



# City Research Online

## City St George's, University of London

**Citation:** Rozeik, R. Y. (1984). The problem of calibrating a microwave network analyzer. (Unpublished Doctoral thesis, The City University)

This is the accepted version of the paper.

This version of the publication may differ from the final published version. To cite this item please consult the publisher's version.

**Permanent repository link:** <https://openaccess.city.ac.uk/id/eprint/35474/>

**Copyright and Reuse:** Copyright and Moral Rights remain with the author(s) and/or copyright holders. Copies of full items can be used for personal research or study, educational, or not-for-profit purposes without prior permission or charge, unless otherwise indicated, provided that the authors, title and full bibliographic details are credited, a hyperlink and/or URL is given for the original metadata page and the content is not changed in any way. For full details of reuse please refer to [City Research Online policy](#).

THE PROBLEM OF CALIBRATING

Page

A MICROWAVE NETWORK

2

ANALYZER

5

9

13

BY

14

16

RASHEL YOUNAN ROZEIK, B.Sc., M.Sc.

21

21

A THESIS SUBMITTED FOR THE DEGREE OF

22

24

DOCTOR OF PHILOSOPHY

27

TO

31

34

DEPARTMENT OF ELECTRICAL & ELECTRONIC ENGINEERING

36

OF

39

THE CITY UNIVERSITY

41

FEBRUARY 1984

43

47

CONTENTS (cont.)

Page

CONTENTS

CHAPTER 2	PREVIOUS CALIBRATION PROCEDURES (Reflection Coefficients)	52
CONTENTS	2.1 Introduction	2
LIST OF TABLES	Set(a) (A direct short and two offset shorts)	6
LIST OF ILLUSTRATIONS	Conclusion (a)	9
ACKNOWLEDGEMENTS	2.2 Set(b) (A direct short, an offset short and open circuit)	13
ABSTRACT	Conclusion (b)	14
INTRODUCTION	2.3 Set(c) (A match termination, a direct short and sliding termination)	16
CHAPTER 1	REFLECTOMETER THEORY	21
1.1	General Reflectometer theory	21
1.2	A Single directional coupler, 3-port	22
1.3	Signal Flow Graphs for directional Coupler 3-port	24
1.4	Flow Graph-analysis of the reflectometer	27
1.5	Basic Reflectometer error model	31
1.6	Directivity	34
1.7	The effect of source match (importance of low SWR)	36
1.8	Directivity error	39
1.9	Source match error	41
1.10	Sources of errors arising in a microwave network analyser	43
1.11	Correcting model	47

CHAPTER 2 THE PRECISION OF CALIBRATION PROCEDURES

page

1.1	Introduction	52
CHAPTER 2	PREVIOUS CALIBRATION PROCEDURES	52
2.1	(Reflection Coefficient)	57
2.1	Introduction	52
2.2	Set(a) [A direct short and two offset shorts]	56
	Conclusion (a)	60
2.3	Set(b) [A direct short, an offset short and open circuit]	63
	Conclusion (b)	65
2.4	Set(c) [A match termination, a direct short and a standard mismatch]	67
	Conclusion (c)	69
2.5	Set(d and e) [A direct short, and offset short and sliding termination]	70
	Calibration with two standards and one sliding termination	70
	Calibration with one standard and two different sliding terminations	74
	Conclusion (d and e)	75
2.6	Correction method using the invariance of the cross-ratio	77
2.7	Previous work on the uncertainty	82
2.7.1	Adam (1968)	82
2.7.2	Hand (1970)	85
2.7.3	Ridella (1973 and 1978)	87
2.7.4	(H.P. method) uncertainty of the magnitude	92
4.7	Final result	171

CONTENTS (cont.)

	page
CHAPTER 3 THE PRECISION OF CALIBRATION PIECES	96
3.1 Introduction	96
3.2 Special properties	97
(1) Short-Circuit termination	97
(2) Tolerance on diameters	101
(3) Tolerance on eccentricity	104
(4) Electrical length	106
(5) Capacitance in the open circuit	113
3.3 Problem associated with the calibration procedure	116
3.3.1 The effect of electric length of reference short-circuit in network analyser calibration	116
3.3.2 The choice of the 3-standards depends on the frequency	121
(I) Procedure I	
(II) Procedure II	
3.3.3 repeatability error	127
CHAPTER 4 MEASUREMENT UNCERTAINTY	131
4.1 Introduction	131
4.2 Analysis of experimental work	133
4.3 The logic of the analysis of variance	139
4.4 Two-dimensional errors (general theory)	143
4.5 Non-linear transformation procedure	150
4.6 Application of the calibration procedure	162
4.7 Final result	171

CONTENTS (cont.)

	page
CHAPTER 5 CONCLUSION	177
APPENDIX	
7.1 Bilinear transformation of scattering parameters	180
7.2 General description of the standards	182
(1) The Connector line	182
(2) Line size	185
General precision for the 7-mm laboratory Connector parameters	186
(A) Mechanical properties	186
(1) Line diameter and tolerances	
(2) Environmental Condition operating	
(3) Connect-disconnect life	
(B) Electrical parameters	187
(1) Maximum frequency limits	
(2) VSWR limits	
(3) Insertion loss	
(4) DC Contact resistance	
7.3 Regression computer program	189
7.4 The effect of electric length of reference short circuit in network analyser	193
7.5 Some statistical definition	196
7.6 Analysis of variance	199
7.7 Correction using any three standards	201
7.8 Computer program	204
REFERENCES	225

	page
LIST OF TABLES	
Table(2.2.1) The unknown matched load with an APC-7 connector was measured through three different mismatches.	137
Table(3.2.1) Impedance of silver short circuit for 50 $\Omega$ with air dielectric	59
Table(3.2.2) Comparison of results for fringe capacitance obtained by other authors	100
Table(3.3.1) Standards used in the calibration procedure.	115
Table(3.3.2) The uncertainty for the magnitude and phase for procedure I and II.	122
Table(3.3.3) The mean values of the uncertainty both in magnitude and phase for procedures I and II.	125
Table(3.3.4) Reflection-coefficient results with confidence levels for measurements on 10.35cm - offset - Short circuit (Based on 60 measurements using the Three-Short circuit correction method).	125
Table(4.2.2) Magnitude of $\rho_{11}$ in dB from measurements of the Eight Standards.	130
Table(4.2.3) Phase of $\rho_{11}$ in degrees from measurements of the Eight Standards.	135
	136

Table(4.2.4)	Standard deviation of $\Gamma_{11}$ in dB from measurement of the Eight Standards.	137
Table(4.2.5)	Standard deviation of $\Gamma_{11}$ in degrees from measurements of the Eight Standards.	138
Table(4.3.1)	Analysis of variance for the dB in Table(4.2.4).	140
Table(4.3.2)	Analysis of variance for the phase in Table(4.2.5).	141
Table(4.4.1)	A hypothetical bivariate distribution for the magnitude and the Phase.	146
Table(4.5.1)	Distribution of 300 corrected values for a single load ( $\rho = .5 \sqrt{10}$ ) when random errors are introduced in the values of the correcting standards at the frequency .5 GHz.	156
Table(4.5.2)	The bivariate distribution from Table(4.5.1).	158
Table(4.5.3)	Distribution of 300 corrected values for a single load ( $\rho = .5 \sqrt{10}$ ) when random errors are introduced in the values of the correcting standards at the frequency .7 GHz.	159
Table(4.5.4)	The bivariate distribution from Table(4.5.3).	161

LIST OF ILLUSTRATIONS

Page

Table(4.6.1)	The measured and the corrected value for the 3 dB coaxial load with an APC-7 connector when measured direct to the network analyzer.	168
Table(4.6.2)	The measured and the corrected value for the 3 dB coaxial load with an APC-7 connector when measured through 2 type N transducers to the network analyzer.	169
Table (4.6.3)	The measured and the corrected value for the 3 dB coaxial load with an APC-7 connector when measured through 2 type N transducers to the network	170
Table (4.7.1)	Magnitude uncertainty (systematic and random errors)	173
Table (4.7.2)	Phase uncertainty (systematic and random errors)	175

LIST OF ILLUSTRATIONS

page

Fig.( 1.1.1)	Basic-Reflectometer	23
Fig.( 1.2.1)	Schematic diagram for a Directional Coupler connected as a 3-Port	23
Fig.( 1.3.1)	Three-port network with detector	26
Fig.( 1.3.3)	Directional-Coupler	26
Fig.( 1.4.1)	Signal flow graph of the Reflectometer	30
Fig.( 1.4.2)	Simplification to Fig (1.4.1)	30
Fig.( 1.5.1)	Reflectometer error network	33
Fig.( 1.6.1)	Effect of Directivity on reflection measure- ment	35
Fig.( 1.7.1)	Source match effect	38
Fig.( 1.8.1)	Directivity effect	40
Fig.( 1.8.2)	Ripple resulting from phase changes as fre- quency is swept	40
Fig.( 1.9.1)	Possible error of full reflection using coupler having a source VSWR of 1.25.	42
Fig.( 1.11.1)	Incident and reflected waves	45
Fig.( 1.11.2)	Effective directivity error	45

Fig.( 1.11.3)	Effective source match error	45
Fig.( 1.11.4)	Reflection error model	46
Fig.(2.1.1)	Reflection measurement system	54
Fig.(2.2.1)	Signal-flow graphs of system under calibration	59
Fig.(2.2.2)	Computer correction using Three Short circuits	62
Fig.(2.3.1)	Measurement correction using Short, Offset Short, and Open Circuits	66
Fig.(2.5.1)	Quantities in $\Gamma$ and $W$ planes for measurement with Two standards and One sliding termination	73
Fig.(2.5.2)	Measurement correction using sliding load	77
Fig.(2.6.1)	Four points in the $\Gamma$ -plane transformed into four other points in the $\rho$ -plane	81
Fig.(2.7.1)	Adam uncertainty.	84
Fig.(2.7.2)	Hand uncertainty.	86
Fig.(2.7.3)	Ridella error model	91
Fig.(2.7.4)	(H.P. Method) Reflection measurement test set	95
Fig.(3.2.1)	Impedance of silver short circuit for 50 $\Omega$ with air dielectric.	99
Fig.(3.2.2)	(a) The measured phases as a function of the frequency for the 7.35 cm and 10.35 cm offset short-circuit. (b) The difference between the measured and the fitted.	107

Fig.(3.2.3)	The measured phases as a function of the frequency for the 20.35 cm and 30.7 cm offset short-circuit. (b) The difference between the measured and the fitted.	108
Fig.(3.2.4)a	(10.35 ±.15)cm offset short line with the connector having susceptance b	112
Fig.(3.2.4)b	The deviation from the line as a function of the frequency	112
Fig.(3.2.5)	Fringe capacitance	115
Fig.(3.3.1)	The phase as a function of the frequency for the eight standards used in the calibration procedure.	123
Fig.(3.3.2)	The distribution of the phase for the eight standards at .7 and 1.5 GHz.	124
Fig.(3.3.3)	The uncertainties in magnitude and phase for procedures I and II.	126
Fig.(3.3.4)	Relative frequency of occurrence of magnitude of reflection coefficient.	129
Fig.(3.3.5)	Relative frequency of occurrence of the phase of the reflection coefficient.	129
Fig.(4.2.1)	Signal-flow graphs of system under calibration.	134
Fig.(4.4.1)	The density for the magnitude and phase represented by a bell-shaped surface	145

Fig.(4.4.2)	Probability density ellipse.	149
Fig.(4.5.1)a	The density distribution for the magnitude and phase in Table(4.6.2).	152
Fig.(4.5.2)	The density distribution for the magnitude and phase in Table(4.6.4).	155
Fig.(4.6.1)	3dB attenuator having type N connector to which was attached a short circuit at one end and a type N to APC7 connector at the other.	164
Fig.(4.6.2)	The measured values of 3-dB with short-circuit measured direct, through 2 type N transducer and "plastic" 2 type N transducer.	165
Fig.(4.6.3)	The corrected values of 3+dB with short-circuit measured direct, through 2 type N transducer and "plastic" 2 type N transducer.	166
Fig. (4.7.1)	The uncertainty curve for the magnitude and phase for systematic and random errors	172

Abstract

ACKNOWLEDGEMENTS

This thesis presents a method for correcting reflection coefficients measurements using network analysers of the heterodyne type.

The author wishes to thank the following people, who have helped in various ways to make this work possible.

Professor A.J.Ellison, for providing the facilities available in the Department of Electrical and Electronic Engineering, The City University.

Dr.A.G.Stainsby, for supervising the project and for his helpful advice and assistance.

Members of my family who, with their support and encouragements throughout my research, have helped me greatly.

Dr.A.G.Stainsby, for supervising the project and for his helpful advice and assistance.

Members of my family who, with their support and encouragements throughout my research, have helped me greatly.

From these calculations, the Abstract of residual error in magnitude and phase is estimated for different magnitudes of reflection coefficient. These are compared with values obtained by other authors.

This thesis presents a method for correcting reflection coefficients measurements using network analysers of the heterodyne type.

In order to test the validity of the calibration procedure a stable load was measured through different mismatching transducers and it was shown that the calibration procedure was effective even for the poorest transition.

The calibration process presented here utilizes three standard loads at each frequency of calibration in order to establish the systematic system error model. Having corrected the results for the systematic errors in the measurement, random errors still remain which cannot be eliminated by any procedure because they are random in their nature. So a statistical approach, has been used to estimate the residual error after corrections have been applied.

A statistical analysis is carried out on repeated measurements of a standard at the same frequency for each of the standards used in the calibration to estimate the standard error in the magnitude and phase for a single network analyser measurement. Making use of a random number generator available in the computer this deviation is applied to a set of theoretically perfect correction measurements and the resultant reflection coefficient calculated. The entire calibration process is repeated many times in a loop, and on each occasion a random value is assigned to the phase angle and magnitude, within limits corresponding to each error source. The uncertainty on a measurement reflection coefficient is then estimated by applying the technique of bivariate distribution to the random variable.

From these calculations the relation of residual error in magnitude and phase is estimated for different magnitudes of reflection coefficient. These are compared with values obtained by other authors.

In order to test the validity of the calibration procedure a stable load was measured through different mismatching transducers and it was shown that the calibration procedure was effective even for the poorest transition.

Methods of characterizing multiport networks using  $H$  or  $Y$  parameters are not suitable above low frequencies as these parameters are not suitable when terminated in the open or short circuit required by these parameters. It is not possible to find more generalised parameters to write for a network in question - parameters which can be measured with reasonable simplicity, even at microwave frequencies. Analysis of the signal flow through a two-port network is one way to do this. The ideal case would be to express a set of parameters when the input and output ports are terminated with their own characteristic impedance at all frequencies. The scattering ( $S$ ) parameters are the set of parameters that are measured under such conditions. An added inherent advantage of these parameters is that they describe the signal flow within the network.

$S$ -parameters are vector quantities, they give magnitude and phase information. Most measurements of microwave components, like attenuation, gain and VSWR have historically been measured only in terms of magnitude, mainly because it was too difficult to obtain both phase and magnitude information. Measuring  $S$ -parameters involves measuring the ratio of the magnitude and relative phase angles of the response to those of the applied signal at the ports of the network when the other ports are terminated in their characteristic impedance. The S.P. network analyzer system used in this work enables one to measure  $S$ -parameters at microwave frequency.

## INTRODUCTION

### Characterization of two ports

Methods of characterizing multiport networks using  $H$  or  $Y$  parameters are not suitable above 1GHz since at these frequencies devices may oscillate when terminated in the open or short circuit required by these parameters. So one would like to find some generalized parameters to write for a network in question - parameters which can be measured with reasonable simplicity, even at microwave frequencies. Analysis of the signal flow through a two-port network is one way to do this. The ideal case would be to express a set of parameters when the input and output ports are terminated with their own characteristic impedance at all frequencies. The scattering (S) parameters are the set of parameters that are measured under such conditions. An added inherent advantage of these parameters is that they describe the signal flow within the network.

S-parameters are vector quantities, they give magnitude and phase information. Most measurements of microwave components, like attenuation, gain and VSWR have historically been measured only in terms magnitude, mainly because it was too difficult to obtain both phase and magnitude information. Measuring S-parameters involves measuring the ratio of the magnitude and relative phase angles of the response to those of the applied signal at the ports of the network when the other ports are terminated in their characteristic impedance. The H.P. network analyser system used in this work enables one to measure S-parameters at microwave frequency.

Such a microwave network analyser measures the reflection coefficient by directly comparing the phase angle and amplitude of the forward and reflected waves. The waves travel along two channels, called reference and test channels respectively. Power is coupled from these channels by means of directional couplers. to a down converter, reducing the frequency to about .11 GHz .The relative phase angle and magnitude of the waves in the test and reference channel are then measured with a vector voltmeter. the network analyser can be constructed by measurements on appropriate standards loads.

As in any system, there are different sources of error associated with the network analyser. For example, the whole of the incident wave may not reach the unknown load. Some of it may appear at the input due to leakage through the coupler, thus causing the directivity error. Also since the measurement system never has exactly constant characteristic impedance, some signal may be reflected back to the unknown device thus causing the source match error. There is a frequency tracking error due to differences between the incident and test couplers. Also measurements frequently have to be made on a device which is fitted with an adaptor from one form of transmission line to that of the reflectometer measurement port. This again can cause mismatch. Noise and frequency drift are also sources of error which affect the value measured by the analyzer. systems are studied, some of which are accounted for in the error model.

It was found that there were no convenient means for accurately characterizing many devices except after detailed study of each error. It is therefore necessary to eliminate or reduce these errors by

different sets of standards. The advantages and disadvantages of each measuring standard components at the frequencies of interest (calibration procedure). The instrument can then be used to measure the required device. The internal system errors are vectorially subtracted from the measurement data through complex mathematical manipulation, correcting the measurement and leaving only the true characteristics of the device. i.e. to recapitulate, the measurement procedure is as follows: 1) calibration; 2) measurement, and 3) correction of the data. A complete error model for the network analyzer can be constructed by measurements on appropriate standards loads.

The purpose of this thesis is to study the sources of error in network analyser measurements of a one port, to divide these into systematic errors (that is those that can be minimized by calibration) and random errors (that is those whose magnitude depends only on the instrument and its method of use) and finally to estimate the residual error in measurement of a reflection coefficient when the instrument has been calibrated using three standards.

In Chapter(1) the theory of reflectometers is explained and the associated errors are investigated. The two most important errors, directivity and source mismatch, are extensively discussed. Also all the sources of error associated with the system are studied, some of which are accounted for in the error model.

Chapter(2) presents a survey of previous work on the calibration of network analyzers for measuring reflection, i.e. a one-port, using

different sets of standards. The advantages and disadvantages of each set are then discussed.

Chapter(3) studies the systematic error associated with the standard used in the calibration procedure. The three main problems affecting the calibration are (1) the effect of incorrect electrical length of reference short-circuit on calibration, (2) The choice of the three standards which depend on the frequency, (3) Repeatability error.

Chapter(4) presents a practical and theoretical way to solve for the overall system error (systematic and random) in three steps. (1) Measuring each of eight standards, ten times. (2) Assigning a standard deviation for the phase and magnitude by means of the analysis of variance. (3) Generating random numbers by using the above standard deviation and applying the bivariate distribution technique. This calibration was used to measure a fixed load over a frequency range through three different mismatches).

The final results for the uncertainty in two different confidence levels are included at the end of this chapter. these results were obtained by using a computer program, developed in Appendix 7.8, which solves a reflectometer error model currently being used in the microwave measurement system. The program makes use of the computers in built random number generator, and the results obtained with this technique apply to all system in general. Furthermore any type of

standard can be use with this program to solve the systematic and random errors.

### 1.1 General Reflectometer Theory:-

Any user with the necessary equipment may determine his own system parameters and put these into the error analysis program to know magnitude and phase uncertainty at the confidence level desired.

The microwave reflectometer in its usual form consists of a pair of directional couplers so arranged that one couples to the forward wave, and the other to the reverse wave. If the couplers were perfect,

The final conclusion are given in Chapter (5). the ratio of the sidearm outputs would be equal to or at least proportional to the magnitude of the reflection coefficient of the termination; and from their relative phases, the phase of the reflection coefficient could be deduced.

In practice, because of imperfections in the directional couplers and other factors, there is some uncertainty in the values obtained.

The basic form of the reflectometer is shown in Fig(1.1.1). If  $b_1$  and  $b_2$  represent the voltage amplitudes of the signals at the respective detectors, the desired response is:-

$$\frac{b_1}{b_2} = \Gamma_0 \text{ or } \frac{b_1}{b_2} = K \Gamma_0$$

where  $\Gamma_0$  is the voltage reflection coefficient of the termination on arm 2, and  $K$  is a constant whose value must be determined.

## CHAPTER (1)

### REFLECTOMETER THEORY

#### 1.1 General Reflectometer Theory:-

The microwave reflectometer in its usual form consists of a pair of directional couplers so arranged that one couples to the forward wave, and the other to the reverse wave. If the couplers were perfect, the ratio of the sidearm outputs would be equal to or at least proportional to the magnitude of the reflection coefficient of the termination; and from their relative phases, the plane of the reflection coefficient could be deduced.

In practice, because of imperfections in the directional couplers and other factors, there is some uncertainty in the values obtained.

The basic form of the reflectometer is shown in Fig(1.1.1). If  $b_3$  and  $b_4$  represent the voltage amplitudes of the signals at the respective detectors, the desired response is:-

$$\frac{b_3}{b_4} = \Gamma_L \text{ or } \frac{b_3}{b_4} = K \Gamma_L$$

where  $\Gamma_L$  is the voltage reflection coefficient of the termination on arm 2, and  $K$  is a constant whose value must be determined.

1.2 A single directional coupler, 3-Port:-

Directional couplers are often considered as a class of lossless 4-ports. But if one arm is internally terminated and the connection is unavailable, it is then classed as a 3-port coupler Fig(1.2.1).

Fig.( 1.1.1) Basic-Reflectometer



Fig.( 1.2.1) Schematic diagram for a Directional Coupler connected as a 3-Port

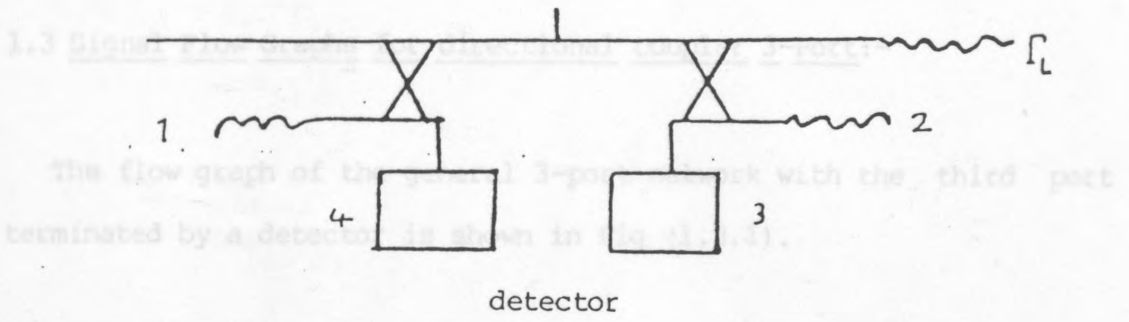
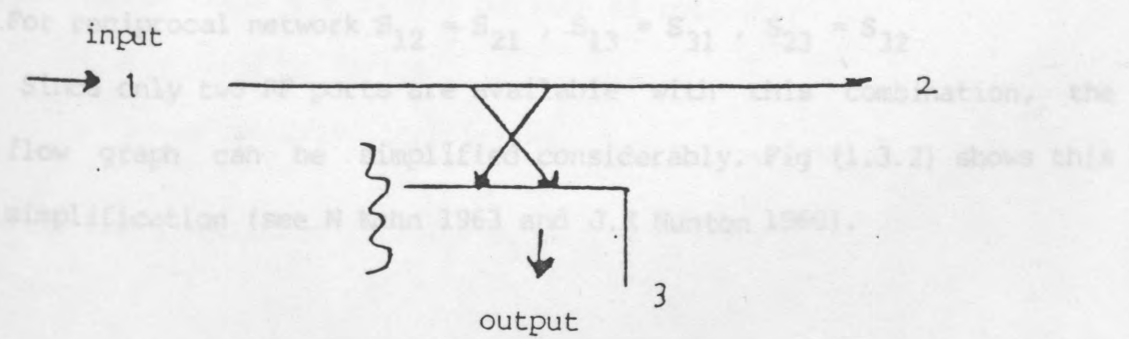


Fig.( 1.1.1) Basic-Reflectometer

$$\begin{aligned}
 b_1 &= S_{11} a_1 + S_{12} a_2 + S_{13} a_3 \\
 b_2 &= S_{21} a_1 + S_{22} a_2 + S_{23} a_3 \\
 b_3 &= S_{31} a_1 + S_{32} a_2 + S_{33} a_3 \\
 a_3 &= b_3 \Gamma_L \\
 R &= \Gamma b_3
 \end{aligned}$$



The relationships involved are:-

Fig.( 1.2.1) Schematic diagram for a Directional Coupler connected as a 3-Port

$$\begin{aligned}
 b_2 &= \Gamma b_1 + C a_2 \\
 R &= K \Gamma a_1 + C a_2
 \end{aligned}$$

### 1.3 Signal Flow Graphs for directional coupler 3-Port:-

The flow graph of the general 3-port network with the third port terminated by a detector is shown in Fig (1.3.1).

The equations described by the flow graph are:-

$$b_1 = S_{11} a_1 + S_{12} a_2 + S_{13} a_3$$

$$b_2 = S_{21} a_1 + S_{22} a_2 + S_{23} a_3$$

$$b_3 = S_{31} a_1 + S_{32} a_2 + S_{33} a_3$$

$$a_3 = b_3 \Gamma_d$$

$$M = Kb_3$$

For reciprocal network  $S_{12} = S_{21}$ ,  $S_{13} = S_{31}$ ,  $S_{23} = S_{32}$

Since only two RF ports are available with this combination, the flow graph can be simplified considerably. Fig (1.3.2) shows this simplification (see N Kuhn 1963 and J.K Hunton 1960).

The relationships involved are:-

$$b_1 = \Gamma_1 a_1 + T a_2$$

$$b_2 = \Gamma_2 a_2 + T a_1$$

$$M = K (C a_1 + C D a_2)$$

$$\Gamma_1 = S_{11} + \frac{S_{13}^2 \Gamma_d}{1 - S_{33} \Gamma_d}$$

$$\Gamma_2 = S_{22} + \frac{S_{23}^2 \Gamma_d}{1 - S_{33} \Gamma_d}$$

$$T = S_{21} + \frac{S_{13} S_{23} \Gamma_d}{1 - S_{33} \Gamma_d}$$

$$C = \frac{S_{31}}{1 - S_{33} \Gamma_d}, \quad D = \frac{S_{32}}{S_{31}}$$

These relationships are written directly through application of the nontouching loop rule. The path  $a_1$  to M is the main coupling direction involving the coupling factor, and effective directivity coefficient these are usually defined as follows :-

C = coupling factor

D = directivity coefficient

while the directivity is  $20 \log S_{31}/S_{32}$

Fig. (1.3.3) Directional-Coupler

1.4 Flow Graph - analysis of the reflectometer:-

In a practical reflectometer system, two identical directional couplers are required, one to sample the incident wave and the other to sample the reflected wave.

A simplified flow graph is shown in Fig. (1.4.1). (The generator and load reflection are indicated by  $\Gamma_d$  and  $M$  respectively.)

Fig. (1.4.1) is further simplified in Fig. (1.4.2) making the same assumptions as in 1.3 above.

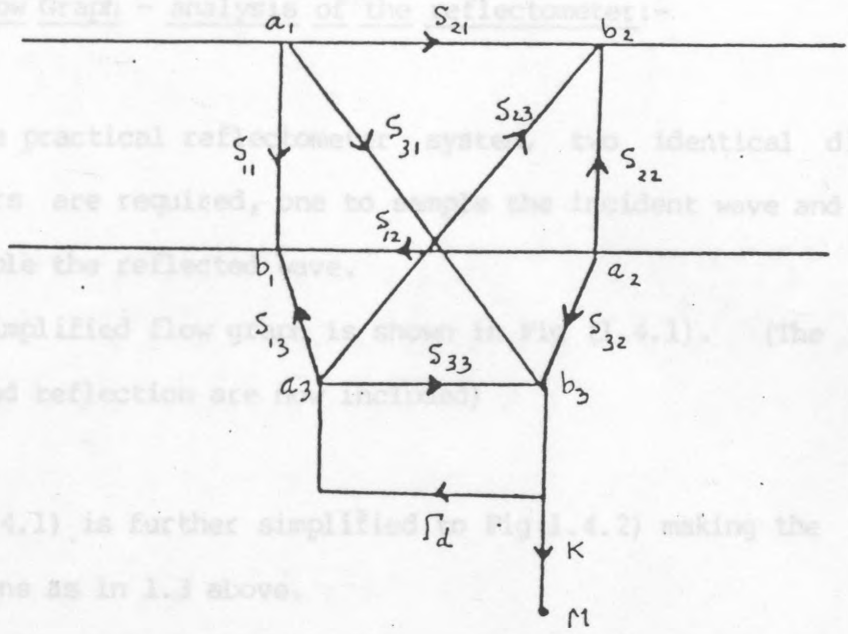


Fig.( 1.3.1) Three-port network with detector

1st order loop:-

2nd order loop:-

3rd order loop:-

Path a → b1:-

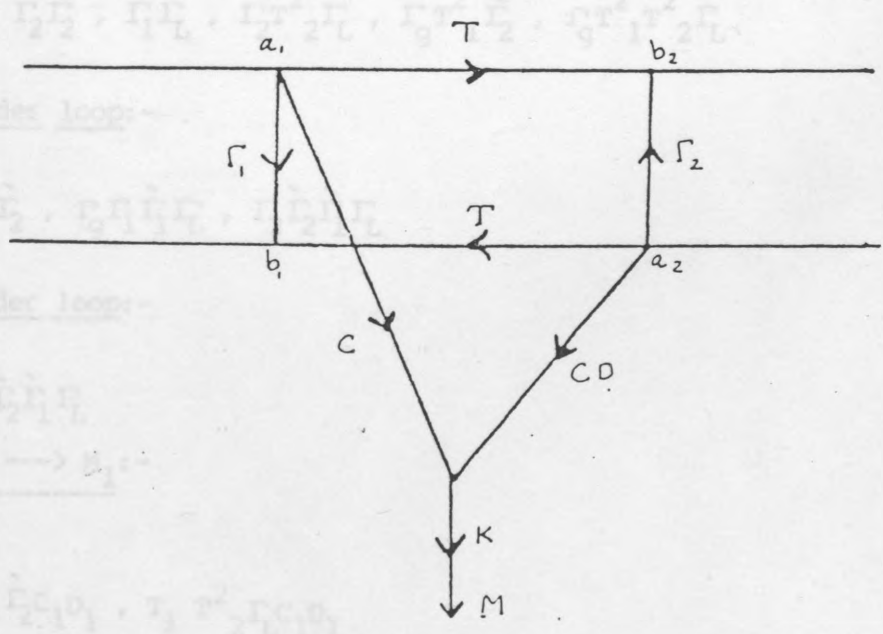


Fig.( 1.3.3) Directional-Coupler

1.4 Flow Graph - analysis of the reflectometer:-

In a practical reflectometer system, two identical directional couplers are required, one to sample the incident wave and the other to sample the reflected wave.

A simplified flow graph is shown in Fig (1.4.1). (The generator and load reflection are now included)

Fig (1.4.1) is further simplified to Fig(1.4.2) making the same assumptions as in 1.3 above.

It is desired to know how the ratio  $M_2/M_1$  related to  $\Gamma_L$  using non-touching loop rule.

1st order loop:-

$$\Gamma_g \Gamma_1, \Gamma_2 \hat{\Gamma}_2, \hat{\Gamma}_1 \Gamma_L, \Gamma_2 T_2^2 \Gamma_L, \Gamma_g T_1^2 \hat{\Gamma}_2, \Gamma_g T_1^2 T_2^2 \Gamma_L$$

2nd order loop:-

$$\Gamma_g \Gamma_1 \Gamma_2 \hat{\Gamma}_2, \Gamma_g \Gamma_1 \hat{\Gamma}_1 \Gamma_L, \Gamma_2 \hat{\Gamma}_2 \hat{\Gamma}_1 \Gamma_L$$

3rd order loop:-

$$\Gamma_g \Gamma_1 \Gamma_2 \hat{\Gamma}_2 \hat{\Gamma}_1 \Gamma_L$$

Path a ---->  $M_1$ :-

$$C_1, T_1 \hat{\Gamma}_2 C_1 D_1, T_1 T_2^2 \Gamma_L C_1 D_1$$

Path a ---->  $M_2$ :-

$$T_1 C_2 D_2, T_1 T_2 \Gamma_L C_2$$

$$M_1/a_1 = C_1 [1 - \Gamma_2 \tilde{\Gamma}_2 - \tilde{\Gamma}_1 \Gamma_L - \Gamma_2 T_2^2 \Gamma_L + \Gamma_2 \tilde{\Gamma}_2 \tilde{\Gamma}_1 \Gamma_L] + T_1 \tilde{\Gamma}_2 C_1 D_1 [1 - \tilde{\Gamma}_1 \Gamma_L] + T_1 T_2^2 \Gamma_L C_1 D_1 /$$

$$[1 - \Gamma_9 \Gamma_1 - \Gamma_2 \tilde{\Gamma}_2 - \tilde{\Gamma}_1 \Gamma_L - \Gamma_9 T_1^2 \tilde{\Gamma}_2 - \Gamma_2 T_2^2 \Gamma_L - \Gamma_9 T_1^2 T_2^2 \Gamma_L + \Gamma_9 \Gamma_1 \Gamma_2 \tilde{\Gamma}_2 +$$

$$\Gamma_9 \Gamma_1 \tilde{\Gamma}_1 \Gamma_L + \Gamma_2 \tilde{\Gamma}_2 \tilde{\Gamma}_1 \Gamma_L - \Gamma_9 \Gamma_1 \Gamma_2 \tilde{\Gamma}_2 \tilde{\Gamma}_1 \Gamma_L]$$

$$M_2/a_1 = T_1 C_2 D_2 [1 - \tilde{\Gamma}_1 \Gamma_L] + T_1 T_2 \Gamma_L C_2 /$$

$$[1 - \Gamma_9 \Gamma_1 - \Gamma_2 \tilde{\Gamma}_2 - \tilde{\Gamma}_1 \Gamma_L - \Gamma_9 T_1^2 \tilde{\Gamma}_2 - \Gamma_2 T_2^2 \Gamma_L - \Gamma_9 T_1^2 T_2^2 \Gamma_L + \Gamma_9 \Gamma_1 \Gamma_2 \tilde{\Gamma}_2 +$$

$$\Gamma_9 \Gamma_1 \tilde{\Gamma}_1 \Gamma_L + \Gamma_2 \tilde{\Gamma}_2 \tilde{\Gamma}_1 \Gamma_L - \Gamma_9 \Gamma_1 \Gamma_2 \tilde{\Gamma}_2 \tilde{\Gamma}_1 \Gamma_L]$$

$$M_2 = \frac{C_2 [T_1 T_2 - T_1 D_2 \tilde{\Gamma}_1] \Gamma_L + C_2 T_1 D_2}{T_1 \Gamma_2 D_1}$$

$$C_1 [-\tilde{\Gamma}_1 + \Gamma_2 \tilde{\Gamma}_2 \tilde{\Gamma}_1 - T_1 \tilde{\Gamma}_2 D_1 \tilde{\Gamma}_1 + T_1 T_2^2 D_1 \tilde{\Gamma}_2 - \Gamma_2 T_2^2 \Gamma_L] \Gamma_L + C_1 [1 - \Gamma_2 \tilde{\Gamma}_2 +$$

$$= \frac{A \Gamma_L + B}{C \Gamma_L + D} \dots\dots (1.4.1)$$

where  $A = C_2 [T_1 T_2 - T_1 D_2 \tilde{\Gamma}_1]$

$B = C_2 T_1 D_2$

$$C = C_1 [-\tilde{\Gamma}_1 + \Gamma_2 \tilde{\Gamma}_2 \tilde{\Gamma}_1 - T_1 \tilde{\Gamma}_2 D_1 \tilde{\Gamma}_1 + T_1 T_2^2 D_1 - \Gamma_2 T_2^2] \Gamma_L$$

$$D = C_1 [1 - \Gamma_2 \tilde{\Gamma}_2 + T_1 \tilde{\Gamma}_2 D_1]$$

Equation (1.4.1) is important because :-

(1) It shows that the measured reflection coefficient " $\rho_m$ " is related to the true reflection coefficient  $\Gamma_L$  by a bilinear transformation (Appendix 7.1).

(2) The constants of a passive bilinear transformation A, B, C, and D may be obtained by three measurements. It is unnecessary to know the individual parameters ( $T_1$ ,  $T_2$ ,  $D_1$ ,  $D_2$ ...) but the scattering parameters may be calculated by use of (Appendix 7.1).

(3) If the constants A, B, C and D of the bilinear transformation are known then  $\Gamma_L$  may be calculated.

(4) Item (3) is of the utmost importance for it clearly demonstrates that an imperfect reflectometer may be used to yield the true measurement of a reflection coefficient if the constants of item (2) are known. This is the basis of computer correction of one port reflection measurements.

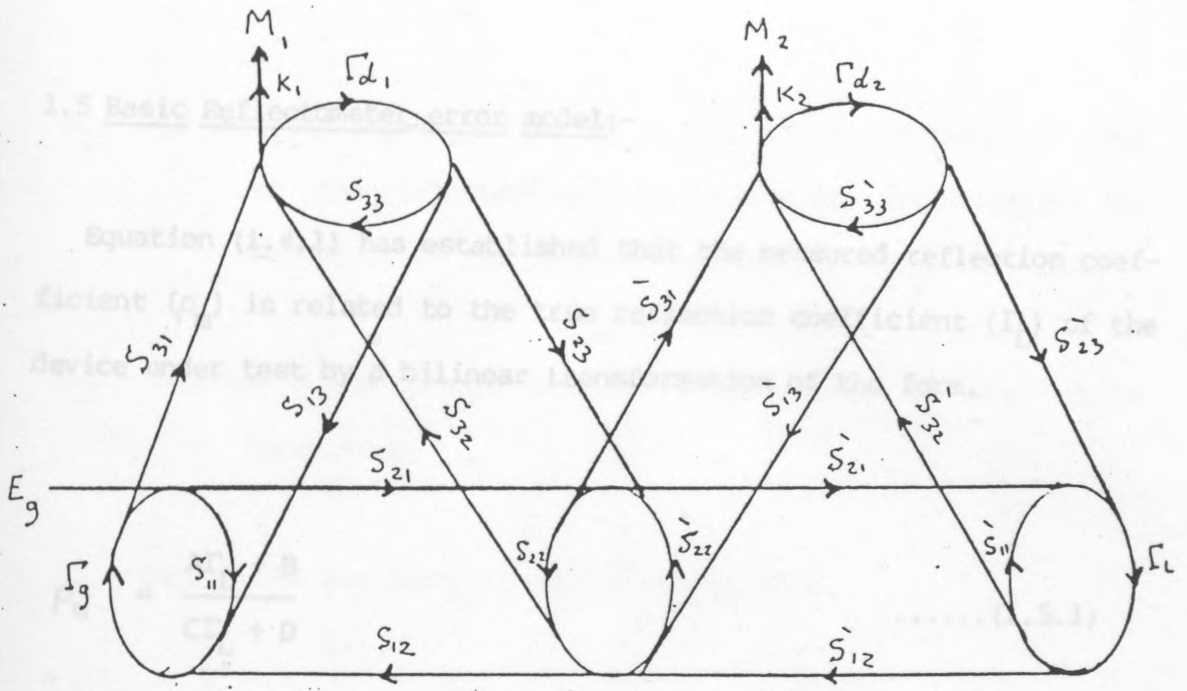


Fig. ( 1.4.1) Signal flow graph of the Reflectometer

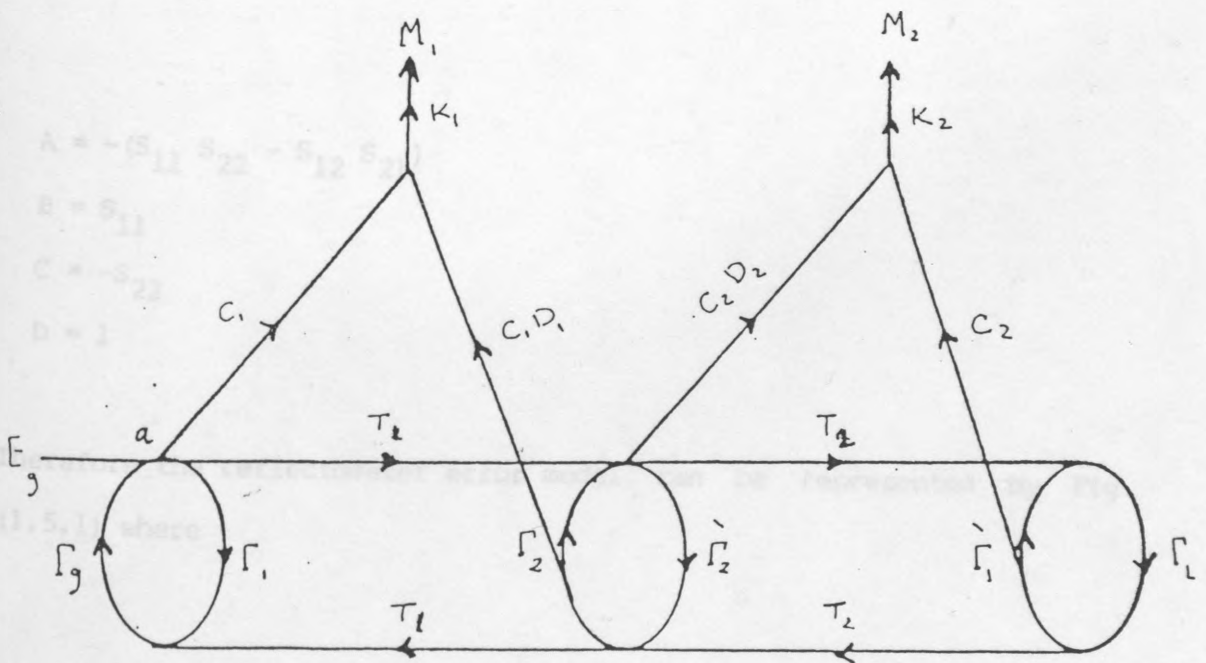


Fig. ( 1.4.2) Simplification to Fig (1.4.1)

1.5 Basic Reflectometer error model:-

Equation (1.4.1) has established that the measured reflection coefficient ( $\rho_m$ ) is related to the true reflection coefficient ( $\Gamma_L$ ) of the device under test by a bilinear transformation of the form.

$$\rho_m = \frac{A\Gamma_L + B}{C\Gamma_L + D} \dots\dots(1.5.1)$$

where A, B, C and D are the complex constants defined by equation (1.4.2). In (Appendix 7.1) it has been shown that a bilinear transformation of equation (1.5.1) can also be expressed by a general set of scattering parameters of the form shown in Fig (1.5.1) where

$$A = -(S_{11} S_{22} - S_{12} S_{21})$$

$$B = S_{11}$$

$$C = -S_{22}$$

$$D = 1$$

Therefore the reflectometer error model can be represented by Fig (1.5.1) where

$S_{11}$  - is the path the signal leaked directly from the incident wave to the reflected wave detector of the reflectometer independent of the device under test (directivity error).

$S_{21}$  - represents the forward incident signal path to the device under test.

$S_{12}$  - represents its return path to the detector.

$S_{22}$  - is the effective reflection coefficient at the output port. (source match error).

$S_{11}$  - is the path the signal leaked directly from the incident wave to the reflected wave detector of the reflectometer independent of the device under test (directivity error).

$S_{21}$  - represents the forward incident signal path to the device under test.

$S_{12}$  - represents its return path to the detector.

$S_{22}$  - is the effective reflection coefficient at the output port. (source match error).

## 1.6 Directivity:-

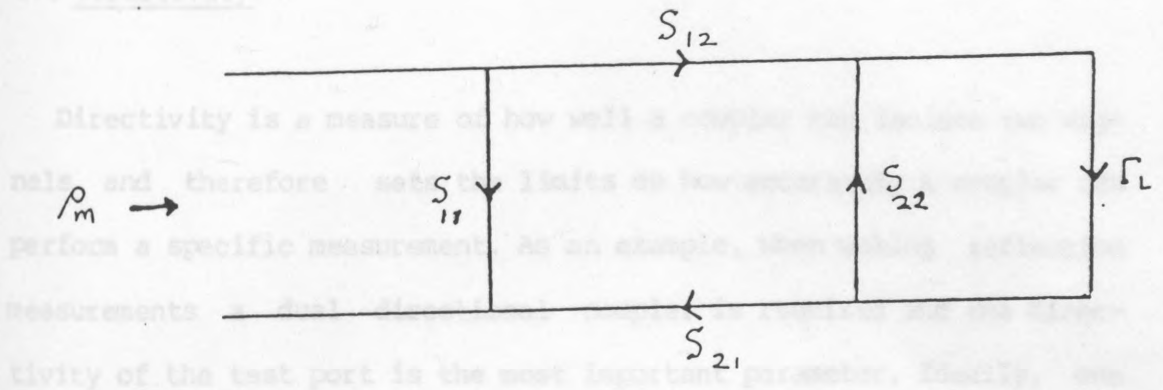


Fig.( 1.5.1) Reflectometer error network

$S_{11}$  - is the path the signal leaked directly from the incident wave to the reflected wave detector of the reflectometer independent of the device under test (directivity error).

$S_{21}$  - represents the forward incident signal path to the device under test.

$S_{12}$  - represents its return path to the detector.

$S_{22}$  - is the effective reflection coefficient at the output port. (source match error).

## 1.6 Directivity:-

Directivity is a measure of how well a coupler can isolate two signals and therefore sets the limits on how accurately a coupler can perform a specific measurement. As an example, when making reflection measurements a dual directional coupler is required and the directivity of the test port is the most important parameter. Ideally, one would like to measure the magnitude of the reflected signal alone. However, because of imperfect directivity, the reflected signal is combined with a small portion of the incident signal. It is important to emphasise that the magnitude of the portion of the incident signal that combines with the reflected signal is dependent strictly on the directivity of the coupler. The figure (1.6.1) graphically shows the effect of directivity error on a reflection measurement.

$K_1$  and  $K_2$ : Coupling coefficients (dB)

$E_{in}$  = Input signal

$D_1$  and  $D_2$ : Directivities (dB)

$E_r$  = Reflected signal from DUT

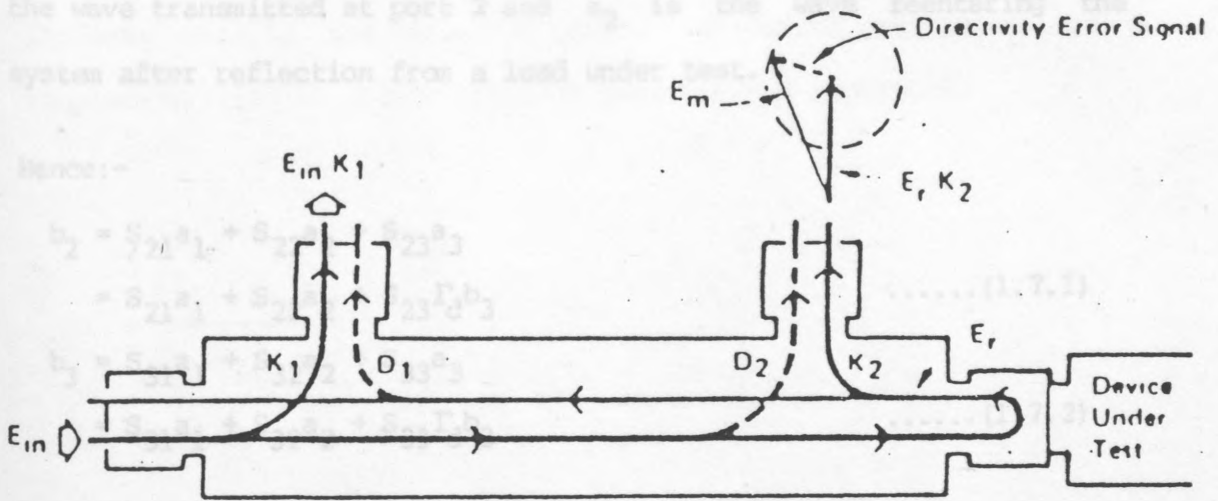
The small portion of the incident signal which combines with the reflected signal is a phasor that is directly additive to the measurement uncertainty. Thus, the higher the directivity the higher the measurement accuracy.

Because the portion of the incident signal that is added to the reflected signal is very small, it adds a negligible amount of uncertainty when measuring large reflections. But as the reflected signal becomes smaller the small portion of the incident signal becomes more significant.

1.7 The effect of source match (importance of low SWR):-

To study the effect of source match, consider the effect of the incident signal coupler as in Fig (1.7.3). This is the same Fig as (1.3.1) but now port 2 is the main signal output port.  $b_2$  is now the wave transmitted at port 2 and  $a_2$  is the wave scattering the system after reflection from a load under test.

Hence:-



$K_1$  and  $K_2$ : Coupling coefficients (dB)  
 $D_1$  and  $D_2$ : Directivities (dB)

$E_{in}$  = Input signal  
 $E_r$  = Reflected signal from DUT  
 $E_m$  = Measured signal (includes directivity error)

Fig.( 1.6.1) Effect of Directivity on reflection measurement

Sub. from equation (1.7.3) into (1.7.2)

$$b_1 = \frac{S_{11}b_2 - S_{21}a_2}{S_{21}} = \frac{S_{11}b_2 - S_{21}a_2}{S_{21}}$$

$$b_2 = \frac{S_{22}b_1 + S_{12}a_1}{S_{12}} = \frac{S_{22}b_1 + S_{12}a_1}{S_{12}}$$

1.7 The effect of source match (importance of low SWR):- ..... (1.7.4)

To study the effect of source match, consider the effect of the incident signal coupler as in Fig (1.7.1). This is the same Fig as (1.3.1) but now Port 2 is the main signal output port.  $b_2$  is now the wave transmitted at port 2 and  $a_2$  is the wave reentering the system after reflection from a load under test.

Hence:-

$$\begin{aligned} b_2 &= S_{21}a_1 + S_{22}a_2 + S_{23}a_3 \\ &= S_{21}a_1 + S_{22}a_2 + S_{23}\Gamma_d b_3 \end{aligned} \quad \text{..... (1.7.1)}$$

$$\begin{aligned} b_3 &= S_{31}a_1 + S_{32}a_2 + S_{33}a_3 \\ &= S_{31}a_1 + S_{32}a_2 + S_{33}\Gamma_d b_3 \end{aligned} \quad \text{..... (1.7.2)}$$

From equation (1.7.1)

$$a_1 = \frac{b_2 - (S_{22}a_2 + S_{23}\Gamma_d b_3)}{S_{21}} \quad \text{..... (1.7.3)}$$

Sub. from equation (1.7.3) into (1.7.2)

$$b_3 = \frac{S_{31}b_2}{S_{21}} - \frac{S_{22}S_{31}a_2}{S_{21}} - \frac{S_{23}S_{31}\Gamma_d b_3}{S_{21}} + S_{32}a_2 + S_{33}\Gamma_d b_3$$

$$b_3 [1 + \Gamma_d (S_{23}S_{31} - S_{33})] = \frac{S_{31}b_2}{S_{21}} - a_2 \frac{[S_{22}S_{31} - S_{32}]}{S_{21}}$$

$$b_2 = b_3 \frac{[S_{21} + \Gamma_d(S_{23} - S_{33}S_{21})]}{S_{31}} + a_2 \frac{[S_{22} - S_{32}S_{21}]}{S_{31}} \quad \dots\dots(1.7.4)$$

The first term in equation (1.7.4)  $b_2/b_3$  represents generator output while the second term is the effective generator reflection coefficient. That is the effective source reflection coefficient of a coupler-levelled or ratio system is given by the expression

$$= \frac{S_{22} - S_{32}S_{21}}{S_{31}}$$

$S_{21} = T =$  transmission coefficient through the coupler

$S_{32}/S_{31} = D =$  Directivity

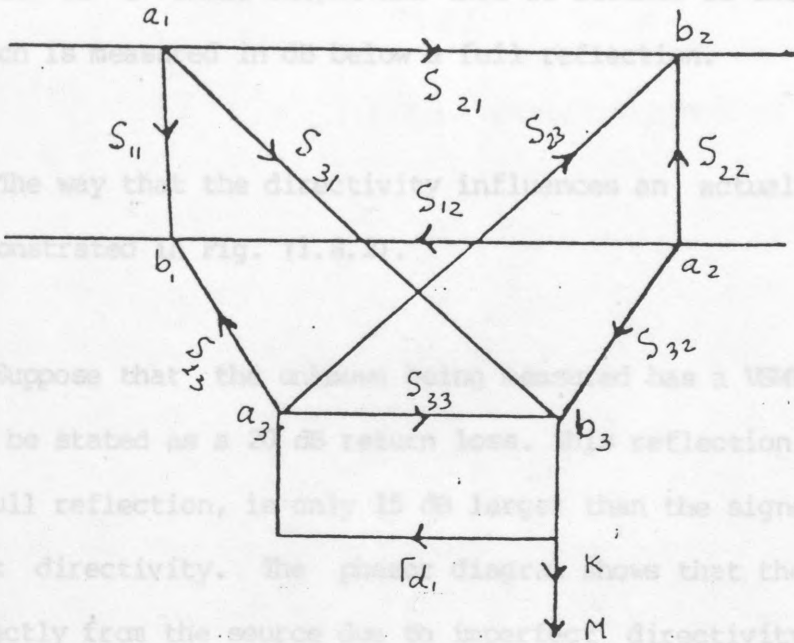
$S_{22} = \Gamma_c =$  output reflection coefficient of couplers main or through arm.

Therefore, the effective source match reflection coefficient =  $\Gamma_c - TD$

$$\dots\dots(1.7.5)$$

1.8 Directivity error

Fig. (1.8-1) illustrates a directional device terminated in an ideal  $Z_0$ . Assume that all energy from the test port is absorbed in  $Z_0$  and none is reflected back to the device. Under these conditions, there is a small output and this is defined as the directivity (D), which is the ratio of the signal received directly from the source to the signal received from the load.



Suppose that the directional coupler has a VSWR of 1.22, which can be stated as a 1.5 dB return loss. This means that the signal due to imperfect directivity is only 15 dB larger than the signal due to imperfect directivity. The phasor diagram shows that the signal received directly from the source due to imperfect directivity combines with the signal reflected from the load to give a resultant which depends upon the phase. Fig. (1.7.1) Source match effect

The limits of the possible error of the measurement are shown alongside. Thus, a 10 dB return loss will appear to be somewhere between 18.58 and 21.70 dB as a consequence of directivity.

### 1.8 Directivity error:-

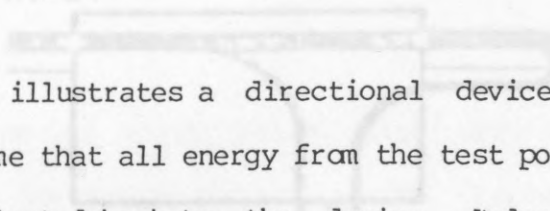
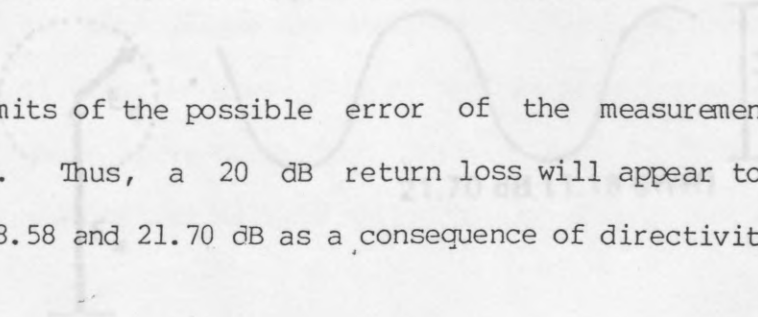


Fig. (1.8.1) illustrates a directional device terminated in an ideal  $Z_0$ . Assume that all energy from the test port is absorbed in  $Z_0$  and none is reflected back to the device. Under these conditions, there is a small output and this is defined as the directivity (D), which is measured in dB below a full reflection.

The way that the directivity influences an actual measurement is demonstrated in Fig. (1.8.2).

Suppose that the unknown being measured has a VSWR of 1.22, which can be stated as a 20 dB return loss. This reflection, 20 dB down from a full reflection, is only 15 dB larger than the signal due to imperfect directivity. The phasor diagram shows that the signal received directly from the source due to imperfect directivity combines with the signal reflected from the load to give a resultant which depends upon the phase relationship of the two signals.



The limits of the possible error of the measurement are shown alongside. Thus, a 20 dB return loss will appear to be somewhere between 18.58 and 21.70 dB as a consequence of directivity.

1.8 Source match

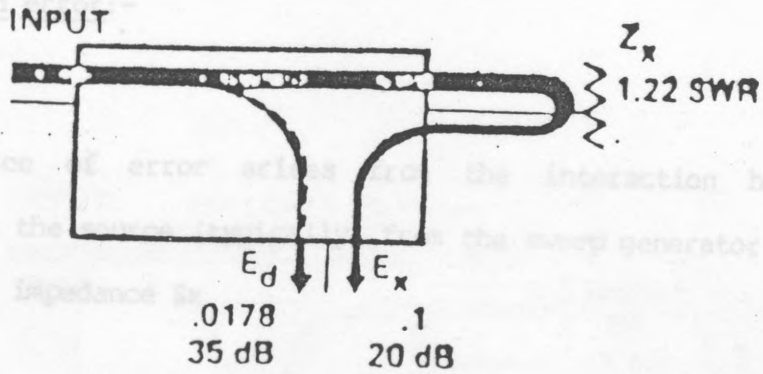


Fig.( 1.8.1) Directivity effect

When a full reflection is reflected back to the signal source, the reflected wave travels unattenuated back to the signal source where it is again reflected unless the source is perfectly matched. This reflected wave passes through the coupler a second time and is re-reflected from the calibrating short or open and summed with the full reflection in the detector.

Since the phase of the reflected signal  $E_x$  in Fig (1.8.1) is arbitrary, the effect of different phasing can lead to ripple in amplitude as a function of frequency of about 1.27 dB of the value with no source mismatch. In practice this ripple should be much smaller than 1.27, but values can vary.

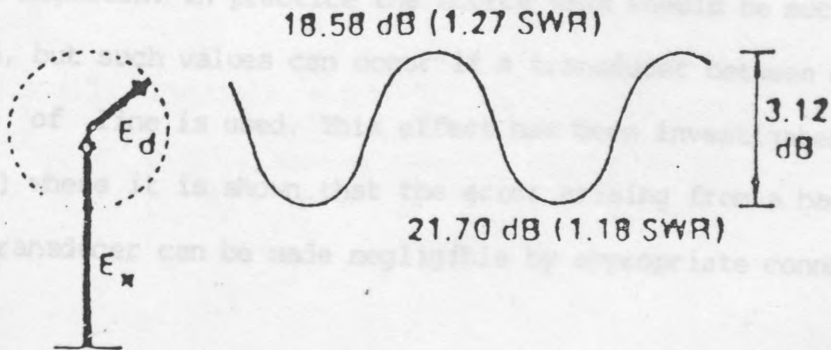


Fig.( 1.8.2) Ripple resulting from phase changes as frequency is swept

### 1.9 Source match error:-

A second source of error arises from the interaction between reflections from the source (typically from the sweep generator) and from the unknown impedance  $Z_x$

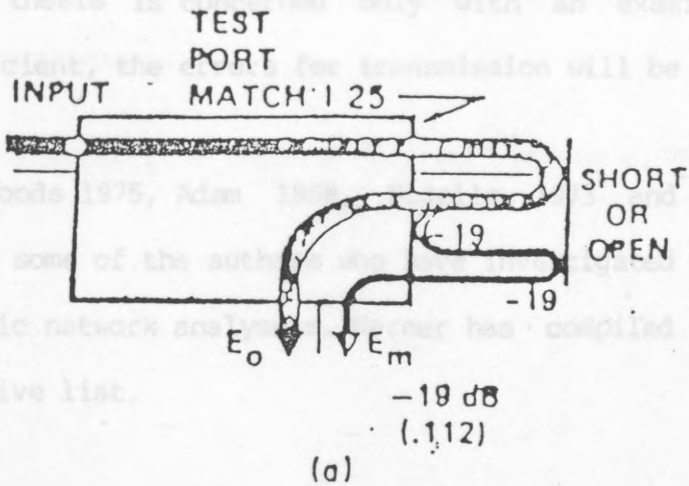
When a full reflection is applied to establish the reference output, the reflected wave travels unattenuated back to the signal source where it is again reflected unless the source is perfectly matched. This reflected wave passes through the coupler a second time and is re-reflected from the calibrating short or open and summed with the full reflection in the detector.

Since the phase of the rereflected signal  $E_m$  in Fig (1.9.1) is arbitrary, the effect of different phasing can lead to ripple in amplitude as a function of frequency of about  $\pm 1.27$  of the value with no source mismatch. In practice the source VSWR should be much smaller than 1.25, but such values can occur if a transducer between different standards of line is used. This effect has been investigated in section (4.6) where it is shown that the error arising from a badly mismatched transducer can be made negligible by appropriate connection.

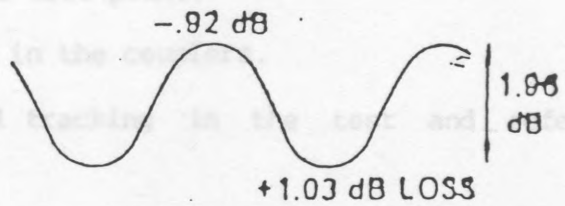
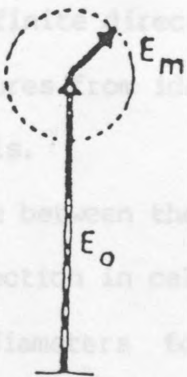
1.10 Sources of errors arising in a microwave network analyzer:-

Although this thesis is concerned only with an examination of reflection coefficient, the error for transmission will be included.

Hand, 1970, Woods 1975, Adam 1978, and Warner 1978 and Warner 1973 are some of the authors who have compiled the following comprehensive list.



- a) Imperfect matching at the test point.
- b) Non-infinite directivity in the coupler.
- c) Departures from identical matching in the test and reference channels.
- d) Leakage between the two channels.
- e) Imperfections in calibration.



RIPPLE DEPENDENT UPON SWEEP WIDTH AND DISTANCE TO MISMATCH.

Fig.( 1.9.1) Possible error of full reflection using coupler having a source VSWR of 1.25.

f) Imperfections in the instrumentation such as frequency and power level non-linearities, gain and phase drifts in the I.F. amplifiers, detectors, attenuator and display circuits.

g) Quantization errors, such as errors in the analogue to digital conversions, rounding off errors in computation.

### 1.10 Sources of errors arising in a microwave network analyser:-

(1) Reflection.

Although this thesis is concerned only with an examination of reflection coefficient, the errors for transmission will be included.

The methods of minimizing these errors will now be discussed.

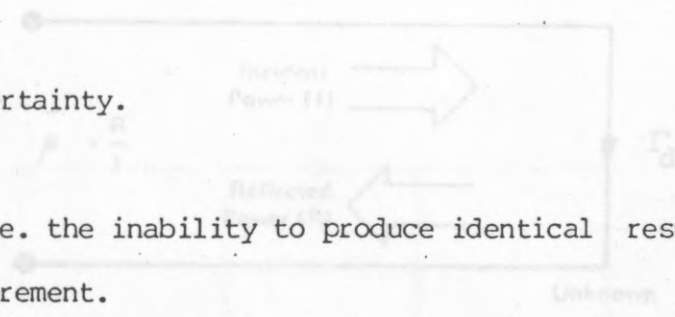
Hand., 1970, Woods 1975, Adam 1968, Ridella 1973 and 1978 and Warner 1973 are some of the authors who have investigated sources of error in automatic network analysers. Warner has compiled the following comprehensive list.

- a) Imperfect matching at the test point.
- b) Non-infinite directivity in the couplers.
- c) Departures from identical tracking in the test and reference channels.
- d) Leakage between the two channels (Transmission measurements).
- e) Imperfection in calibration standards (these are caused by incorrect diameters for the inner and outer conductors, an error in the length of the offset short, contact resistances between the inner and outer conductors, eccentricity in the coaxial line, line losses and discontinuity capacities).
- f) Imperfections in the instrumentation such as frequency and power level non-linearities, gain and phase drifts in the I.F. amplifiers, detectors, attenuator and display circuits.
- g) Quantization errors, such as errors in the analogue to digital conversions, rounding off errors in computation.

h) Connector uncertainty.

i) Noise.

j) Instability i.e. the inability to produce identical results for the same measurement.



The methods of minimizing these errors will now be discussed.

Fig. ( 1.11.1) Incident and reflected waves



Fig. ( 1.11.2) Effective directivity error

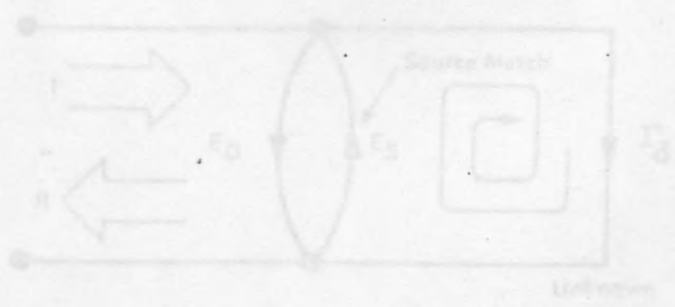


Fig. ( 1.11.3) Effective source match error

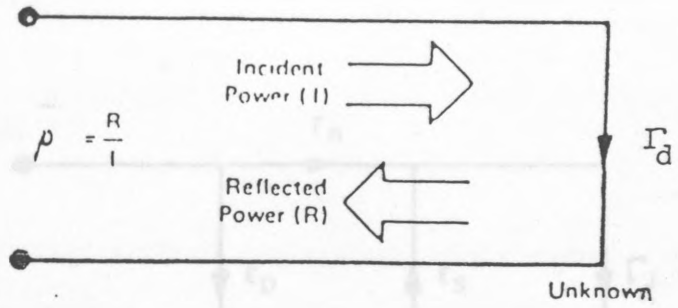


Fig.( 1.11.1) Incident and reflected waves

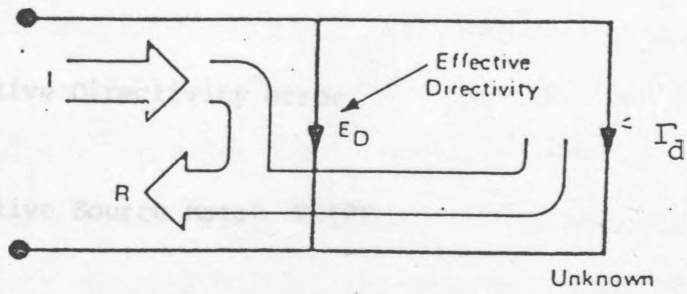


Fig.( 1.11.2) Effective directivity error

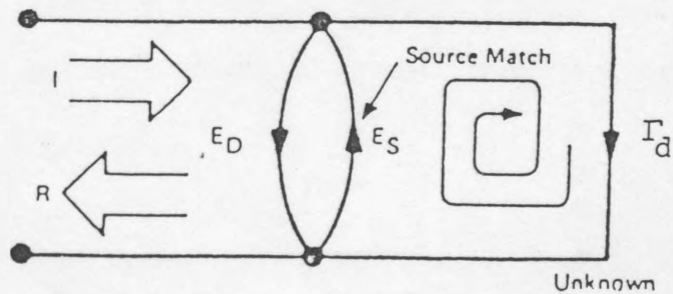


Fig.( 1.11 3) Effective source match error

1.11 Correcting model :-

Let us consider measurement of reflection coefficient (magnitude and phase) of some unknown one-port device. No matter how careful we are, the measured data will differ from the actual. The major sources of error are Effective Directivity error, Effective Source Match and Tracking error which will now be discussed in more detail with reference to Fig (1.11.4) Reflection error model

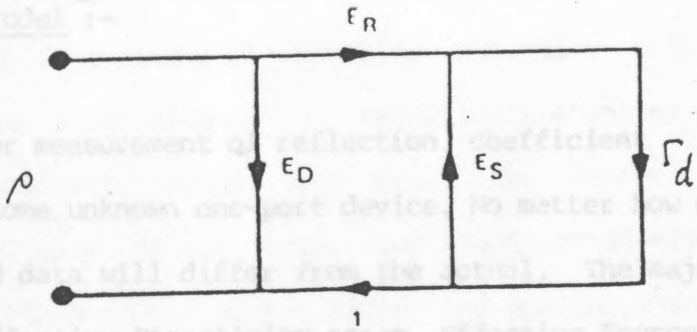


Fig.( 1.11.4) Reflection error model

Reflection coefficient is measured by first separating the incident voltage  $E_D$  : Effective Directivity error (1) then taking the ratio of the two values. Ideally, (2) consists only of the wave reflected  $E_D$  : Effective Source Match error (2). Unfortunately all of the incident wave does not always reach the unknown. Some of (1) may appear  $E_R$  : Tracking error (3) due to leakage through the signal separation device (coupler). Also, some of (2) may be reflected by imperfect adaptors between signal coupler and the measurement plane. The vector sum of the leakage and miscellaneous reflections is the ratio Effective Directivity,  $E_D$ . Unfortunately, our measurement is distorted when the Effective Directivity error signal combines vectorially with the actual reflected signal from the unknown. (Fig (1.11.3)).

Since the measurement system test port is never exactly the characteristic impedance (normally 50 ohms), some of the reflected signal is re-reflected at the test port for other impedance transitions further

### 1.11 Correcting model :-

Let us consider measurement of reflection coefficient (magnitude and phase) of some unknown one-port device. No matter how careful we are, the measured data will differ from the actual. The major sources of error are Effective Directivity error, Effective Source Match and Tracking error which will now be discussed in more detail with reference to Fig (1.11.1).

Reflection Coefficient is measured by first separating the incident voltage wave (I) from the reflected voltage wave (R) then taking the ratio of the two values. Ideally, (R) consists only of the wave reflected by the test device ( $\Gamma_D$ ) Fig (1.11.2). Unfortunately all of the incident wave does not always reach the unknown. Some of (I) may appear at the measurement system input due to leakage through the signal separation device (coupler). Also, some of (I) may be reflected by imperfect adaptors between signal coupler and the measurement plane. The vector sum of the leakage and miscellaneous reflections is the ratio Effective Directivity,  $E_D$ . Understandably, our measurement is distorted when the Effective Directivity error signal combines vectorially with the actual reflected signal from the unknown,  $\Gamma$  Fig (1.11.3).

Since the measurement system test port is never exactly the characteristic impedance (normally 50 ohms), some of the reflected signal is re-reflected at the test port (or other impedance transitions further

down the line) back to unknown, adding to the original incident signal (I). This effect causes the magnitude and phase of the incident wave to vary as a function of  $\Gamma_d$ . Levelling the source to produce constant (I) reduces this error, but since the source cannot be levelled at the test device input, levelling cannot eliminate all power variations. This re-reflection effect and the resultant incident power variation is caused by the Effective Source Match error,  $E_S$  Fig (1.11.3).

Tracking (frequency response) error is caused by variations in magnitude and phase flatness versus frequency between the test and reference signal paths. These are due mainly to imperfectly matched samplers and differences between incident and test couplers. The vector sum of these variations is the Reflection Tracking error,  $E_R$ .

It can be shown that these three errors are mathematically related to the actual,  $\Gamma_d$  and measured,  $\rho$ , data by the following equation:-

$$\rho = E_D + \frac{\Gamma_d (E_R)}{1 - E_S \Gamma_d} \dots\dots (1.11.1)$$

$$= S_{11} + \frac{S_{12} S_{21} \Gamma_d}{1 - S_{22} \Gamma_d} \dots\dots (1.11.2)$$

$$\rho = \frac{-(S_{11}S_{22} - S_{12}S_{21})\Gamma_d + S_{11}}{-S_{22}\Gamma_d + 1} \quad \text{Silva and Nigam} \dots \dots (1.11.3)$$

Where  $S_{11}$  = Directivity Error  
 $S_{22}$  = Source Match Error  
 $S_{12}S_{21}$  = Tracking Error

If we knew the value of these three errors and the measured test device response at each frequency, we could simply solve the above equation for  $\Gamma_d$  to obtain the actual device response. Because each of these errors changes with frequency, it is necessary that their values be known at each test frequency. They are found by measuring (calibrating) the system at the measurement plane using three independent standards whose  $\Gamma_d$  is known at all frequencies.

Many authors have suggested different sets of calibration pieces for determining the constants of equation (1.11.2).

- a) a direct short and two offset shorts.
- b) a direct short, an offset short and an open circuit.
- c) a matched termination, a direct short and a standard mismatch.
- d) a direct short, an offset short and a sliding termination whose reflection coefficient need not be known.
- e) a direct short and two sliding terminations the first with a high reflection coefficient and the second with a low one, neither of which need be known.

Method (a) was proposed by Da Silva and Mcphun (1973) and it is particularly suitable for microstrip work and also for tasks where space restrictions rule out the use of a precision matched sliding termination. Care must be exercised when choosing the offset lengths.

Method (b) was derived by Shurmer (1973) for carrying out measurements on microwave transistors mounted in microstrip. In the open circuit the discontinuity capacitance is then present but this can be taken into account.

Gould and Rhodes (1973) described method (c). Their standard mismatch is a commercially-available item with a V.S.W.R of  $1.5 \pm 5\%$  over the band 1 to 4 GHz. This calibration technique does not require precise measurements of the signal frequency as the three standards are frequency insensitive and they are all used at the same place.

Method (d) and (c) were devised by Kasa (1974) the full theory underlying these two techniques has been published in (1974). The calibration constants are obtained by direct calculation. Kasa neglected the line attenuation in the sliding terminations but Engen (1974) has included it.

Woods (1975) has pointed out that the calibration procedure described by Hand (1970) overlooks the small impedance changes that occur when the reflection/transmission switches are changed over. To avoid this shortcoming, he had suggested that these switches should be

In an S-parameter test set, as opposed to a pure reflectometer, the ports used for transmission and reflection measurements may be interchanged by means of switches. Woods (1975) has pointed out that the calibration procedure described by Hand (1970) overlooks the small impedance changes that occur when the reflection/transmission switches are changed over. To avoid this shortcoming, he had suggested that these switches should be eliminated by using three receiving channels. He has carried out a completely rigorous analysis of this proposed new scheme. By adapting it, the random errors caused by non-repeatability of the switches would be eliminated and two 10dB pads usually included would become unnecessary, resulting in an improved dynamic range. Three single-port standards would be needed to do the calibration.

A large variety of error models and calibration procedures has been proposed to date, all differing in degree of complexity and effectiveness. A common feature of all the proposed error models is the attempt at representing the repeatable system errors by means of the scattering response of a virtual error network, assumed to interface the device under test to an ideal error-free network analyzer system.

The various proposed error models differ, however, in the assumed topological configuration of the specific error network and in the number of independent complex parameters required for their full characterization.

The removal of the computed measurement error from uncalibrated measurements must be performed through a parameter transformation.

## CHAPTER (2)

### PREVIOUS CALIBRATION PROCEDURES:- (reflection-measurement)

#### 2.1 Introduction:-

Ever since the introduction of automated microwave instrumentation for the characterization of microwave components and networks through scattering-parameter measurements, the need has been recognised for automated system-calibration procedures. These were expected to be capable of providing a representation of the repeatable system errors, usable for correcting uncalibrated measurements.

A large variety of error models and calibration procedures has been proposed to date, all differing in degree of complexity and effectiveness. A common feature of all the proposed error models is the attempt at representing the repeatable system errors by means of the scattering response of a virtual error network, assumed to interface the device under test to an ideal error-free network analyzer system.

The various proposed error models differ, however, in the assumed topological configuration of the specific error network and in the number of independent complex parameters required for their full characterization.

The removal of the computed measurement error from uncalibrated measurements must be performed through a parameter transformation,

equivalent to removing the virtual error network from the measurement interface. A common feature of all proposed calibration procedures is the reliance upon simple, idealized standards for which:-

A) All standards must be electrically connectable to physically replace the unknown X at its definition interface, using the same type of electrical connection. This implies that all the used standards be 1-port as the unknown network X to be measured.

B) The reflection coefficients of the standards at the port of connection must be theoretically calculable or otherwise known from primary measurement. This restricts the types of component usable in standards to a few extremely simple circuit elements for which the relevant electrical parameters may be theoretically postulated or determined by primary 1-port measurements. Typical elements are short circuits, open circuits, segments of beadless coaxial air line or waveguide .

C) At least one of the standards must contain a fully known impedance-reference component.

The single port error model, used in reflection measurements, is a virtual error-two-port assumed to be inserted between the single-measurement port of an ideal error-free reflectometer and the unknown reflection to be measured Fig (2.1.1). This model requires the specification of three independent complex parameters at each frequen-

Any three known ports can be used to characterize the error network. Provided that they have different reflection coefficients. For example :-

$\rho/\theta$  and  $\rho/\theta + \pi$  are not different. As will be seen later the reflection coefficients should be well separated on the complex plane. The standards most used in the literature have been, the matched load ( $\rho = 0$ ), the short ( $\rho = -1$ ), the shunted open ( $\rho = 1$ ), and either of the

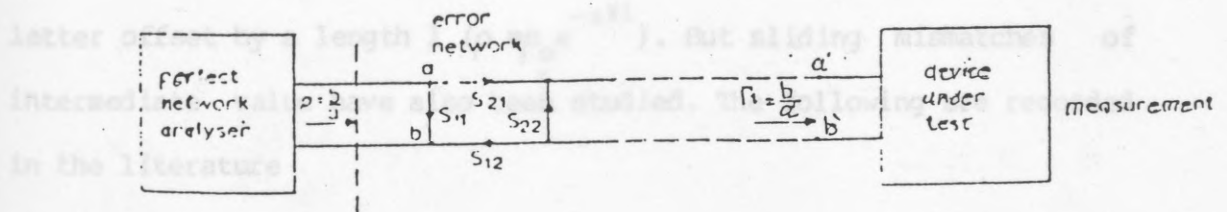


Fig.(2.1.1) Reflection measurement system

Any three known one ports can be used to characterize the error network. Provided that they have different reflection coefficients. For

example :- as proposed by Silva and McPhun 1973. This is the case when correction is made using all short circuit calibration pieces. The

$\rho/\theta$  and  $\rho/(\theta + \pi)$  are not different. As will be seen later the reflection coefficients should be well separated on the complex plane. The standards most used in the literature have been, the matched load ( $\rho = 0$ ), the short ( $\rho = -1$ ), the shrouded open ( $\rho \approx 1$ ), and either of the latter offset by a length  $l$  ( $\rho = \rho_0 e^{-2\gamma l}$ ). But sliding mismatches of intermediate value have also been studied. The following are recorded in the literature

$$\dots\dots(2.2.1)$$

$$P_2 = S_{11} - \frac{S_{21}S_{12}e^{-j2\theta}}{1 + S_{22}e^{-j2\theta}}$$

$$\dots\dots(2.2.2)$$

$$P_1 = S_{11} - \frac{S_{21}S_{12}e^{-j2(\theta+\pi)}}{1 + S_{22}e^{-j2(\theta+\pi)}}$$

$$\dots\dots(2.2.3)$$

Solving Equations (2.2.1) - (2.2.3)

$$S_{11} = \frac{P_1 P_2 (e^{-j2\theta} - 1) - P_2 P_3 (e^{+j2\theta} - 1) - P_1 P_3 (e^{-j2\theta} - e^{+j2\theta})}{e^{-j2\theta} - 1 (P_2 - P_3) - (e^{+j2\theta} - 1) (P_3 - P_1)}$$

$$\dots\dots(2.2.4)$$

2.2 Set (a) [a direct short and two offset shorts]:- ..... (2.2.5)

This was proposed by Silva and McPhun 1973. This is the case when correction is made using all short circuit calibration pieces. The offset lengths of the standard are assumed to be lossless and the phase change between terminations are  $\theta$  and  $\theta'$  respectively. The test device is removed, and the error network is terminated in turn by the three-short-circuits shown in Figure (2.2.1). From the basic theory,

$$\rho_1 = S_{11} - \frac{S_{21}S_{12}}{1+S_{22}} \quad \dots\dots (2.2.1)$$

$$\rho_2 = S_{11} - \frac{S_{21}S_{12}e^{-j2\theta}}{1+S_{22}e^{-j2\theta}} \quad \dots\dots (2.2.2)$$

$$\rho_3 = S_{11} - \frac{S_{21}S_{12}e^{-j2(\theta+\theta')}}{1+S_{22}e^{-j2(\theta+\theta')}} \quad \dots\dots (2.2.3)$$

Solving Equations (2.2.1) - (2.2.3)

$$S_{11} = \frac{\rho_1\rho_2(e^{-j2\theta}-1) - \rho_2\rho_3(e^{+j2\theta}-1) - \rho_1\rho_3(e^{-j2\theta} - e^{+j2\theta})}{(e^{-j2\theta}-1)(\rho_2 - \rho_3) - (e^{+j2\theta}-1)(\rho_2 - \rho_1)} \quad \dots\dots (2.2.4)$$

$$S_{22} = \frac{e^{j2\theta}(\rho_2 - S_{11}) + S_{11} - \rho_1}{(\rho_1 - \rho_2)} \dots\dots (2.2.5)$$

$$S_{21}S_{12} = (S_{11} - \rho_1)(1 + S_{22}) \dots\dots (2.2.6)$$

For the device under test, with a reflection coefficient  $\Gamma_L$

$$\rho = S_{11} + \frac{S_{21}S_{12}\Gamma_L}{\Gamma_L - S_{22}}$$

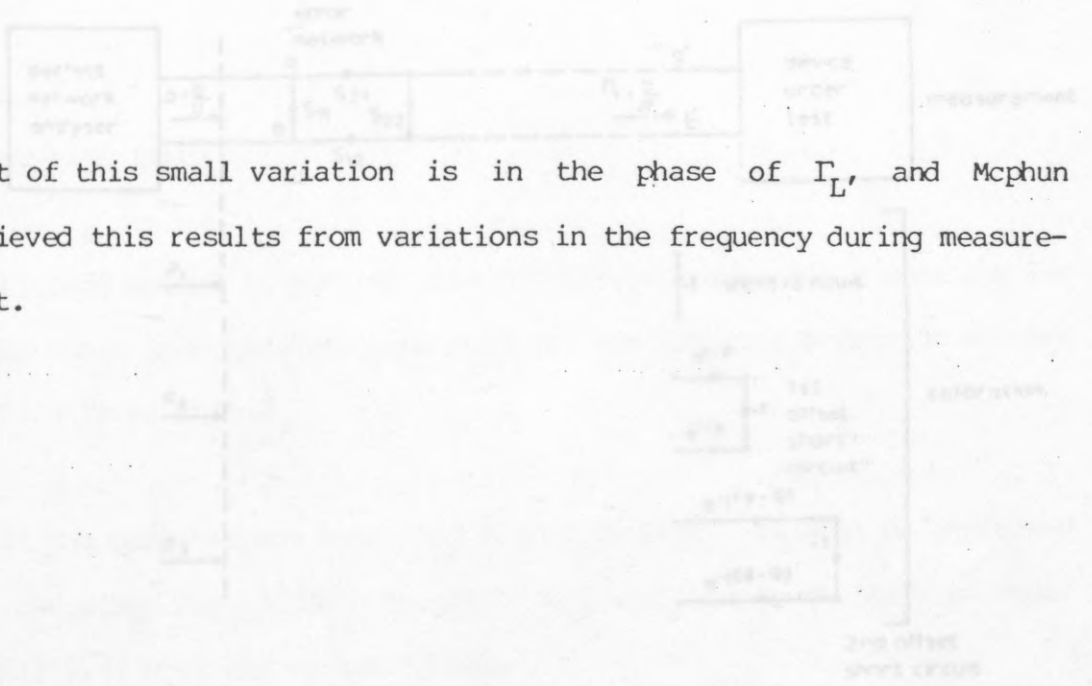
.....(2.2.7)

from which

$$\Gamma_L = \frac{\rho - S_{11}}{S_{22} \rho + S_{21}S_{12} - S_{11}S_{22}} \dots\dots (2.2.8)$$

Thus, with the substitution of  $S_{11}$ ,  $S_{22}$  and  $S_{12}S_{21}$  from Equations (2.2.4)-(2.2.6) into Equations (2.2.8), the value of  $\Gamma_L$  can be obtained.

The measurements shown in Table (2.2.1) were made manually, whereby the unknown (a coaxial matched load with APC 7 Connector was measured through three different mismatches. In each case, the calibration was carried out on the "unknown" side of the mismatch. When the results are compared on Smith chart, it is seen that the maximum variation in  $\Gamma_L$  can be contained within a circle corresponding to  $|\Gamma| = 0.0035$ .



Most of this small variation is in the phase of  $\Gamma_L$ , and McPhun believed this results from variations in the frequency during measurement.

Fig.(2.2.1) Signal-flow graphs of system under calibration

Table(2.2.1) The unknown matched load with an APC-7 connector was measured through three different mismatches.

Conditions of measurements	Measured reflection coefficient			Frequency	Calculated errors			Device under test	
	$\rho_1$	$\rho_2$	$\rho_3$		$S_{11}$	$S_{21}$	$S_{22}$	Measured $\rho$	Corrected
Through instrument*	1	1	1	1.01143	0.021	0.998	0.012	0.003	0.003
Through instrument* and out of 0.2dB mismatch	1	0.98	1	1.01131	0.020	0.998	0.0114	0.006	0.003
Through instrument* and out of 0.2dB mismatch	1	0.97	1	1.01128	0.019	0.997	0.0107	0.005	0.002

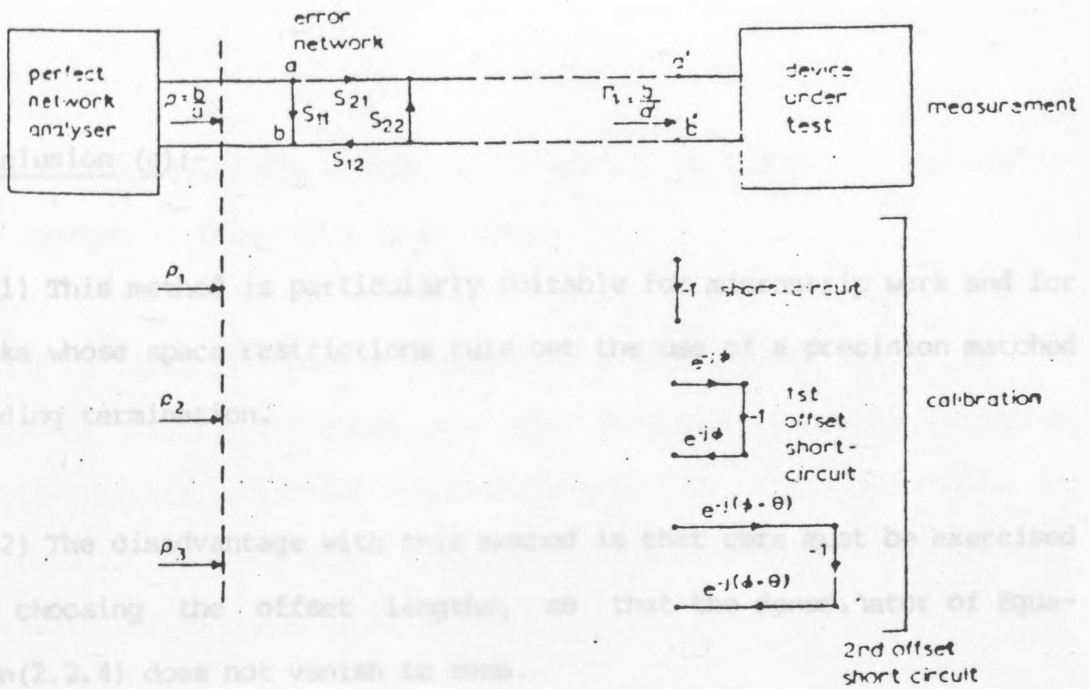


Fig.(2.2.1) Signal-flow graphs of system under calibration

Table(2.2.1) The unknown matched load with an APC-7 connector was measured through three different mismatches.

Conditions of measurements	Measured reflection coefficient			Frequency GHz	Calculated errors			Device under test	
	$\rho_1$	$\rho_2$	$\rho_3$		$S_{11}$	$S_{21} S_{12}$	$S_{22}$	Measured $\rho$	Corrected
Through instrument*	1 $\angle -180$	1 $\angle -70$	1 $\angle 43$	1.01143	0.022 $\angle -18.24$	0.999 $\angle -0.77$	0.022 $\angle -162.5$	0.025 $\angle -68$	0.0199 $\angle -124$
Through instrument* and pair of o.s.m. connectors	1 $\angle -180$	0.98 $\angle -69$	1 $\angle 48$	1.01215	0.020 $\angle 89.7$	0.994 $\angle 1.5$	0.00918 $\angle 132$	0.006 $\angle -178$	0.021 $\angle -108$
Through instrument* and pair of GR 874 connectors	1 $\angle -180$	0.98 $\angle -68$	1 $\angle 47$	1.01220	0.0187 $\angle 44.14$	0.994 $\angle 1.47$	0.0187 $\angle 137.3$	0.005 $\angle -92$	0.022 $\angle -128$

Conclusion (a):-

(1) This method is particularly suitable for microstrip work and for tasks whose space restrictions rule out the use of a precision matched sliding termination.

(2) The disadvantage with this method is that care must be exercised in choosing the offset lengths, so that the denominator of Equation(2.2.4) does not vanish to zero.

(3) At a particular frequency of measurement the offset lengths must not be chosen so that the calibration reflection coefficients measured are  $1/\theta$ ,  $1/(\theta+2\pi)$ ,  $1/(\theta+2n\pi)$  etc. where n is any integer. For, if this was the case, then the error network cannot be solved.

(4) The offset lengths should be chosen to produce large calibration reflection coefficient angle differences to minimise the inaccuracies involved in specifying offset lengths. For example if the ability to measure a mechanical length is limited to  $\pm 0.01\text{mm}$ , then choosing an offset length of  $0.1\text{mm}$  is obviously unwise for a  $\pm 10\%$  uncertainty would be involved in specifying the offset length.

(5) Unnecessary mechanical difficulties would arise in maintaining the concentricity of the inner conductor if the offset lengths were made too long. Support by bead etc. is not favoured as discontinuities albeit small, will be produced. Furthermore, errors inac-

curately specifying the electrical length of the offset , especially with changes in frequency, could result.

(6) Da Silva 1978 used a single set of measurement data, in the frequency range 4-6 GHz but calculated the correction using erroneous lengths for his correcting standards Fig (2.2.2). From the results it is readily deduced that the two offset lengths must be carefully specified for accurate correction.

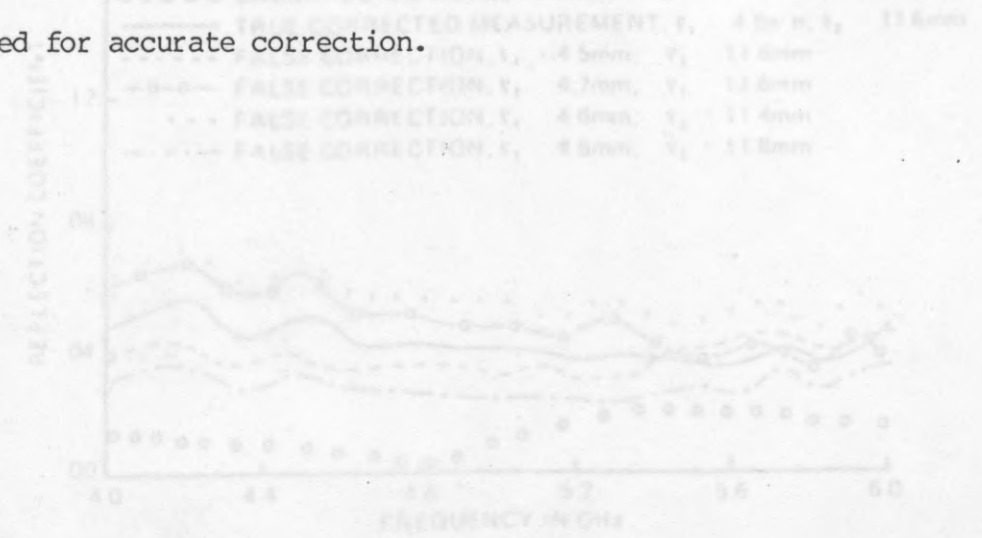


Fig. (2.2.2) Computer correction using three Short circuits

2.3 Set (b) Is direct short, an offset short and open circuit):-

This is the case when correction is carried out using calibration standards consisting of a short circuit, an offset short circuit, and an open circuit (lossless). If all the line lengths are considered to be lossless

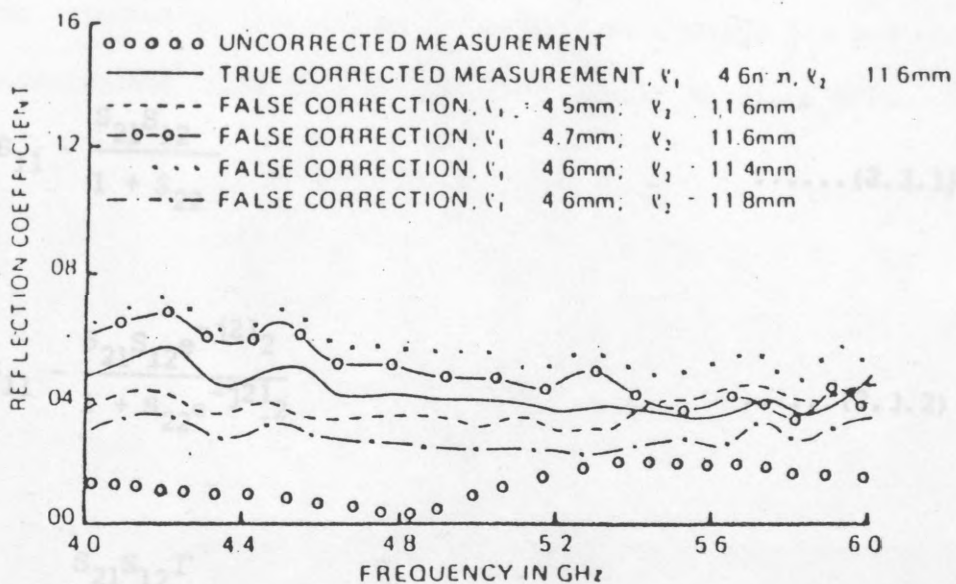


Fig.(2.2.2) Computer correction using Three Short circuits

From Equations (2.3.1) - (2.3.3)

$$S_{11} = \frac{P_1 P_2 (1 - e^{-2\gamma \ell_1}) - P_3 P_3 (1 - e^{-2\gamma \ell_2}) - P_1 P_2 (1 - e^{-2\gamma \ell_1})}{P_1 e^{-2\gamma \ell_1} - P_2 (1 - e^{-2\gamma \ell_2}) - P_1 (1 - e^{-2\gamma \ell_1})}$$

.....(2.3.4)

2.3 Set (b) [a direct short, an offset short and open circuit]:-

This is the case when correction is carried out using calibration standards consisting of a short circuit, an offset short circuit, and an open circuit  $\Gamma$ (lossless). If all the line lengths are considered to be lossless

$$\rho_1 = S_{11} - \frac{S_{21}S_{12}}{1 + S_{22}} \quad \dots\dots(2.3.1)$$

$$\rho_2 = S_{11} - \frac{S_{21}S_{12}e^{-j2l_2}}{1 + S_{22}e^{-j2l_2}} \quad \dots\dots(2.3.2)$$

$$\rho_3 = S_{11} + \frac{S_{21}S_{12}\Gamma}{1 - S_{22}\Gamma} \quad \dots\dots(2.3.3)$$

From Equations (2.3.1) - (2.3.3):

$$S_{11} = \frac{\rho_1\rho_2(1 - \Gamma e^{-2jl_2}) - \rho_2\rho_3(\Gamma + e^{-2jl_2}) + \rho_3\rho_1(\Gamma e^{-2jl_2} + e^{-2jl_2})}{\rho_1(e^{-2jl_2} + \Gamma) - \rho_2(\Gamma e^{-2jl_2} + e^{-2jl_2}) + \rho_3\Gamma(e^{-2jl_2} - 1)} \quad \dots\dots(2.3.4)$$

$$S_{22} = \frac{S_{11} - \rho_1 + e^{+2j\beta}(\rho_2 - S_{11})}{\rho_1 - \rho_2} \quad \dots\dots(2.3.5)$$

$$S_{12}S_{21} = (S_{11} - \rho_1)(1 + S_{22}) \quad \dots\dots(2.3.6)$$

In practice it is difficult to produce an open circuit due to the stray capacitance and resistance across the terminals. Various methods for calculating the capacitance are known (more discussion about it in Chapter 3). An iterative method based in measurement is given by Da Silva 1978 in his thesis (3).

This method was devised by Shurmer 1973 for carrying out measurements on microwave transistors mounted in microstrip jig and practical measurements using this system were made by Da Silva 1978.

A set of measurements of a load was the results of corrections using the above method are shown in fig (2.3.1). It is readily deduced that the corrected results depend on the accuracy of the value taken for the stray capacitance of the final termination.

If a satisfactory calculation of the open circuit capacitance can be made, then this method is probably easier to use than that using short circuits in measurements in a two-port line.

Conclusion (b):-

In practice it is difficult to produce an open circuit due to the stray capacitance and resistance across the terminals. Various methods for calculating the capacitance are known (more discussion about it in Chapter (3) ). An accurate method based in measurement is given by Da Silva 1978 in his Appendix (3).

A set of measurements of a load and the results of corrections using the above method are shown in Fig (2.3.1). It is readily deduced that the corrected results depend on the accuracy of the value taken for the stray capacitance of the final termination.

If a satisfactory calculation of the open circuit capacitance can be made, then this method is physically easier to use than that using short circuits in measurements in microstrip line.

Fig.(2.3.1) Measurement correction using Short, Offset Short, and Open Circuits

2.4 Set (c) (a matched termination, a direct short and a standard mismatch):

This method described by Gould and Rhodes 1971. The calibration is performed using a 50 ohm termination, a standard mismatch and a short circuit.

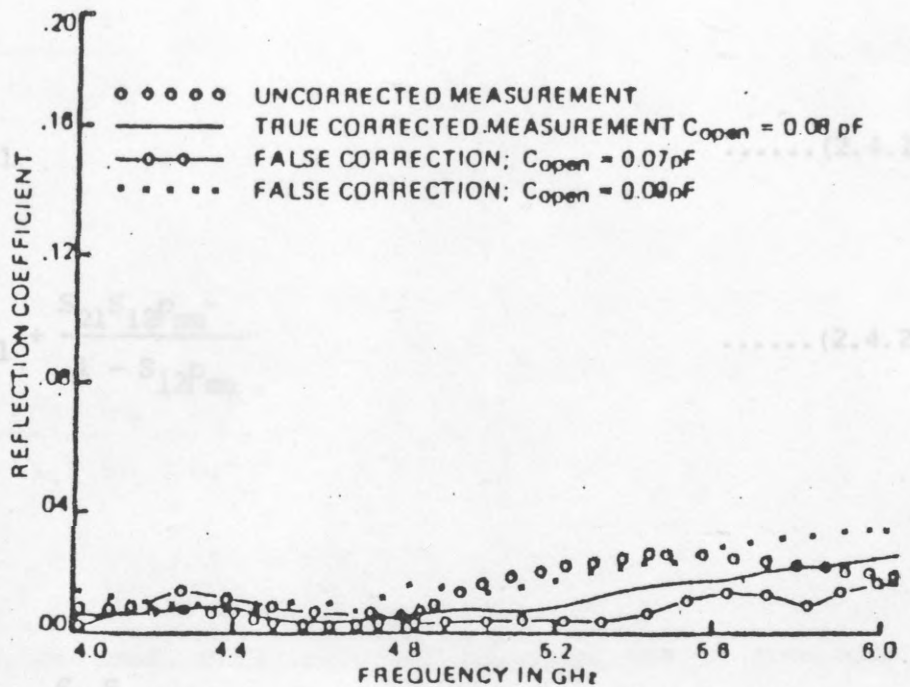


Fig.(2.3.1) Measurement correction using Short, Offset Short, and Open Circuits

where  $\rho_{em}$  is the reflection coefficient of the standard mismatch at the same reference plane as the short circuit and 50 ohm terminations. If  $\rho$  is the measured reflection coefficient of the device under test, the correction reflection coefficient  $\Gamma_p$  is given by,

2.4 Set (c) [a matched termination, a direct short and a standard mismatch]:-

This method described by Gould and Rhodes 1973. The calibration is performed using a 50 ohm termination, a standard mismatch and a short circuit.

$$\rho_1 = S_{11} \quad \dots\dots (2.4.1)$$

$$\rho_2 = S_{11} + \frac{S_{21}S_{12}\rho_{sm}}{1 - S_{12}\rho_{sm}} \quad \dots\dots (2.4.2)$$

and

$$\rho_s = S_{11} - \frac{S_{21}S_{12}}{1 + S_{22}} \quad \dots\dots (2.4.3)$$

where  $\rho_{sm}$  is the reflection coefficient of the standard mismatch at the same reference plane as the short circuit and 50 ohm terminations. If  $\rho$  is the measured reflection coefficient of the device under test, the correction reflection coefficient  $\Gamma_L$  is given by,

$$\rho = S_{11} + \frac{S_{21}S_{12}\Gamma_L}{1 - S_{22}\Gamma_L} \quad \dots\dots(2.4.4)$$

In methods a and b the phase of the standard is directly proportional to frequency. Sub.  $S_{11}$ ,  $S_{22}$  and  $S_{21}S_{12}$  Equation (2.4.4) becomes: frequency to a greater accuracy.

$$\Gamma_L = \frac{1}{K(1 + 1/\rho_{sm}) - 1} \quad \dots\dots(2.4.5)$$

where  $K$  is a constant which changes only slowly with frequency. This calibration technique does not require precise measurements of the signal frequency as the three standards are frequency insensitive and they are all used at the same plane.

$$K = \frac{(\rho - \rho_3)(\rho_1 - \rho_2)}{(\rho - \rho_1)(\rho_3 - \rho_2)}$$

The device used as a standard mismatch was a commercially available item with a VSWR of  $2.5 \pm 5\%$  over the band 1 to 4 GHz. The value of  $\rho_{sm}$  used in the calculation can either be obtained from precision slotted-line measurements, or by using the network analyzer and measuring offset short circuits after the three calibrations have been performed, and finding an optimum value for  $\rho_{sm}$  for the magnitude of reflection coefficients of the short circuits to be unity.

Conclusion (c):-

In methods a and b the phase of the standard is directly proportional to frequency and hence calibration requires measurements of frequency to a greater accuracy.

Since  $\rho_{sm}$  changes only slowly with frequency, Once it has been calibrated over its operative bandwidth swept-frequency measurements can be simply performed using relatively inaccurate frequency measurement. This calibration technique does not require precise measurements of the signal frequency as the three standards are frequency insensitive and they are all used at the same plane.

The same relationship exists between the constant  $W$  of a linear complex reflectometer network analyzer and the reflection coefficient,  $\Gamma$ , to be measured. In this case the parameters  $a, b$  and  $c$  have to be determined by a calibration procedure.

2.3.1 set (d) [ calibration with two standards and one sliding termination ]:-

Russ describes procedures that require one standard and one sliding termination or one standard and two different sliding terminations to determine  $a, b$  and  $c$ . The technique is applicable for two-port measurements and especially for automatic network analyzer calibration.

## 2.5 calibration using sliding termination:-

Two methods were devised by Kasa (1974), Fitzpatrick (1978) and Engen (1974) using sliding termination.

A linear two-port transforms the load reflection coefficient  $\Gamma$  into the input reflection coefficient  $W$ . The connection between  $\Gamma$  and  $W$  is generally described by the equation:

$$W = \frac{a\Gamma + b}{c\Gamma + 1}$$

where  $a$ ,  $b$  and  $c$  are complex parameters.

The same relationship exists between the readout  $W$  of a linear complex reflectometer network analyzer and the reflection coefficient,  $\Gamma$ , to be measured. In this case the parameters  $a$ ,  $b$  and  $c$  have to be determined by a calibration procedure.

### 2.5.1 set (d) [ calibration with two standards and one sliding termination ]:-

Kasa describes procedures that require two standards and one sliding termination or one standard and two different sliding terminations to determine  $a$ ,  $b$  and  $c$ . The evaluation is applicable for two-port measurements and especially for automatic network analyzer calibration.

The sliding termination can be described by:

$$\Gamma = re^{j(\theta_0 - \theta)}$$

where  $r$ ,  $\theta$  and  $\theta_0$  are respectively the magnitude, the initial phase angle and the varying phase angle. Neither  $r$  nor  $\theta_0$  need to be known, the only requirement is that  $r$  and  $\theta_0$  be constant.

Two standard terminations  $\Gamma_1$  and  $\Gamma_2$  are used, in addition to the sliding termination  $\Gamma_s$ . The corresponding system response is denoted by  $W_1$ ,  $W_2$  and  $W_{si}$  where  $i=1, \dots, N$  and  $N$  is the number of sliding termination positions  $N \geq 3$ , for which the response is measured. As it is well known, the points  $W_{si}$  lie on a circle on the complex plane which will be denoted by  $W_s$ . The circle  $W_s$  is characterized by the center  $W_0$  and the radius  $R$  Fig(2.5.1). These parameters can be determined from the measurement points by a circle fitting procedure.

From the transform of unknown standards we obtain:

$$W_1 \Gamma_1 C + W_1 = a \Gamma_1 + b$$

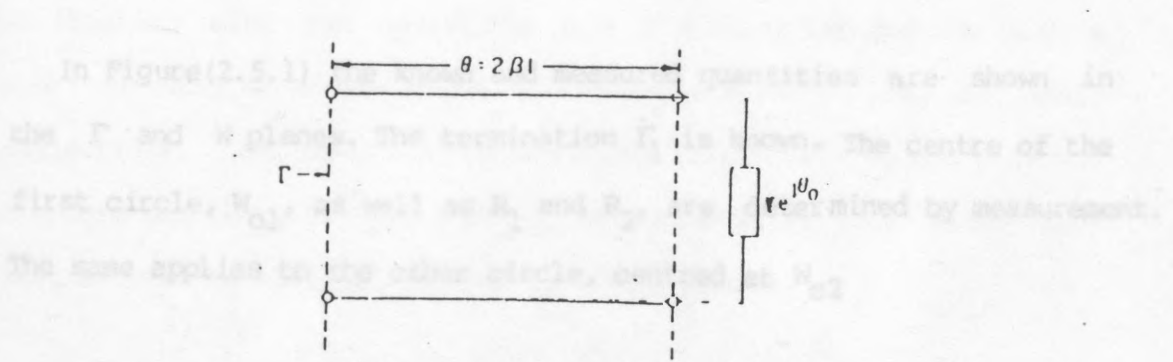
$$W_2 \Gamma_2 C + W_2 = a \Gamma_2 + b$$

A third equation can be obtained by exploiting the circles in the  $\Gamma$  and  $W$  planes:

$$(b - W_0)^* = \frac{CR^2}{a - CW_0}$$

Where the asterisk denotes the complex conjugate. These equations can be transformed to a second-degree equation for  $b$ , which can be solved either by iteration or by explicit quadrature. Once  $b$  is known,  $a$  and  $c$  can be determined from a linear equation system.

2.5.2 set (e) ( calibration with one standard and two different sliding termination ):-



Schematic of sliding termination.

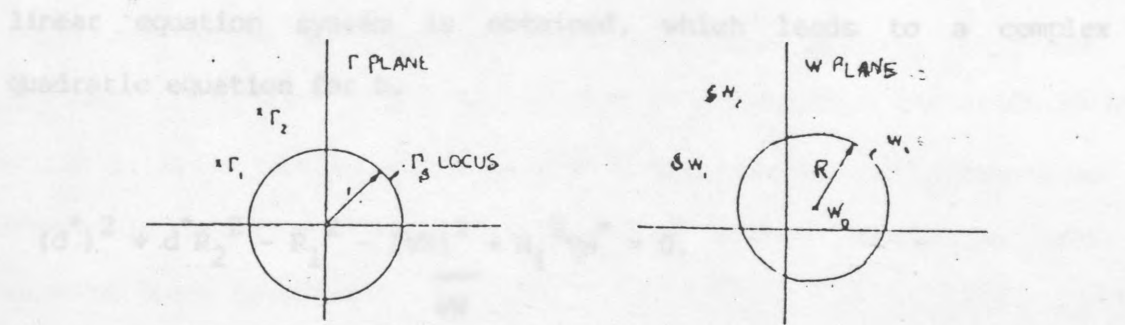


Fig.(2.5.1) Quantities in  $\Gamma$  and  $w$  planes for measurement with Two standards and One sliding termination

Once  $\theta$  is known,  $a$  and  $c$  can be evaluated from a linear equation system.

Conclusion (d and e):-

2.5.2 set (e) [ calibration with one standard and two different sliding termination ]:-

(1) The first procedure provides exact formulas for the usual calibration with two standards and a sliding termination (e.g. a

In Figure(2.5.1) the known and measured quantities are shown in the  $\Gamma$  and  $W$  planes. The termination  $\Gamma_1$  is known. The centre of the first circle,  $W_{01}$ , as well as  $R_1$  and  $R_2$ , are determined by measurement. The same applies to the other circle, centred at  $W_{02}$

From the transformation of the standard and the circles a non-linear equation system is obtained, which leads to a complex quadratic equation for  $b$ .

$$(d^*)^2 + d^* R_2^2 - R_1^2 - \frac{\Gamma \nabla W_1^2}{\nabla W} + R_1^2 \nabla W^* = 0,$$

(3) Kasa neglected the line extension to the sliding termination

where  $d = b - W_{01}$  and  $\nabla W = W_{02} - W_{01}$ .

Once  $b$  is known,  $a$  and  $c$  can be evaluated from a linear equation system.

Conclusion (d and e):-

(1) The first procedure provides exact formulae for the usual calibration with two standards and a sliding termination (e.g. a short circuit, an offset short circuit and a sliding load of small reflection). The second procedure makes it possible to use only one standard and two different sliding terminations. (e.g. a short circuit as well as sliding load and a sliding short).

(2) Da Silva 1978 had a set of measurements using this technique which are shown in Figure (2.5.2). From these results, it is seen that even if the line length is in error by  $\pm 2\%$ , this variation is not critical. It is generally agreed that if the offset lengths cannot be accurately specified, then the sliding load method should be used whenever space permits.

(3) Kasa neglected the line attenuation in the sliding termination but Engen 1974 has included it.

Fig. (2.5.2) Measurements using sliding load

## 2.6 Correction method using the invariance of the cross-ratio:-

In correction systems involving bilinear transformation, the calculation of the corrected results is often tedious and especially if the complex constants of the bilinear transformation are to be derived. Neatly (1973) has proposed a simpler mathematical approach by utilising the invariance properties of the cross-ratios of the bilinear transformation.

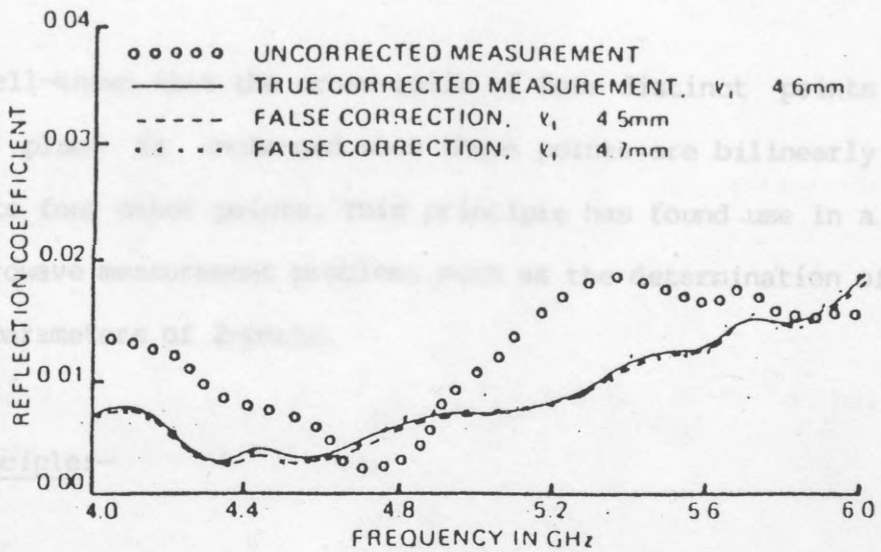


Fig.(2.5.2) Measurement correction using sliding load

Consider the linear transformation:-

$$\Gamma = \frac{A\Gamma' + B}{C\Gamma' + D} \quad \dots (2.5.1)$$

## 2.6 Correction method using the invariance of the cross-ratio:-

In correction systems involving bilinear transformation, the calculation of the corrected results is often tedious and especially if the complex constants of the bilinear transformation are to be derived. Beatty (1972) has proposed a simpler mathematical approach by utilising the invariance properties of the cross-ratios of the bilinear transformation.

It is well-known that the cross-ratio of four distinct points in a complex plane is unchanged when these points are bilinearly transformed to four other points. This principle has found use in a number of microwave measurement problems such as the determination of scattering parameters of 2-ports.

The principle:-

The principle of invariance of the cross ratio is briefly illustrated as follows:-

Consider the linear transformation:-

$$p = \frac{A\Gamma + B}{C\Gamma + D} \quad \dots\dots (2.6.1)$$

where  $\rho$  and  $\Gamma$  are complex variables, and A, B, C and D are complex coefficients.

As shown in Figure (2.6.1) four points in the  $\Gamma$ -plane are transformed by equation (2.6.1) into four other points in the  $\rho$ -plane.

According to the principle of invariance, the cross-ratio of the  $\Gamma$ 's is equal to the cross-ratio of the  $\rho$ 's or

$$\frac{(\rho_1 - \rho_2)(\rho_3 - \rho_4)}{(\rho_2 - \rho_3)(\rho_4 - \rho_1)} = \frac{(\Gamma_1 - \Gamma_2)(\Gamma_3 - \Gamma_4)}{(\Gamma_2 - \Gamma_3)(\Gamma_4 - \Gamma_1)} \quad \dots\dots\dots (2.6.2)$$

In Fig (2.6.1) each point,  $\rho$  is related to  $\Gamma$  by a bilinear transformation of the form (2.6.1).

For the 2-port network the relation between  $\rho$  and  $\Gamma$  and the scattering parameter:-

$$\rho = \frac{-(S_{11}S_{22} - S_{12}S_{21})\Gamma + S_{11}}{-S_{22}\Gamma + 1} \quad \dots\dots\dots (2.6.3)$$

or

$$\rho = S_{11} + \frac{S_{12}S_{21}\Gamma}{1 - S_{22}\Gamma} \quad \dots\dots\dots (2.6.4)$$

which is the same as equation (2.6.1)

Hence:-

$$\begin{aligned} \rho_1 - \rho_2 &= S_{11} + \frac{S_{12}S_{21}\Gamma_1}{1 - S_{22}\Gamma_1} - S_{11} - \frac{S_{12}S_{21}\Gamma_2}{1 - S_{22}\Gamma_2} \\ &= \frac{S_{12}S_{21}[\Gamma_1(1 - S_{22}\Gamma_2) - \Gamma_2(1 - S_{22}\Gamma_1)]}{(1 - S_{22}\Gamma_1)(1 - S_{22}\Gamma_2)} \\ \rho_1 - \rho_2 &= \frac{S_{12}S_{21}(\Gamma_1 - \Gamma_2)}{(1 - S_{22}\Gamma_1)(1 - S_{22}\Gamma_2)} \dots\dots (2.6.4) \end{aligned}$$

Similarly it can show that:-

$$\rho_3 - \rho_4 = \frac{S_{12}S_{21}(\Gamma_3 - \Gamma_4)}{(1 - S_{22}\Gamma_3)(1 - S_{22}\Gamma_4)} \dots\dots (2.6.5)$$

Thus:-

$$\begin{aligned} (\rho_1 - \rho_2)(\rho_3 - \rho_4) &= \frac{S_{12}^2 S_{21}^2 (\Gamma_1 - \Gamma_2)(\Gamma_3 - \Gamma_4)}{(1 - S_{22}\Gamma_1)(1 - S_{22}\Gamma_2)(1 - S_{22}\Gamma_3)(1 - S_{22}\Gamma_4)} \\ \frac{(\rho_1 - \rho_2)(\rho_3 - \rho_4)}{(\rho_2 - \rho_3)(\rho_4 - \rho_1)} &= \frac{(\Gamma_1 - \Gamma_2)(\Gamma_3 - \Gamma_4)}{(\Gamma_2 - \Gamma_3)(\Gamma_4 - \Gamma_1)} \dots\dots (2.6.6) \end{aligned}$$

which proves that from the measured  $\rho$  the corrected value  $\Gamma$  can be obtained without actually calculating the error model parameters.

The method has the apparent advantage of computing out the correction directly from the measurements of the standards without the necessity of calculating error parameters. However, if more than one unknown has to be measured, the method of calculating error parameters enables these to be derived once only and then the correction for subsequent measurements of unknowns is relatively short. also the error parameters separate out the function of each error and associate it with directivity, source match etc.

Fig. (2.6.1) The circle in the  $\Gamma$ -plane transformed into four other points in the  $\rho$ -plane

2.7 Previous work on the uncertainty:-

Some of the authors referred in section 2.2 to 2.5 above have also discussed the resulting uncertainties in a computer correction measurement.

2.7.1 Adam 1966

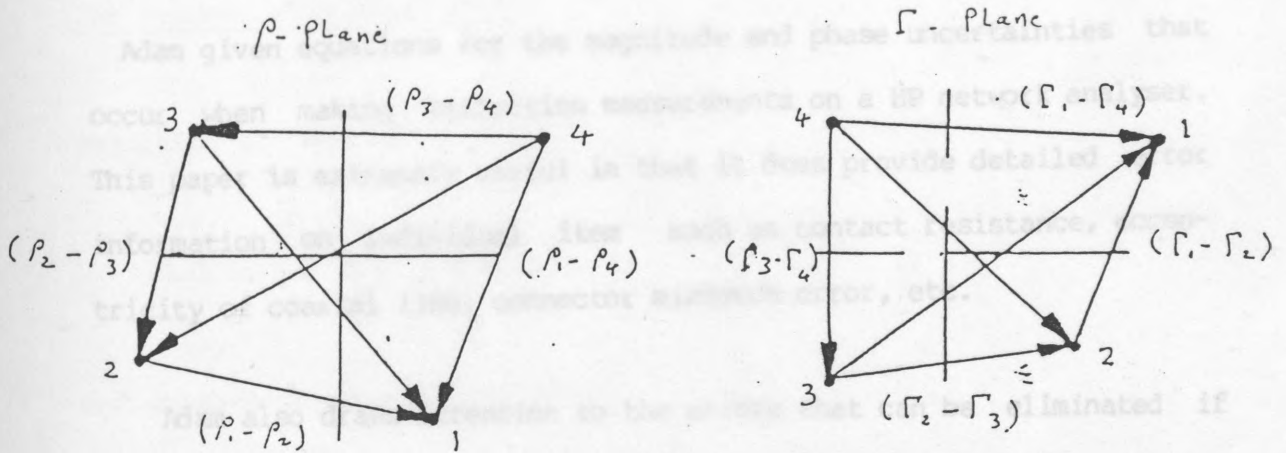


Fig.(2.6.1) Four points in the  $\Gamma$ -plane transformed into four other points in the  $\rho$ -plane

For reflection type measurements, the calculated system uncertainty to be:-

For systems without phase lock:-

magnitude of uncertainty was:

$$+(0.003 \pm 0.015\rho \pm 0.01\rho^2)$$

## 2.7 Previous work on the uncertainty:-

Some of the authors referred in section 2.2 to 2.5 above have also discussed the resulting uncertainties in a computer correction measurement.

### 2.7.1 Adam 1968

Adam given equations for the magnitude and phase uncertainties that occur when making reflection measurements on a HP network analyser. This paper is extremely useful in that it does provide detailed error information on individual item such as contact resistance, eccentricity of coaxial line, connector mismatch error, etc.

Adam also draws attention to the errors that can be eliminated if it is ensured that in a repeat of any measurement the harmonic converter always uses the same harmonic number. This could be ensured by phase-locking or in the latest analyses it is ensured by using synthesized signal generation.

For reflection type measurements, Adams claims the calculated system uncertainty to be:-

For system without phase lock:-

magnitude of uncertainty was:

$$+(0.003 \pm 0.015\rho \pm 0.01\rho^2)$$

phase-angle uncertainty was:

$$+[0.5 \pm \tan^{-1} 0.003/\rho \pm 4 \tan^{-1} (0.015\rho)]$$

For systems with phase lock:-

magnitude of uncertainty was:

$$+(0.0015 \pm 0.005\rho \pm 0.003\rho^2)$$

and phase-angle uncertainty was:

$$+[0.25^\circ \pm \tan^{-1} 0.0015/\rho \pm 4 \tan^{-1} (0.005\rho)]$$

where  $\rho$  is the magnitude of the reflection coefficient  $\Gamma$  and  $S_{11} \ll \rho$  in the equations relating to angle error.

Adam does not give the information and neither does he indicate clearly as to how those figures were deduced or obtained.

The equations above have been calculated over the frequency range .1 to 2GHz and the results are shown in Fig (2.7.1)

Fig. (2.7.1) Magnitude uncertainty.

2.7.2 (and 1970)

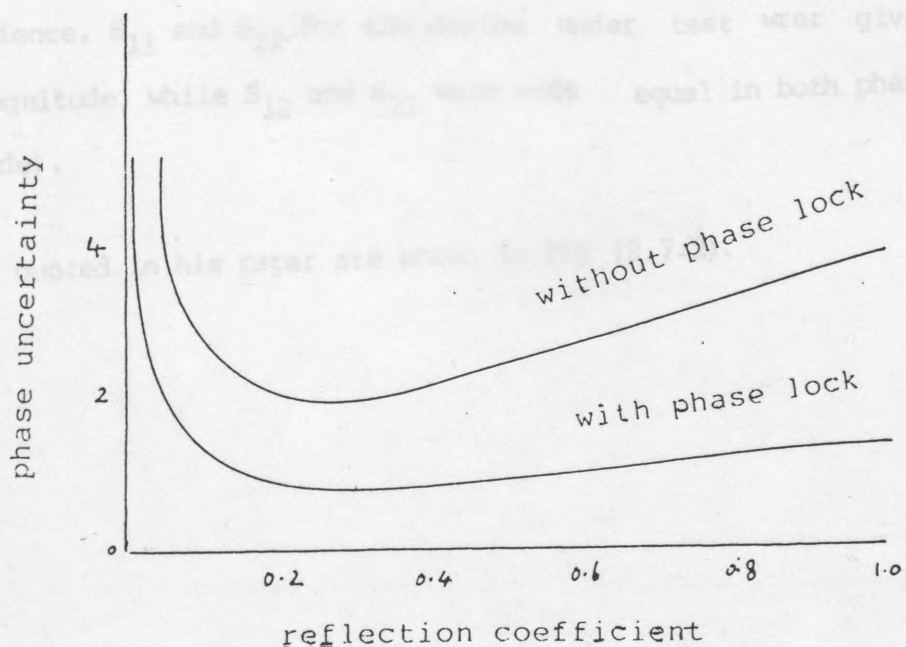
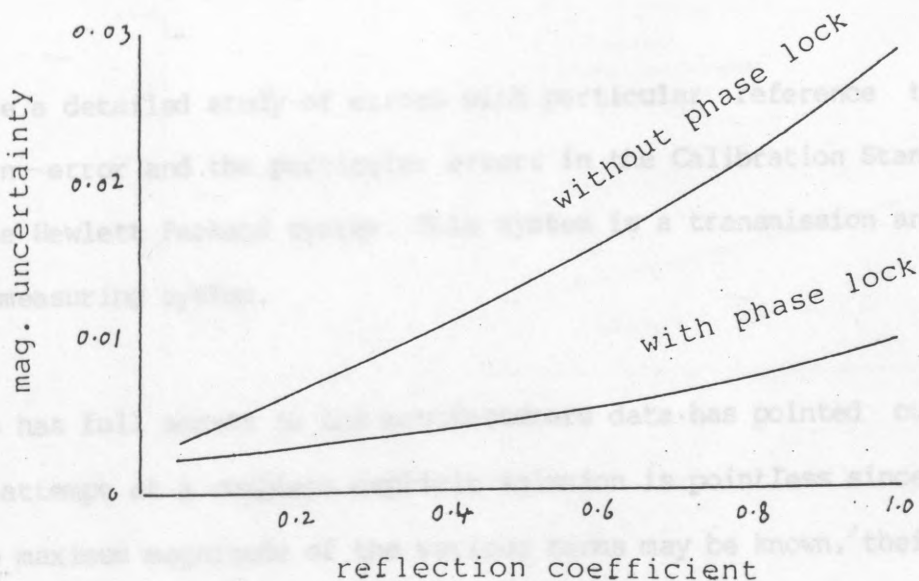


Fig. (2.7.1) Adam uncertainty.

### 2.7.2 Hand 1970

Hand made a detailed study of errors with particular reference to noise, gain error and the particular errors in the Calibration Standards on the Hewlett Packard system. This system is a transmission and reflection measuring system.

Hand who has full access to the manufacturers data has pointed out that any attempt at a complete explicit solution is pointless since, whereas the maximum magnitude of the various terms may be known, their phases are in general quite unpredictable. Hand also tried combining the random-phase errors with the rest of the sum of the squares (RMS) values of amplitudes but finally decided on a statistical method of analysis.

(For convenience,  $S_{11}$  and  $S_{22}$  for the device under test were given the same magnitude, while  $S_{12}$  and  $S_{21}$  were made equal in both phase and magnitude).

The results quoted in his paper are shown in Fig (2.7.2).

2.7.3 Ridella 1973 and 1978

Be discussed some of the errors of computerized network analyzers, in particular, the instrumentation errors when measuring reflection-coefficients.

His system can be used by the user to flow each Fig (5.1.3)

$\Gamma$  represents the reflection coefficient of the components of calibration

$S_{11}, S_{22}, S_{12}, S_{21}$  represent the error correction parameters of the system which can be obtained at each frequency during calibration.

$N + E_p$  represents the total equivalent noise of the system which affects the repeatability of the measurement. This term is a function of connector, switch performances, frequency stability, instrumentation noise, drift deviation, quantization, computational accuracy, quantization error;

The calibration procedure consists in measuring standard components from which the error matrix parameters are determined, whose accuracy

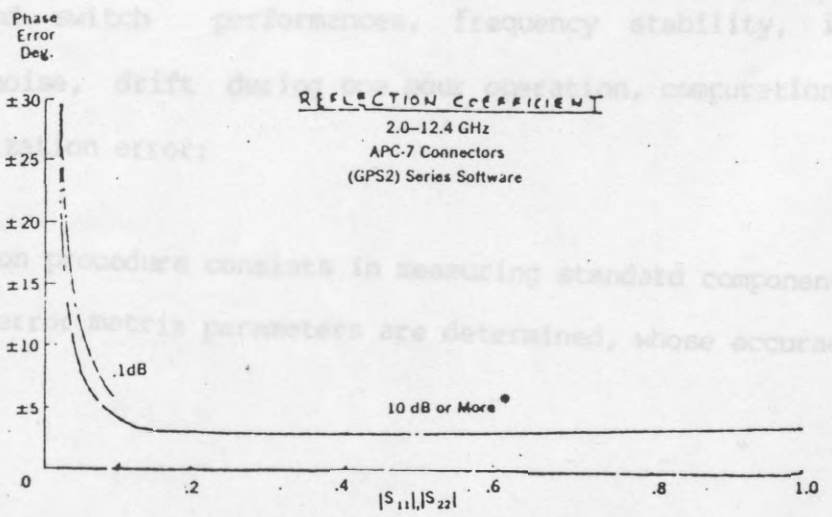
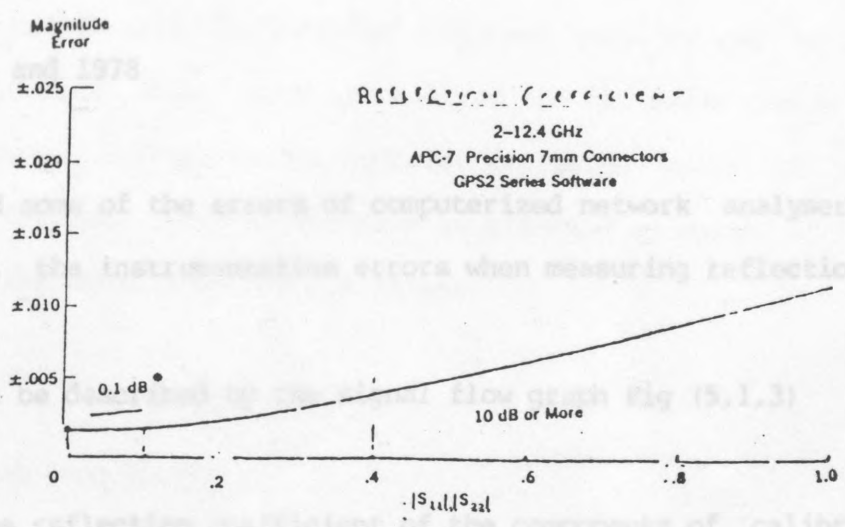


Fig. (2.7.2) Band uncertainty.

2.7.3 Ridella 1973 and 1978

He discussed some of the errors of computerized network analysers, in particular, the instrumentation errors when measuring reflection-coefficients.

His system can be described by the signal flow graph Fig (5.1.3)

$\Gamma$  represents the reflection coefficient of the components of calibration

$S_{11}, S_{22}, S_{12}, S_{21}$  represent the error correction parameters of the system which can be obtained at each frequency during calibration.

$N + E_p$  represents the total equivalent noise of the system which affects the repeatability of the measurement. This term is a function of connector and switch performances, frequency stability, instrumentation noise, drift during one hour operation, computational accuracy, quantization error;

The calibration procedure consists in measuring standard components from which the error matrix parameters are determined, whose accuracy

is affected by two factors: Calibration component accuracy and noise. Finally, the device under test is measured and the error matrix is taken into account. This gives the computer corrected value of the reflection coefficient. This measurement is affected by noise. He categorizes the error into four families:-

(deviation not shown)

- (1) Measurement repeatability
- (2) Calibration repeatability
- (3) Calibration standard inaccuracy
- (4) Instrumentation error

1) Measurement repeatability:-

which takes into account noise during the measurement.

$$\sigma_{I(MR)} = \frac{N}{S_{12}} + E1$$

Experimental results shown:

$  \Gamma  $	$  \sigma_{I(MR)}  $	$\angle \sigma_{I(MR)}$
0	0.0015	0
0.3	0.003	$0.3^\circ$
1	0.007	$0.5^\circ$

4) Instrumentation error:

2) Calibration repeatability:-

which takes into account noise during calibration

$$\sigma_{\Gamma}(\text{CR}) = \frac{-N}{S_{21}} - \Gamma E + \frac{\Gamma^2 N}{S_{21}}$$

3) Calibration Standards inaccuracy:-

$$\sigma_{\Gamma_c} = -\dot{\Gamma}_1 - \frac{\Gamma^2 [4S_{22}\dot{\Gamma}_1 + \dot{\Gamma}_2 + \dot{\Gamma}_3 - 2]}{2} + \frac{\Gamma^2 [2\dot{\Gamma}_1 + \dot{\Gamma}_2 - \dot{\Gamma}_3]}{2}$$

where  $\dot{\Gamma}_1$ ,  $-\dot{\Gamma}_2$  and  $\dot{\Gamma}_3$  are the reflection coefficient of the load, the short and the open.

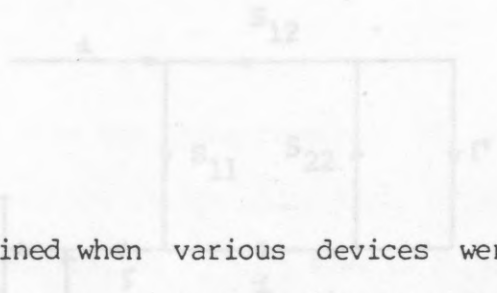
Experimental results show:

$ \Gamma $	$ \sigma(\Gamma_c) $	$\angle \sigma(\Gamma_c)$
0	0.007	0
0.3	0.007	1.4°
1	0.009	1.2°

4) Instrumentation error:

$$|\nabla\Gamma_1| \leq 0.008 \Gamma$$

$$\Delta\Gamma_I \leq 0.80$$



Ridella has reported the results obtained when various devices were measured on four different network analysers. However, the error expressions which he has arrived at differ considerably from those of Adam 1968. He also points out that the error curves issued by Hewlett Packard have been modified very often over the years.

$\Gamma$  represents the reflection coefficient of the components of calibration or in resonance.

$S_{11}$ ,  $S_{22}$ ,  $S_{12}$  represent the error correction of the system which can be obtained at each frequency during calibration.

$N + E_p$  represents the total equivalent noise of the system which affects the repeatability of the measurement. This term is a function of connector and switch performances, frequency stability, instrumentation noise, drift during one hour operation, computational accuracy, quantization error;

2.7.4. (R.P. method) Uncertainty of the magnitude:— H.P. supposed any reflection measuring system can be represented by three constants A, T and C. The assumed flow-graph is given in Fig (2.7.3)

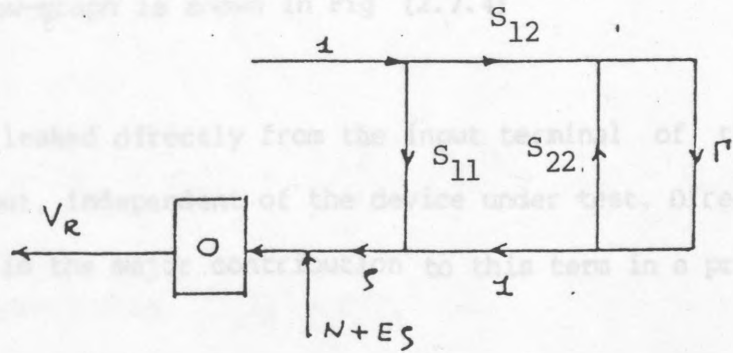


Fig. (2.7.3) Ridella error model

$\Gamma$  represents the reflection coefficient of the components of calibration or in measure:

$S_{11}$   $S_{22}$   $S_{12}$  represent the error correction of the system which can be obtained at each frequency during calibration.

$N + E_p$  represents the total equivalent noise of the system which affects the repeatability of the measurement. This term is a function of connector and switch performances, frequency stability, instrumentation noise, drift during one hour operation, computational accuracy, quantization error;

2.7.4 (H.P. method) Uncertainty of the magnitude:— H.P supposed any reflection measuring system can be represented by three constants A, T and C. The assumed flow-graph is shown in Fig (2.7.4)

A represents power leaked directly from the input terminal of the test set to its output, independent of the device under test. Directivity in the coupler is the major contribution to this term in a practical test set.

T represents the system scaling factor. The coupling of the test set to the detector and the display sensitivities are the major contributors to the scaling factor.

C represents the source match or the equivalent reflection looking back into the last coupler.

It will be noted that A corresponds to the  $S_{11}$  of previous authors C, the  $S_{22}$  and  $1+T$  corresponds to the product  $S_{12}S_{21}$

By application of Mason's non-touching loop rule, it can be shown:—

$$\Gamma_m = A + \frac{(1 + T) \Gamma_A}{1 - C\Gamma_A} \quad \dots\dots (2.7.1)$$

This is a vector relationship, i.e., all  $\Gamma$ 's, A, T, and C are complex quantities. The maximum errors can be expected by assuming worst case addition of all terms.

therefore  $\text{Max error} = E = \Gamma_m - \Gamma_A$

$$E = A + \frac{(1+T)\Gamma_A}{1 - C\Gamma_A} - \Gamma_A$$

$$= A + (1+T)\Gamma_A(1 + C\Gamma_A + C^2\Gamma_A^2 + C^3\Gamma_A^3 + \dots) - \Gamma_A$$

ignoring the higher order terms,  $C^2\Gamma_A^2 + C^3\Gamma_A^3 \dots$

$$\approx A + (1+T)\Gamma_A(1 + C\Gamma_A) - \Gamma_A$$

$$= A + T\Gamma_A + C\Gamma_A^2 + TC\Gamma_A^2$$

The term  $TC\Gamma_A^2$  is negligible since T and C are both small

$$\approx A + T\Gamma_A + C\Gamma_A^2 \quad \dots\dots\dots (2.7.2)$$

Since T is not known, both a calibration standard (short circuit) and the unknown are measured when a reflectometer is employed, and it is necessary to apply (5.1.2) to both condition:-

$$\Gamma_{\text{short}} = \Gamma_A + (A + T\Gamma_A + C\Gamma_A^2)$$

$$= -1 + (A - T + C) \text{ where } \Gamma_A = -1 \text{ for short circuit (standard)}$$

$\Gamma_{\text{unknown}} = \Gamma_A + (A + T\Gamma_A + C\Gamma_A^2)$  where  $\Gamma_A$  = the actual reflection coefficient of the unknown. The measurement is performed by taking the ratio of  $\Gamma_{\text{unknown}}$  and  $\Gamma_{\text{short}}$  (or the difference in dB, if the two quantities are measured in return loss).

$$\Gamma_{\text{displayed}} = \frac{\Gamma_{\text{unknown}}}{1 - \Gamma_{\text{short}}} = \frac{\Gamma_A + A + T\Gamma_A + C\Gamma_A^2}{1 - (A - T + C)}$$

$$= [\Gamma_A + A + T\Gamma_A + C\Gamma_A^2] [1 + (A - T + C) - (A - T + C)^2 + \dots]$$

$$\approx [\Gamma_A + A + T\Gamma_A + C\Gamma_A^2] [1 + A - T + C]$$

$$= \Gamma_A + A + T\Gamma_A + C\Gamma_A^2 + A[\Gamma_A + A + T\Gamma_A + C\Gamma_A^2]$$

$$- T[\Gamma_A + A + T\Gamma_A + C\Gamma_A^2] + C[\Gamma_A + A + T\Gamma_A + C\Gamma_A^2]$$

eliminating higher order terms.

$$\approx \Gamma_A + [A + (T + A - T + C)\Gamma_A + C\Gamma_A^2]$$

$$= \Gamma_A + [A + (A + C)\Gamma_A + C\Gamma_A^2]$$

Thus the uncertainty in  $\Gamma_{\text{displayed}} - \Gamma_A = \Delta\Gamma = A + (A + C)\Gamma_A + C\Gamma_A^2$

$$= A + B\Gamma_A + C\Gamma_A^2$$

..... (2.7.3)

where  $B = A + C =$  Calibration error.

By replacing  $\Gamma$  with its scalar equivalent  $\rho$ , it is possible to obtain equation.

$$\Delta\rho = A + B\rho + C\rho^2$$

..... (2.7.4)

where the values of the A and C coefficients are determined by the directivity and source match errors respectively, while B is composed of frequency response, instrument, and calibration errors.

THE PRECISION OF CALIBRATION PIECES

3.1 Introduction

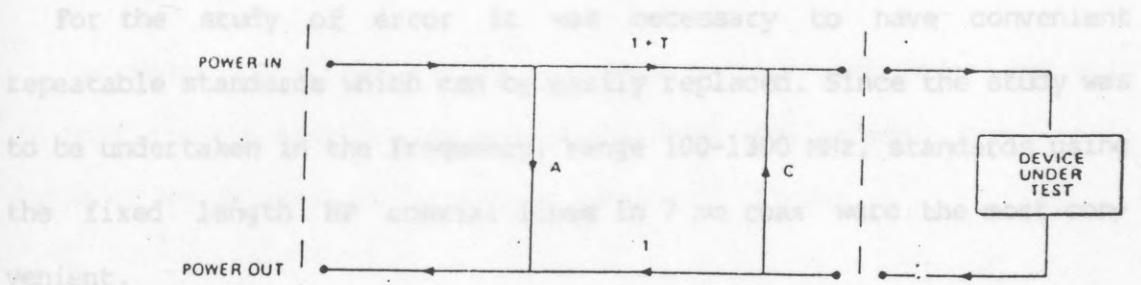


Fig. (2.7.4) (H.P. Method) Reflection measurement test set

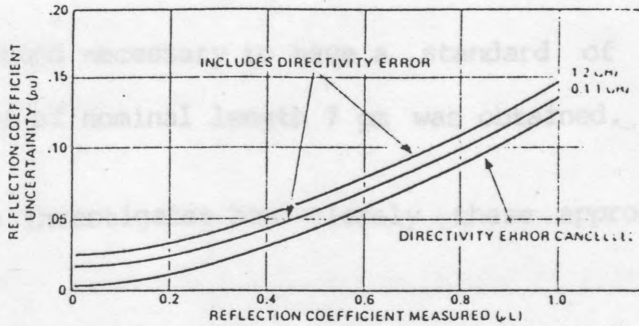
Magnitude accuracy:

$$\rho_u = \pm(0.015 + 0.03 \rho_L + 0.06 \rho_L^2) \text{ 0.11-1.0 GHz.}$$

$$\rho_u = \pm(0.025 + 0.03 \rho_L + 0.06 \rho_L^2) \text{ 1.0-2.0 GHz.}$$

$\rho_u$  = magnitude uncertainty.

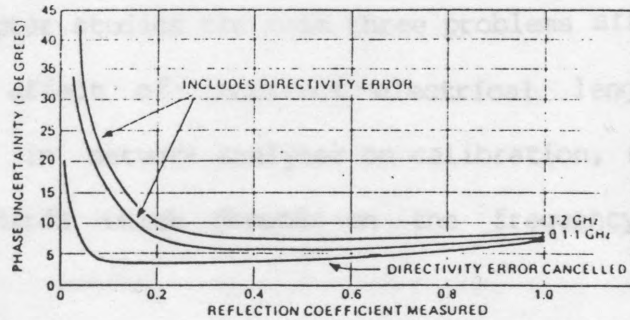
$\rho_L$  = measured reflection coefficient magnitude.



Phase accuracy:

$$\Phi_u = \sin^{-1} \rho_u / \rho_L \text{ for } \Phi_u < 90^\circ.$$

$\Phi_u$  = phase uncertainty.



## CHAPTER (3)

### THE PRECISION OF CALIBRATION PIECES

#### 3.1 Introduction

For the study of error it was necessary to have convenient repeatable standards which can be easily replaced. Since the study was to be undertaken in the frequency, range 100-1300 MHz, standards using the fixed length HP coaxial lines in 7 mm coax were the most convenient.

A available were two rigid lines with APC-7 connectors at either end of lengths 10 cm nominal (electrical length 10.35) and 20 cm nominal (electrical length 20.35).

A standard short circuit was available and a standard open was made to terminate the lines.

It was subsequently found necessary to have a standard of intermediate length and a line of nominal length 7 cm was obtained.

The following section investigates how closely these approach to ideal standards.

Appendix (7.2) describes the points common to the coaxial standards. Also this chapter studies the main three problems affecting the calibration (1) The effect of incorrect electrical length of reference short-circuit in network analyzer on calibration, (2) The choice of the three standards which depends on the frequency. (3) Repeatability error.

### 3.2 Special properties for 7-mm laboratory connector:-

#### 3.2.1 Short-circuit termination;-

The short-circuiting annulus will have a finite impedance, but this is sufficiently small to be ignored for most applications. For certain types of measurement it is however, just significant

The terminating impedance equals the short-circuit  $Z_S$  given by :

$$Z_S = R_S (1+j) \quad (\text{see D.Wood 1961,1971 and J.Zorzy})$$

where

$$R_S = \sqrt{\frac{\omega \mu_0}{2 \sigma}} \frac{1}{2\pi} \ln (b/a)$$
$$= 2.303 \sqrt{f/\sigma} \log_{10} (b/a) \text{ ohm}$$

( $R_S$  is plotted in Fig (3.2.1) against the frequency for a silver short circuit on a 50 ohm coaxial line and tabulated in Table (3.2.1)) - where  $f$  is in gigahertz and  $\sigma$  in siemens per metre.

An ideal short circuit has a reflection coefficient  $\rho_S = -1+j0$  in cartesian form, or  $\rho_S = 1/\pi$  in polar form, with the angle expressed in radians. In practice, the impedance of the short circuit is so small that it is a sufficiently good approximation to calculate the reflection coefficient in relation to  $Z_0$  (50 ohm) rather than (complex  $Z_0$ ).

The reflection coefficient of the short circuit:

$$\rho_s = \frac{z_s - z_0}{z_s + z_0} = \frac{z_s/z_0 - 1}{z_s/z_0 + 1} = \frac{z_s/z_0 + 1 - 2}{z_s/z_0 + 1} = 1 - \frac{2}{z_s/z_0 + 1}$$

$$= 1 - 2(z_s/z_0 + 1)^{-1} = 1 - 2(1 - z_s/z_0 + (z_s/z_0)^2 - z_s/z_0)^3 \dots$$

(By binomial expansion)

By ignoring 2<sup>nd</sup>-order quantities and taking the angle to be substantially equal to the tangent, we obtain:

$$\rho_s = 1 - 2 + \frac{2z_s}{z_0} = -1 + \frac{2R_s(1+j)}{z_0}$$

$$\rho_s = -1 + \frac{2R_s(1+j)}{z_0} \quad \text{in Cartesian form} \quad \dots\dots (3.2.1)$$

OR

$$\rho_s = \frac{(1 - 2R_s/z_0)}{z_0} \angle \pi - 2R_s/z_0 \quad \text{in polar form} \quad \dots\dots (3.2.2)$$

Fig. (3.2.1) Impedance of Silver Short Circuit for 30 GHz

Our investigations are made in the frequency range .1 - 1.4 GHz. Then it is seen that in this range  $R_s$  is about 1 mΩ. It is thus also negligible and only differs from 180 degrees by 0.02 degree at 1.4 GHz (the highest frequency used in the measurements described in chapter 3).

Table (3.2.1)

IMPEDANCE OF SILVER SHORT CIRCUIT FOR 50 OHM WITH AIR DIELECTRIC

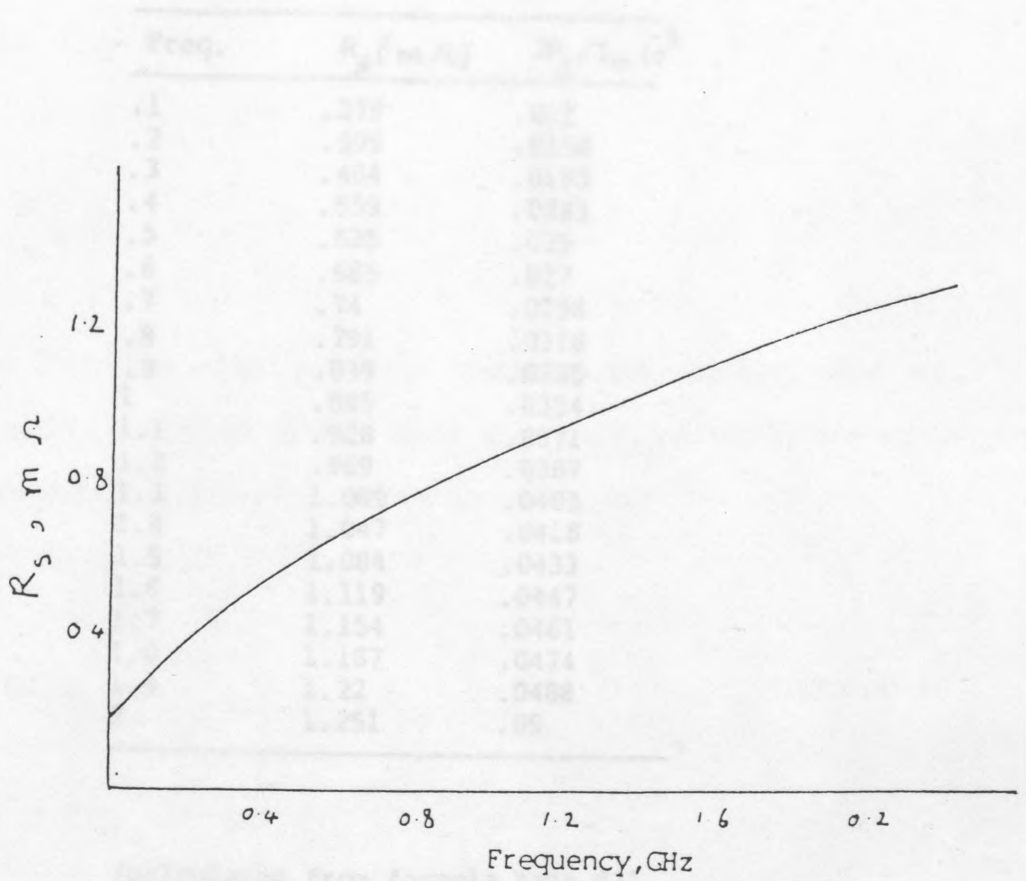


Fig. (3.2.1) Impedance of Silver Short Circuit for 50 with air dielectric.

(calculated from formula page 83)

Table (3.2.1)

IMPEDANCE OF SILVER SHORT CIRCUIT FOR 50Ω WITH AIR DIELECTRIC

The formula generally used to compute the characteristic impedance of a coaxial line is

$$Z_0 = 60 \ln \frac{b}{a}$$

where b and a are the outer and inner diameters respectively. The effect of small radii is accounted for by the correction factor in the outer conductor radius b as:

$$Z_0 = 60 \ln \frac{b}{a} \left[ 1 + \frac{0.0042}{b} \right]$$

Subtracting (3.2.3) and (3.2.4)

(calculated from formula page 83)

Freq.	$R_s (m\Omega)$	$2R_s/Z_0 \cdot 10^{-3}$
.1	.279	.011
.2	.395	.0158
.3	.484	.0193
.4	.559	.0223
.5	.625	.025
.6	.685	.027
.7	.74	.0296
.8	.791	.0316
.9	.839	.0335
1	.885	.0354
1.1	.928	.0371
1.2	.969	.0387
1.3	1.009	.0403
1.4	1.047	.0418
1.5	1.084	.0433
1.6	1.119	.0447
1.7	1.154	.0461
1.8	1.187	.0474
1.9	1.22	.0488
2	1.251	.05

from the expansion of:

### 3.2.2 Tolerance on diameters:-

$$\ln(1+x) = x - \frac{x^2}{2} + \frac{x^3}{3} - \frac{x^4}{4} + \dots \quad (\text{neglecting } 2^{\text{nd}} \text{ order})$$

The formula generally used to compute the characteristic impedance of a coaxial line is:

$$Z_0 = 60 \ln \frac{b}{a} \quad \dots\dots(3.2.3)$$

where b and a are the outer and inner diameter respectively. The effect of small errors  $\Delta a$  in the inner conductor, radius a, and  $\Delta b$  in the outer conductor, radius b, can be expressed as:

$$Z_0 + \Delta Z_0 = 60 \ln \frac{b + \Delta b}{a + \Delta a} \quad \dots\dots(3.2.4)$$

Subtracting (3.2.3) and (3.2.4)

$$\Delta Z_0 = 60 \ln \frac{b + \Delta b}{a + \Delta a} - \ln \frac{b}{a}$$

$$= 60 \ln \frac{b + \Delta b}{a + \Delta a} \cdot \frac{a}{b}$$

$$= 60 \ln \frac{1 + (\Delta b/b)}{1 + (\Delta a/a)} = 60 \left\{ \ln \left( 1 + \frac{\Delta b}{b} \right) - \ln \left( 1 + \frac{\Delta a}{a} \right) \right\}$$

$$\Delta Z_0 = 60 \left\{ \Delta b/b - \Delta a/a \right\}$$

From the expansion of:

So due to the small change in the characteristic impedance of the transmission line, the reflection coefficient will be small unless and the reflection equal to:

$$\ln(1+x) = x - \frac{x^2}{2} + \frac{x^3}{3} - \frac{x^4}{2} \dots \text{(neglecting 2}^{\text{nd}} \text{ order)}$$

$$\% \Delta Z_0 = \frac{60 \times 100}{Z_0} \left[ \frac{\Delta b}{b} - \frac{\Delta a}{a} \right] \dots \text{per cent}$$

which expresses the fact that the percent change in characteristic impedance is given approximately by  $60/Z_0$  times the percent change in inner or outer diameter. Therefore, for a line of about 50 ohms, the error in characteristic impedance due to incorrect inner or outer diameter will be 1.2 times the percent error in either diameter.

To study the effect of small errors  $\Delta a$  in the inner conductor, (radius  $a$ ) and  $\Delta b$  in the outer conductor (radius  $b$ ). Thus, if a line with  $Z_0 = 50$ ,  $2b = 7.00$  mm, and  $2a = 3.04$  mm, if  $2\Delta b = \pm .005$  mm and  $2\Delta a = \pm .002$  mm. Then.

$$\% \Delta Z_0 = 120 \left( \frac{\Delta b}{b} + \frac{\Delta a}{a} \right) = \pm .164$$

This is the largest possible uncertainty in the measurement of impedance with a line having the given dimensional errors and would correspond to VSWR of 1.001

### 3.2.3 Tolerances on Eccentricity

So due to the small change in the characteristic impedance of the transmission line, this line will no longer be reflectionless and the reflection equal to:

$$\rho = \frac{(Z_0 \pm \Delta Z_0) - 50}{(Z_0 \pm \Delta Z_0) + 50}$$

(See C. Wejnichel 1964)

$$(\text{Max}) \Delta Z_c = 60 \left( \frac{\Delta b}{b} + \frac{\Delta a}{a} \right) = .0822$$

For small eccentricities, it can be shown that this reduces to:

$$\rho(\text{Max}) = \sim .00082$$

This it will be seen in (page 116) is two orders smaller than the uncertainty due to random electronic effects and it will thus be ignored.

where  $L$  is the inductance per unit length, and  $v$  is the velocity of light:

$$\frac{1}{\sqrt{\epsilon_0}} = \frac{L}{\sqrt{\mu_0}}$$

$$Z_0 = \frac{1}{2\pi \epsilon_0} \ln \left( \frac{2b}{a} \sqrt{\frac{\mu_0}{\epsilon_0}} \right) \quad (3.2.5)$$

If we compare this equation (3.2.5) with the equation of the characteristic impedance of a perfect line:

$$Z_0 = \frac{1}{2\pi} \sqrt{\frac{\mu}{\epsilon}} \ln \frac{b}{a} \quad (3.2.6)$$

We observe that the difference is:

### 3.2.3 Tolerances on Eccentricity:-

The capacitance per unit length of a coaxial line with eccentricity (e) is given by:

$$C = 2\pi\epsilon \left[ \frac{\cosh^{-1} \left[ \frac{b^2 + a^2 - 4e^2}{2ba} \right]^{-1}}{2ba} \right]^{-1} \quad (\text{see C.Weinschel 1964})$$

For small eccentricities, it can be shown that this reduced to:

$$C = 2\pi\epsilon \left[ \frac{\ln \frac{b}{a} \cdot \left[ 1 - \frac{4e^2}{b^2 - a^2} \right]^{-1}}{a} \right]^{-1}$$

$$\text{Since } Z_0 = \sqrt{\frac{L_0}{C}} = \frac{1}{\sqrt{LC}}$$

Where  $L_0$  is the inductance per unit length, and  $v$  is the velocity of light:

$$= \frac{1}{\sqrt{\frac{\mu\epsilon}{c^2}}} = \frac{1}{\sqrt{L_0 C}}$$

$$Z_0 = \frac{1}{2\pi\sqrt{\frac{\mu}{\epsilon}}} \ln \left[ \frac{b \left[ 1 - \frac{4e^2}{b^2 - a^2} \right]}{a} \right] \quad \dots\dots (3.2.5)$$

If we compare this equation (3.2.5) with the equation of the characteristic impedance of a perfect line:

$$Z_0 = \frac{1}{2\pi\sqrt{\frac{\mu}{\epsilon}}} \ln \frac{b}{a} \quad \dots\dots (3.2.6)$$

We observe that the difference is:

$$\nabla Z_0 = 60 \ln \left[ \frac{1 - 4e^2}{d^2 - a^2} \right] = \frac{-240e^2}{d^2 - a^2}$$

For a 50 ohm line therefore:

$$\nabla Z_0 = - \frac{240 e^2}{.81 d^2} = -296 \frac{e^2}{d^2}$$

Mechanical tolerances on the line diameters govern the uncertainty in the calculated value of  $Z_0$ . This can be expressed as a fractional error in  $Z_0$  in terms of the diameter tolerances.

If  $e = .05$  mm

$$\nabla Z_0 = -.015$$

$$\rho = .00015$$

If  $e = .1$  mm

$$\nabla Z_0 = -0.0604$$

$$\rho = .0006$$

This reflection coefficient is neglected for the frequency range considered.

### 3.2.4 Electrical length:-

The expression for the equivalent electrical length is:

$$\phi = \beta l_E \quad (\text{see H.Vifian 1976})$$

where  $l_E$  = electrical length in vacuum

$\phi$  = insertion phase (phase shift through the propagation medium)

$\beta$  = phase constant of the propagation.

The electrical length of an ideal transmission line stays constant with frequency and the insertion phase characteristic is strictly proportional to frequency. Therefore, an ideal electrical length can be simulated by a frequency proportional phase shift, where the slope of the phase characteristic determines the electrical length.

In general, the phase characteristic in practice is not strictly a linear function of frequency and, therefore, the electrical length varies.

Fig (3.2.2) represents the measured phase as a function of frequency for the 7.35 cm and 10.35 cm offset short-circuit. Fig (3.2.3) the same for 20.35cm and 30.7cm.

Also shown is difference between the measured and the fitted value for the same lengths. (See Appendix (7.3))

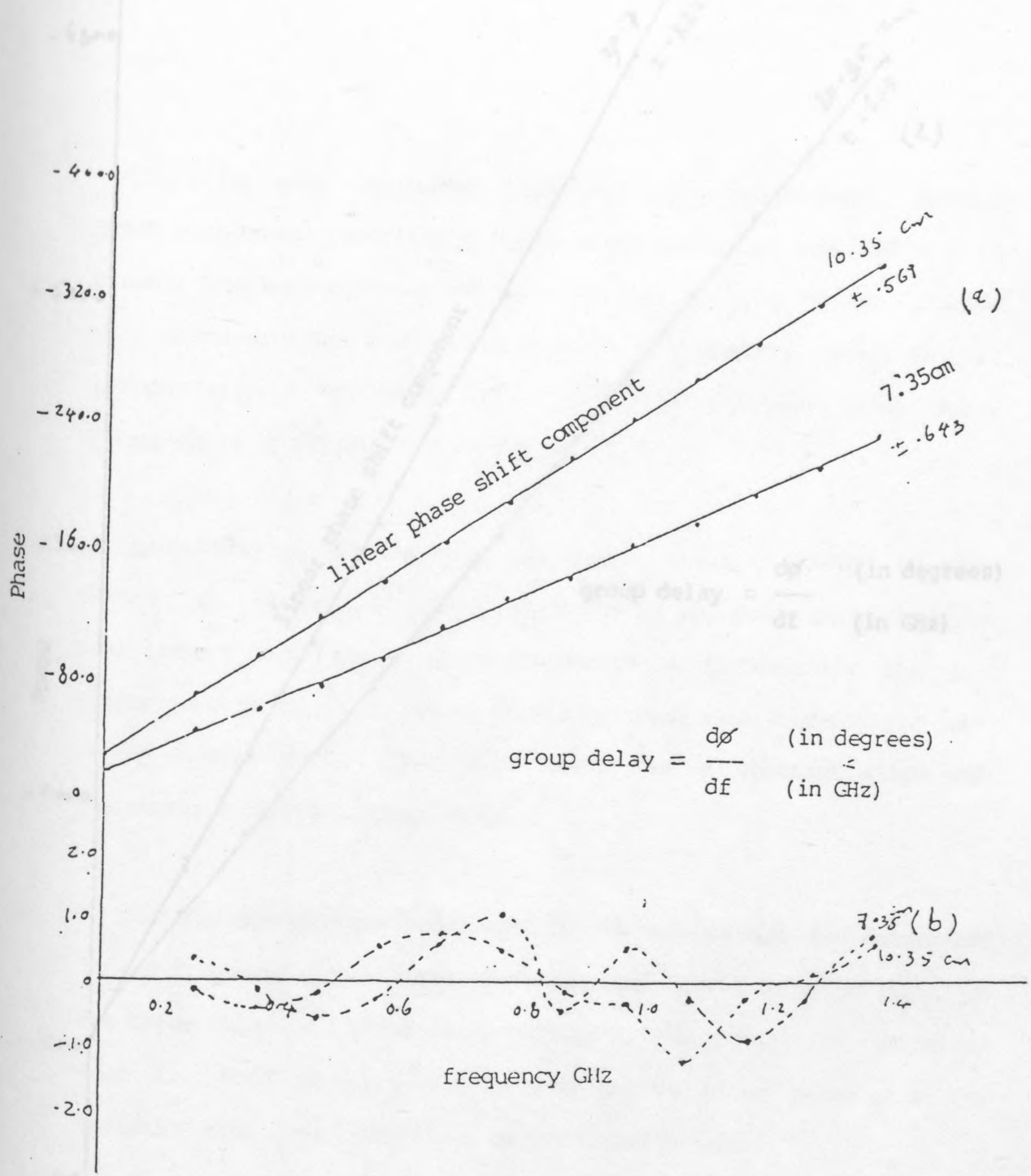


Fig (3.2.2) (a) The measured phase as a function of the frequency for the 7.35cm and 10.35 cm offset short-circuit. (b) The difference between the measured and the fitted.

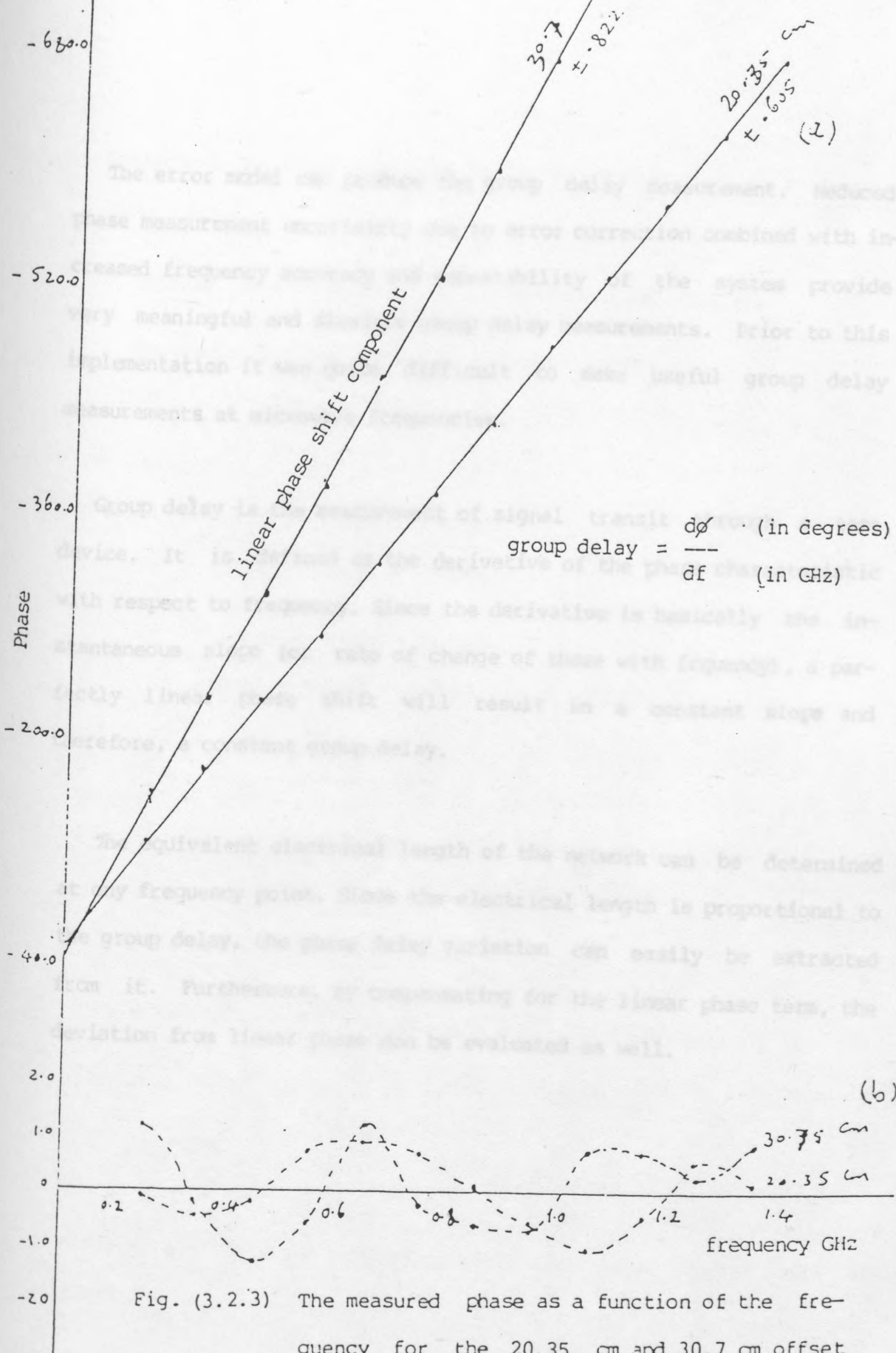


Fig. (3.2.3) The measured phase as a function of the frequency for the 20.35 cm and 30.7 cm offset short-circuit. (b) The difference between the measured and the fitted.

The error model can produce the group delay measurement. Reduced phase measurement uncertainty due to error correction combined with increased frequency accuracy and repeatability of the system provide very meaningful and flexible group delay measurements. Prior to this implementation it was quite difficult to make useful group delay measurements at microwave frequencies.

Group delay is the measurement of signal transit through a test device. It is defined as the derivative of the phase characteristic with respect to frequency. Since the derivative is basically the instantaneous slope (or rate of change of those with frequency), a perfectly linear phase shift will result in a constant slope and therefore, a constant group delay.

The equivalent electrical length of the network can be determined at any frequency point. Since the electrical length is proportional to the group delay, the phase delay variation can easily be extracted from it. Furthermore, by compensating for the linear phase term, the deviation from linear phase can be evaluated as well.

3.2.4.1 Reflection coefficient of line having connector distant l from the short circuit:-

Suppose the connector has a susceptance b Fig (3.2.4)a

The normalized admittance at A =  $j(b - \cot\beta l)$

Thus 
$$\rho = \frac{1 - j(b - \cot\beta l)}{1 + jb - j\cot\beta l}$$

$$= \frac{\sin\beta l + j\cos\beta l - j\sin\beta l}{\sin\beta l - j\cos\beta l + j\sin\beta l}$$

$$= \frac{-\cos\beta l + j\sin\beta l + b\sin\beta l}{\cos\beta l + j\sin\beta l - b\sin\beta l}$$

$$= -\frac{e^{-j\beta l} - b\sin\beta l}{e^{j\beta l} - b\sin\beta l}$$

$$= -e^{-j2\beta l} (1 - e^{j\beta l} b\sin\beta l) (1 - e^{-j\beta l} b\sin\beta l)^{-1}$$

For the AEC-7 connector  $b \ll 1$ ,

$$\rho = -e^{-j2\beta l} (1 - e^{j\beta l} b\sin\beta l) (1 + e^{-j\beta l} b\sin\beta l + \dots)$$

$$= -e^{-j2\beta l} (1 - b\sin\beta l (e^{j\beta l} - e^{-j\beta l})) - b^2 \sin^2\beta l + \dots$$

$$= -e^{-j2\beta l} (1 - j2b\sin^2\beta l) + \text{term in } b^2$$

But  $-1 \cdot e^{-j2\beta l}$  is the reflection coefficient of a shorted line of length l

Thus the deviation from the line is given by

$$\nabla \text{ phase angle} = \frac{e^{-j2\beta l}}{1 - j2b \sin^2 \beta l} - \frac{e^{-j2\beta l}}{1 - j2b \sin^2 \beta l}$$

$$\text{Deviation is } \arctan(-2b \sin^2 \beta l) \dots \dots (3.2.7)$$

The pattern will thus give a sinusoidal variation of phase varying twice per 360°. The amplitude will be b. Also the regression line will not strictly be the line corresponding to the perfect short. It will be a line parallel to it but different by one amplitude.

Fig (3.2.2)a and Fig (3.2.2)b show that the length of the offset short line is  $(10.35 \pm .15)$  cm and its phase change is  $\pm 1$  degree.

To satisfy the above phase change requirement in equation (3.2.7), the value of b has been found to be  $.0095 \approx .01$  Fig (3.2.4)b by successive approximation.

$$(.018 + .00f) \text{ where } f \text{ is the frequency in GHz}$$

Thus at 2GHz the reflection coefficient according to this formula is .02

To derive curve Fig (3.2.4)b, the value of susceptance has been adjusted so that the deviation coincides with that measured in Figs 3.2.2b and 3.2.3b. These value of b required for this excursion is considerably less than that quoted for APC 7 connection. Further more periodicity in the experimental curve is much greater than the calculated curve of Fig (3.2.4)b. This suggests that in practice the reflections due to APC 7 connectors can be compared with reflections due to the source mismatch or other elements further into the reflectometer.

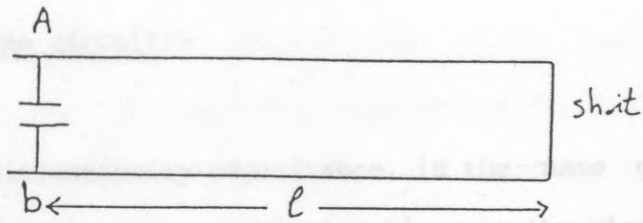


Fig.(3.2.4)a (10.35 +.15)cm offset short line with the connector having susceptance b

The normalized admittance at A =  $j(b - \cot\beta l)$

Thus 
$$\rho = \frac{1 - j(b - \cot\beta l)}{1 + jb - j\cot\beta l}$$

arctan  $(-2b\sin\beta l)$

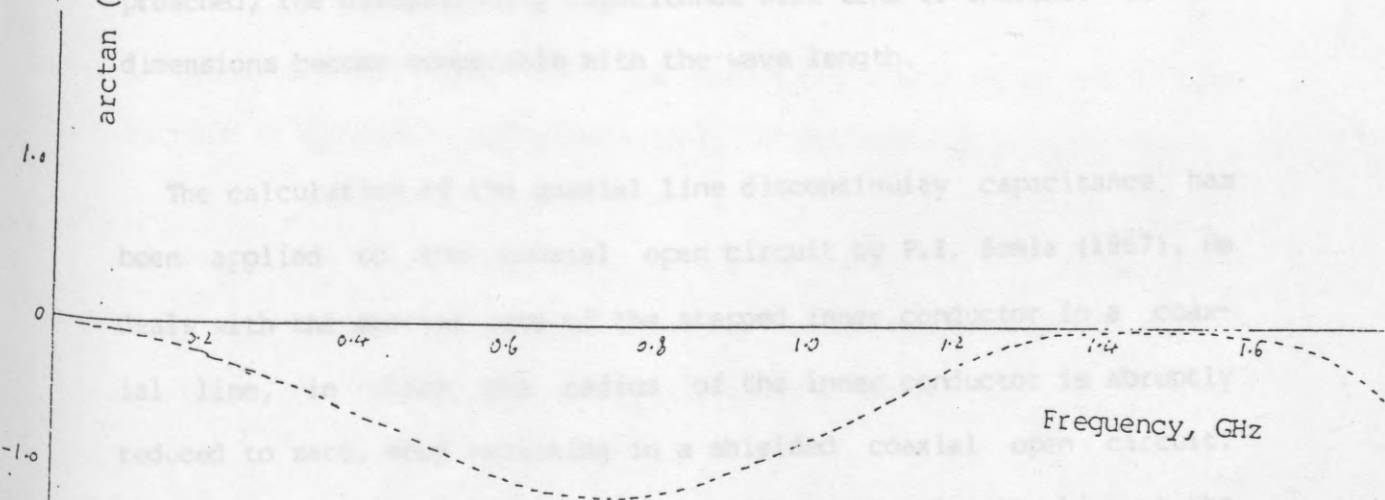


Fig (3.2.4)b The deviation from the line as a function of the frequency

### 3.2.5 Capacitance in the open circuit:-

Step capacitance, or discontinuity capacitance, is the name given to the capacitance which occurs in transmission lines at the plane of a sudden change of geometry (discontinuity), and causes reflections, apart from reflections caused by any sudden change of the characteristic impedance of the line. As an example, if the dimensions of a coaxial line from a given transverse plane onwards are suddenly scaled up, thus keeping constant the characteristic impedance of the transmission line, this line will no longer be reflectionless because of the disturbance of the field pattern in the vicinity of the discontinuity. As the upper frequency limit of the connector system is approached, the discontinuity capacitance will tend to increase as the dimensions become comparable with the wave length.

The calculation of the coaxial line discontinuity capacitance has been applied to the coaxial open circuit by P.I. Somla (1967). He deals with the special case of the stepped inner conductor in a coaxial line, in which the radius of the inner conductor is abruptly reduced to zero, thus resulting in a shielded coaxial open circuit. The computed values of the step capacitance shunting the line at the discontinuity (open-circuit), and the effective position of the open circuit are given in Table (1), and in graphical form. Figure(1) in this reference.

Woods (1972), by interpolation of Somla's data (1967) has calculated the values of the discontinuity capacitance for different coaxial line dimensions to four significant digits. However, Woods's and Somla's results differ significantly from those obtained by Risley (1969) and are closer to measured values.

The method used here depends on the Marcuvitz (Handbook vol.10). He made a study of a similar discontinuity with hollow inner conductor. He expressed the values of step capacitance as an equivalent length of coaxial line terminated by a perfect open circuit. This equivalent line has the same characteristic impedance as the original coaxial line.

Using Marcuvitz expression the equivalent length of an APC 7 open circuit is 0.11 cm as compared with 0.119 for Somla's

Table (3.2.2) Comparison of results for fringe capacitance

Fig (3.2.5) represents the fringe capacitance in the open-circuit and Table (3.2.2) a comparison results for the capacitance and equivalent electric length obtained by different authors.

### 3.1 Problems associated with

Having established that a perfectly defined standard is not possible, and having studied the deviations of the standards, three more problems in the calibration procedure are studied. The first

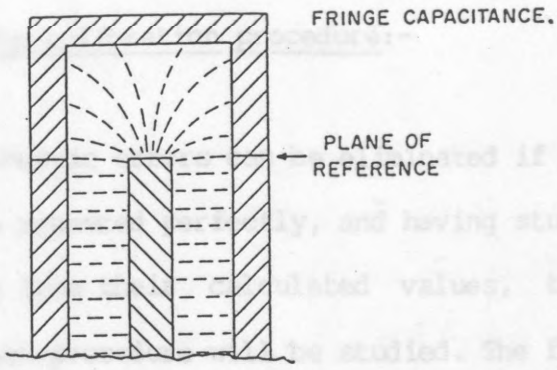


Fig (3.2.5) Fringe capacitance

studies the effect of an incorrect value for the electric length in one of the standards used in the calibration and derives the mathematical formulae for the uncertainty in the magnitude and phase of the corrected value for the device under test.

The second problem studies how to choose standards and how the choice depends on the frequency. The third problem studies the

Table (3.2.2) Comparison of results for fringe capacitance

obtained by other authors

	$f$ (MHz)	$C$ (fF)	$l$ (cm)
Somig's	0.001	79.70	0.1194
	1000	not available	
Woods	0.001	79.70	0.1194
	1000	79.70	
Razaz & Davics	0.001	79.88	0.1197
	1000	79.917	0.1198

We now examine the effect on a measurement of assuming an incorrect value for the electrical length of one of the standards. The uncorrected measurement of reflection coefficient,  $\rho$  is related to the true value of  $\Gamma$  by:-

### 3.3 Problems association with the calibration procedure:-

Having established that systematic errors can be eliminated if perfectly defined standards can be measured perfectly, and having studied the deviations of the standards from their calculated values, three more problems in the calibration procedure will be studied. The first studies the effect of an incorrect value for the electric length in one of the standards used in the calibration and derives the mathematical formula for the uncertainty in the magnitude and phase of the corrected value for the device under test. There will therefore

be a residual error in the final corrected measurement of the unknown. The second problem studies how to choose standards and how the choice depends on the frequency. The third problem studies the repeatability error or the capability of the system to repeat the same measurement and the effect of random error in the calibration procedure.

#### 3.3.1 The effect of electric length of reference short-circuit in network analyser calibration:-

We now examine the effect on a measurement of assuming an incorrect value for the electrical length of one of the standards. The uncorrected measurement of reflection coefficient,  $\rho$  is related to the true value of  $\Gamma$  by:-

$$\rho = S_{11} + \frac{S_{12}S_{21}\Gamma}{1 - S_{22}\Gamma} \dots\dots(3.3.1)$$

If we now measure an unknown impedance with reflection coefficient  $\Gamma$ ,

The evaluation of  $S_{11}$ ,  $S_{22}$  and the product  $S_{12} \cdot S_{21}$  at each frequency of interest is referred to as the calibration of the network analyser. Measurements of  $\rho$  for a short, an open-circuit and an offset short are used to solve equation (3.3.1) for  $S_{11}$ ,  $S_{22}$  and  $S_{12}S_{21}$ .

Substitution of equations (3.3.2) - (3.3.4) into (3.3.1) gives:-

If the reflection coefficient of the off-set-short is wrongly specified by assuming an incorrect value of  $\Gamma_c$ , then the resulting values for  $S_{11}$ ,  $S_{22}$  and  $S_{12}S_{21}$  will be in error. There will therefore be a residual error in the final corrected measurement of the unknown impedance.

$\Gamma$  (the final corrected measurement of the unknown if one of the stan-

From equation (3.3.1) can be seen that:-

$$S_{11} + \frac{S_{12} S_{21}}{1 - S_{22}} = \hat{S}_{11} + \frac{\hat{S}_{12} \hat{S}_{21}}{1 - \hat{S}_{21}} \dots\dots(3.3.2) \quad \text{open-circuit}$$

$$S_{11} - \frac{S_{12} S_{21}}{1 + S_{22}} = \hat{S}_{11} - \frac{\hat{S}_{12} \hat{S}_{21}}{1 + \hat{S}_{12}} \dots\dots(3.3.3) \quad \text{short-circuit}$$

$$S_{11} - \frac{S_{12} S_{21} \Gamma_c}{1 + S_{22} \Gamma_c} = \hat{S}_{11} - \frac{\hat{S}_{12} \hat{S}_{21} \hat{\Gamma}_c}{1 + \hat{S}_{22} \hat{\Gamma}_c} \dots\dots (3.3.4) \text{ off-set-short}$$

If we now measure an unknown impedance with reflection coefficient  $\Gamma$ ,

Differentiation of (3.3.7) with respect to  $a$  gives the maximum

$$S_{11} + \frac{S_{12} S_{22} \Gamma}{1 - S_{22} \Gamma} = \hat{S}_{11} + \frac{\hat{S}_{12} \hat{S}_{21} \hat{\Gamma}}{1 - \hat{S}_{22} \hat{\Gamma}} \dots\dots (3.3.5) \text{ device under test}$$

i.e.  $a = 0, 2\pi, \dots$  (see Appendix (7.4))

Substitution of equations (3.3.2) - (3.3.4) into (3.3.5) gives:-

Again from equation (3.3.5) we can find the expression for the phase of  $\hat{\Gamma}$ .

$$\hat{\Gamma} = \frac{\Gamma - \Gamma_c + \hat{\Gamma}_c - \Gamma \Gamma_c \hat{\Gamma}_c}{1 - \hat{\Gamma}_c + \Gamma \hat{\Gamma}_c - \Gamma_c \hat{\Gamma}_c} \dots\dots (3.3.6)$$

Equation (3.3.6) relates "in error" error corrected measurement  $\hat{\Gamma}$  (The final corrected measurement of the unknown if one of the standards used in the calibration is in error) to the true value  $\hat{\Gamma}$  of reflection coefficient.

The relation between  $\Gamma$  and  $\hat{\Gamma}$  is seen to be independent of the network analyser error network.

Let  $\Gamma$ ,  $\hat{\Gamma}$ ,  $\Gamma_c$  and  $\hat{\Gamma}_c$  have angles  $a$ ,  $\hat{a}$ ,  $b$  and  $\hat{b}$ . Then from equation (3.3.6) we can find an expression for the magnitude of  $\hat{\Gamma}$ .

By assuming  $|\hat{\Gamma}_c| = |\Gamma_c| = 1$  and let  $|\Gamma| = r$  from equation (3.3.6)

Differentiation (3.3.10) with respect to  $a$  and equal to zero.

$$|\dot{\Gamma}|^2 = \frac{[r \cos a - \cos b + \cos \hat{b} - r \cos(a+b+\hat{b})]^2 + [r \sin a - \sin b + \sin \hat{b} - r \sin(a+b+\hat{b})]^2}{[1 - r \cos(a+b) + r \cos(a+\hat{b}) - \cos(b+\hat{b})]^2 + [-r \sin(a+b) + r \sin(a+\hat{b}) - \sin(b+\hat{b})]^2} \dots\dots (3.3.7)$$

where  
 Differentiation of (3.3.7) = 0 with respect to a gives the maximum

$$A = 4r^2 (1 - \cos b \cos \hat{b})^2 - \sin^2 b \sin^2 \hat{b}$$

$$B = 2r^2 (1+r^2) (\cos b - \cos \hat{b}) [2(1 - \cos b \cos \hat{b}) - \sin b \sin \hat{b}]$$

$$C = (1+r^2) \sin a (\cos b - \cos \hat{b}) = 0 \dots\dots \text{condition} \quad (3.3.8)$$

i.e.  $a = 0, 2\pi, \dots$  (see Appendix (7.4))

sub. by the condition (3.3.8) in (3.3.7) given the maximum  $|\dot{\Gamma}|$

Again from equation (3.3.6) we can find the expression for the phase of  $\dot{\Gamma}$ .

As an example suppose that the third standard has a reflection coefficient 0.97 (D) and a phase angle (b) 52.41, but due to erroneous measurement it is assumed to be 0.95 (D) with phase angle 55.72 (b)

$$\tan^{-1} \Gamma = \tan^{-1} \frac{2r \sin b \sin \hat{b} \sin a}{(1+r^2) (\cos \hat{b} - \cos b) + 2r(1 - \cos b \cos \hat{b}) \cos a} \quad (3.3.9)$$

Equation (3.3.7) and (3.3.10) represents the uncertainty in the magnitude and phase in the final corrected measurement of the unknown therefore the phase difference (error in the phase) E

If only one of the standards used in the calibration is in error. The same expression  $E = \tan^{-1} \Gamma - \tan^{-1} \hat{\Gamma}$  and difficult to solve if we suppose the three standards in error.

$$E = a - \tan^{-1} \frac{2r \sin b \sin \hat{b} \sin a}{(1+r^2) (\cos \hat{b} - \cos b) + 2r(1 - \cos b \cos \hat{b}) \cos a} \dots\dots (3.3.10)$$

Differentiation (3.3.10) with respect to a and equal to zero.

therefore  $\cos a = \frac{-B + \sqrt{B^2 - 4AC}}{2A}$  condition .... (3.3.11)

The usual procedure for the calibration of network analyzers for where reflection measurements is based on the utilization of three standards

$$A = 4r^2 [(1 - \cos b) \cos b]^2 - \sin^2 b \sin^2 b$$

$$B = 2r^2 (1+r^2) (\cos b - \cos b) [2(1 - \cos b) \cos b - \sin b \sin b]$$

$$C = (1+r^2)^2 (\cos b - \cos b)^2 + 4r^2 \sin^2 b \sin^2 b - 4r^2 (1 - \cos b) \cos b \sin b \sin b$$

Procedure I:-

sub. by the condition (3.3.11) in equation (3.3.10) gives the maximum E

This is based on using the same set of three standards in all the

As an example, suppose that our third standard has a reflection coefficient 0.97 ( $\tilde{I}$ ) and a phase angle ( $\tilde{b}$ ) 52.11, but due to erroneous measurement it is assumed to be 0.95 ( $I$ ) with phase angle 55.72 ( $b$ ) then the calculated error in the magnitude is equal to 0.02 and in the phase is equal to 4.468.

To improve the precision, we used for calibration at any

Equation (3.3 7) and (3.3.10) represents the uncertainty in the magnitude and phase in the final corrected measurement of the unknown if only one of the standards used in the calibration is in error. The same expression will be very complex and difficult to solve if we suppose the three-standards in error.

This is not such a disadvantage as may at first appear since a perfect short and an open of very small electrical lengths are readily calculable.

to closeness in the phase difference between the standards.

### 3.3.2 The choice of the 3-standards depends on the frequency:-

The usual procedure for the calibration of network analyzers for reflection measurements is based on the utilization of three standards of reflection for each frequency. In this section we compare the results obtained with two procedures of calibration.

#### Procedure I:-

This is based on using the same set of three standards in all the frequency range (.1 to 2 GHz). The components which are used are: a short circuit, an open circuit and an 10.35 cm offset short circuit.

#### Procedure II:-

To improve the precision, we used for calibration at any frequency the set of three components whose phase spacings were nearest to be 120 degrees (when the three measured reflection coefficients whose phase spacings were 120 degree plotted in the complex plane their values lie on the unit circle. The intersection of the medians of the triangle formed by connecting these three points, coincides with the centre of the circle). The components needed for standards were chosen as in table (3.3.1) From Fig (3.3.1) and Fig (3.3.2) we see at the frequency .7 and 1.5GHz we can not calculate the s-error matrix due to closeness in the phase difference between the standards.

TABLE (3.3.1)

Freq	3-standard
.1	3 5 8
.2	2 4 7
.3	3 6 8
.4	2 3 4
.5	1 2 3
.6	1 7 8
.8	4 5 8
.9	4 5 6
1	1 2 3
1.1	5 6 7
1.2	2 5 7
1.3	2 5 7
1.4	4 5 8
1.6	3 5 8
1.7	1 3 6
1.8	5 6 8
1.9	5 6 7
2	2 3 4

standard no (1)	short-circuit
standard no (2)	10.35 offset-short
standard no (3)	20.35 offset-short
standard no (4)	30.70 offset-short
standard no (5)	open-circuit
standard no (6)	10.35 offset-open
standard no (7)	20.35 offset-open
standard no (8)	30.70 offset-open

standards used in the calibration procedure

For both procedures, the uncertainty of the magnitude and phase has been calculated. The method of calculation of the uncertainties is described in Chapter (4), and the results are given in table (3.3.2) and illustrated in Fig (3.3.3). The Table excludes certain frequencies where the error is indeterminate. The discontinuities shown in Fig (3.3.3) occur at these frequencies.

Table (3.3.3) gives the mean value of the uncertainty in magnitude and phase for each of the two procedures. The results given in this table confirm that procedure II should give rise to less uncertainty than procedure I.

standard no (1)	short-circuit
standard no (2)	10.35 offset-short
standard no (3)	20.35 offset-short
standard no (4)	30.70 offset-short
standard no (5)	open-circuit
standard no (6)	10.35 offset-open
standard no (7)	20.35 offset-open
standard no (8)	30.70 offset-open

standards used in the calibration procedure

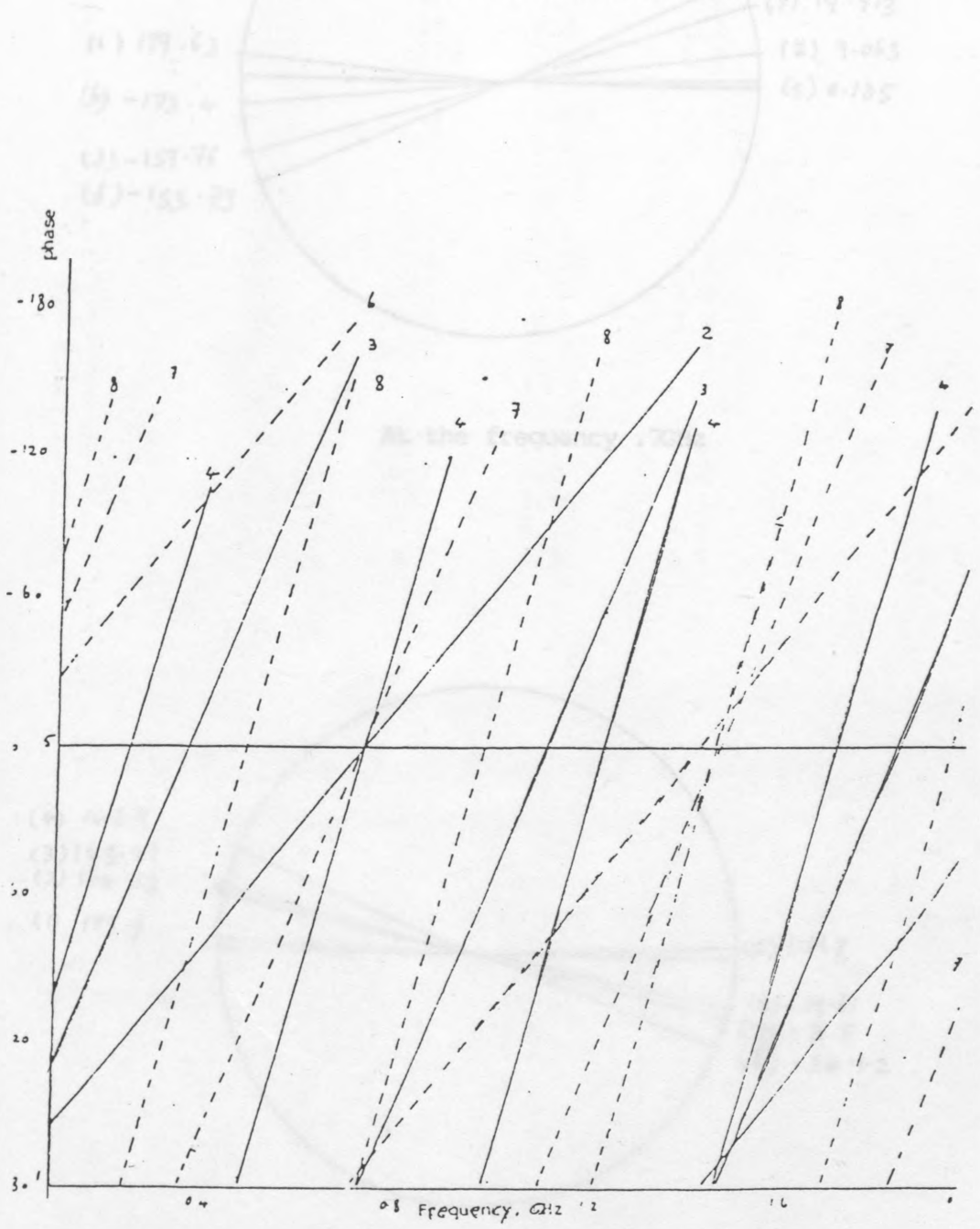


Fig.(3.3.1) The phase as a function for the eight-standards used in the calibration procedure.

Table (3.3.2)

THE UNCERTAINTY OF AMPLITUDE AND PHASE FOR PROCEDURES I AND II

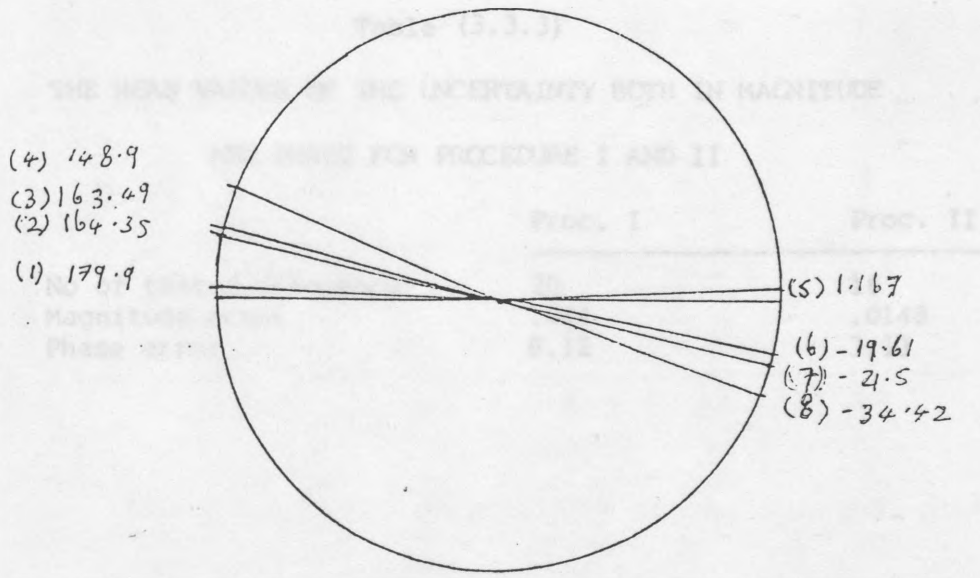
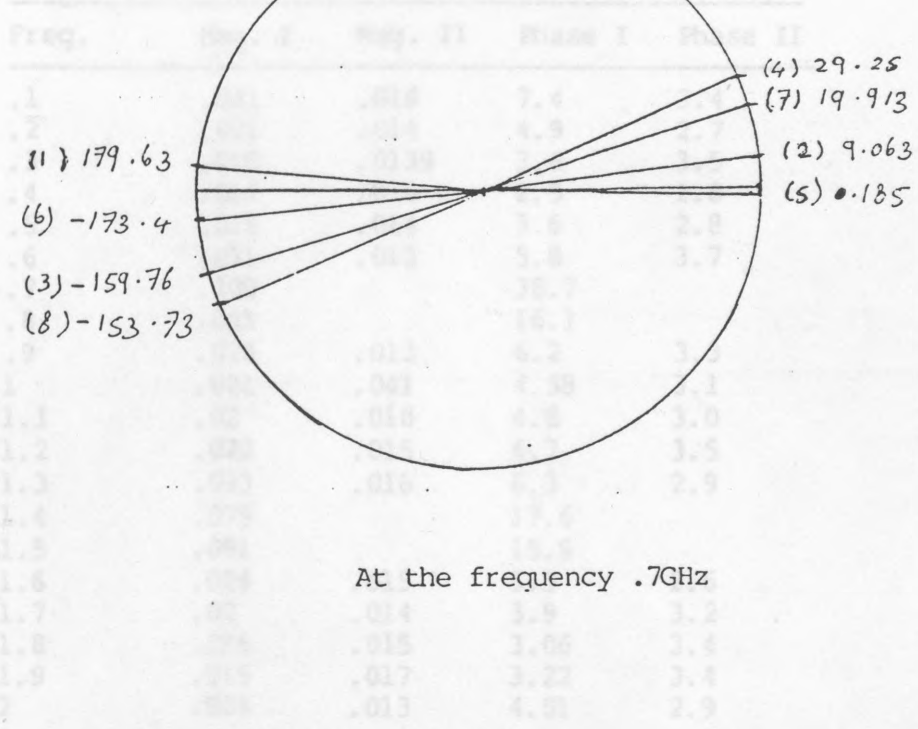


Fig (3.3.2) the distribution of the phase for the eight standards

Table (3.3.2)

THE UNCERTAINTIES IN MAGNITUDE AND PHASE FOR PROCEDURES I AND II

Freq.	Mag. I	Mag. II	Phase I	Phase II
.1	.041	.016	7.4	3.4
.2	.021	.014	4.9	2.7
.3	.018	.0139	3.6	3.5
.4	.014	.016	2.5	2.8
.5	.018	.014	3.6	2.8
.6	.031	.013	5.8	3.7
.7	.103		38.7	
.8	.061		16.1	
.9	.026	.013	6.2	3.3
1	.021	.041	4.38	3.1
1.1	.02	.018	4.8	3.0
1.2	.022	.015	4.7	3.5
1.3	.033	.016	6.3	2.9
1.4	.079		17.6	
1.5	.091		15.9	
1.6	.024	.015	5.3	2.6
1.7	.02	.014	3.9	3.2
1.8	.016	.015	3.06	3.4
1.9	.015	.017	3.22	3.4
2	.024	.013	4.51	2.9

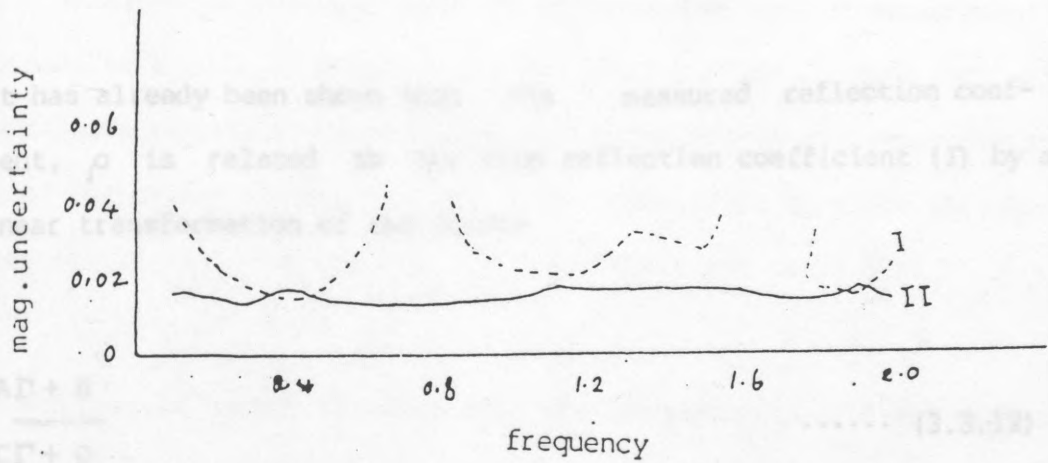
Table (3.3.3)

THE MEAN VALUES OF THE UNCERTAINTY BOTH IN MAGNITUDE  
AND PHASE FOR PROCEDURE I AND II

	Proc. I	Proc. II
No of tested frequency	20	16
Magnitude error	.044	.0148
Phase error	8.12	3.13

Fig. (3.3.3) The uncertainties in magnitude and phase for procedures I and II.

3.3.3 The instability (repeatability) of corrected network-analyser measurements of reflection coefficients error:-



where A, B, C and D are complex constants of the transformation.

Correction methods use three calibrations to establish the values of these constants. These constants are then used in conjunction with a measured reflection coefficient to calculate the true reflection coefficient.

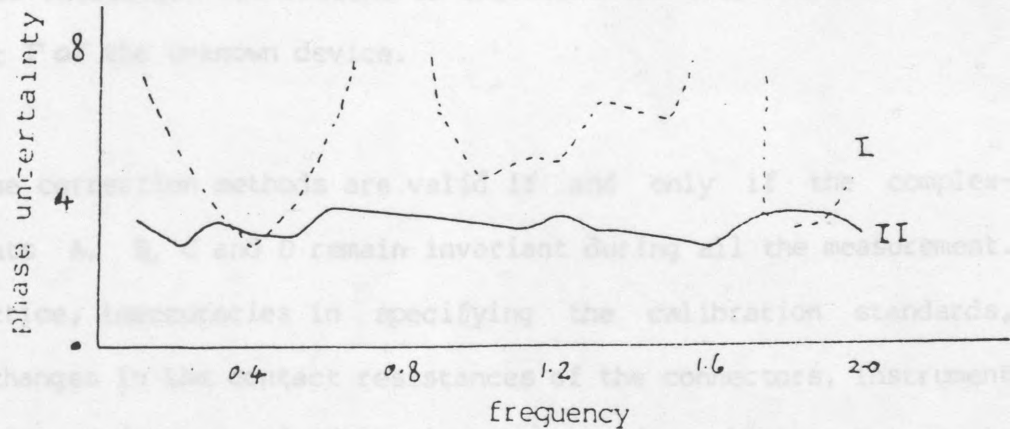


Fig.(3.3.3) The uncertainties in magnitude and phase for procedures I and II.

The method used to verify the stability of the system was taking repeated measurements of the same device to establish the accuracy

3.3.3 The instability (repeatability of corrected network-analyser measurements of reflection coefficients) error:-

It has already been shown that the measured reflection coefficient,  $\rho$  is related to the true reflection coefficient ( $\Gamma$ ) by a bilinear transformation of the form:-

$$\rho = \frac{A\Gamma + B}{C\Gamma + D} \quad \dots\dots (3.3.12)$$

where A, B, C and D are complex constants of the transformation.

Correction methods use three calibrations to establish the values of these constants. These constants are then used in conjunction with a measured reflection coefficient to calculate the true reflection coefficient  $\Gamma$  of the unknown device.

These correction methods are valid if and only if the complex-constants A, B, C and D remain invariant during all the measurement. In practice, inaccuracies in specifying the calibration standards, e.g. changes in the contact resistances of the connectors, instrument amplitude and frequency drift, noise, etc. produce slight changes in these constants and it is inevitable that random errors result.

The method used to verify the stability of the system was taking repeated measurements of the same device to establish the accuracy

limits and confidence level of the measurements. For this method, three short-circuits were used and 60 corrected sets of measurements were made of a line of length 10.35 cm. short-circuit. Each set of measurements comprised three calibration measurements and one measurement of the device followed by the usual computation to yield the corrected result. The frequency of measurement was set to .5 GHz.

The sort of spread obtained when the frequency is held as constant as possible is shown in Fig (3.3.4) and Fig (3.3.5) which represents the relative frequency occurrence of magnitude and phase of reflection coefficient. (A counter was used so that the oscillation frequency at the time of measurements was accurate to  $\pm 0.005$  MHz).

The statistical data from the measurement are presented in Table (3.3.4)

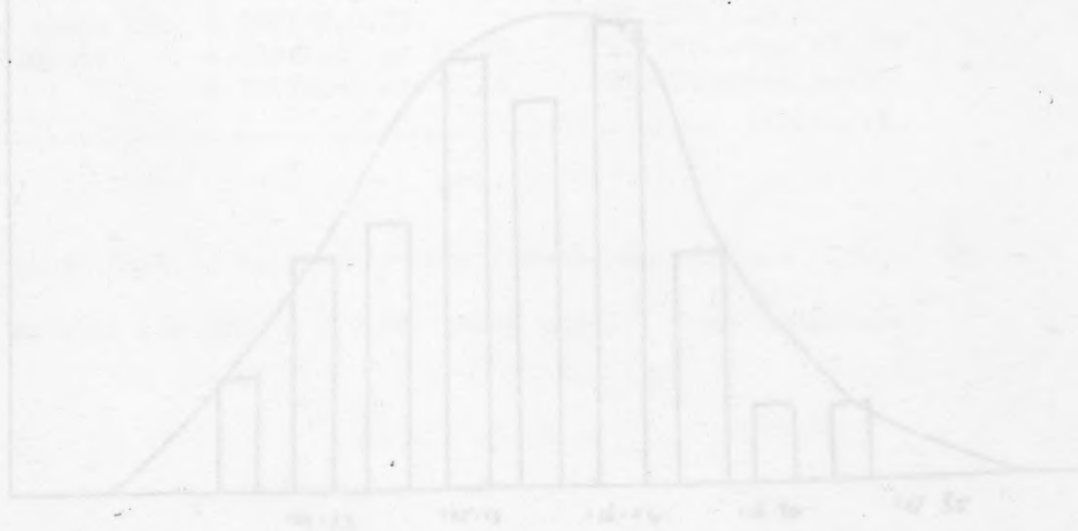


Fig. (3.3.5) Relative frequency of occurrence of the phase of the reflection coefficient.

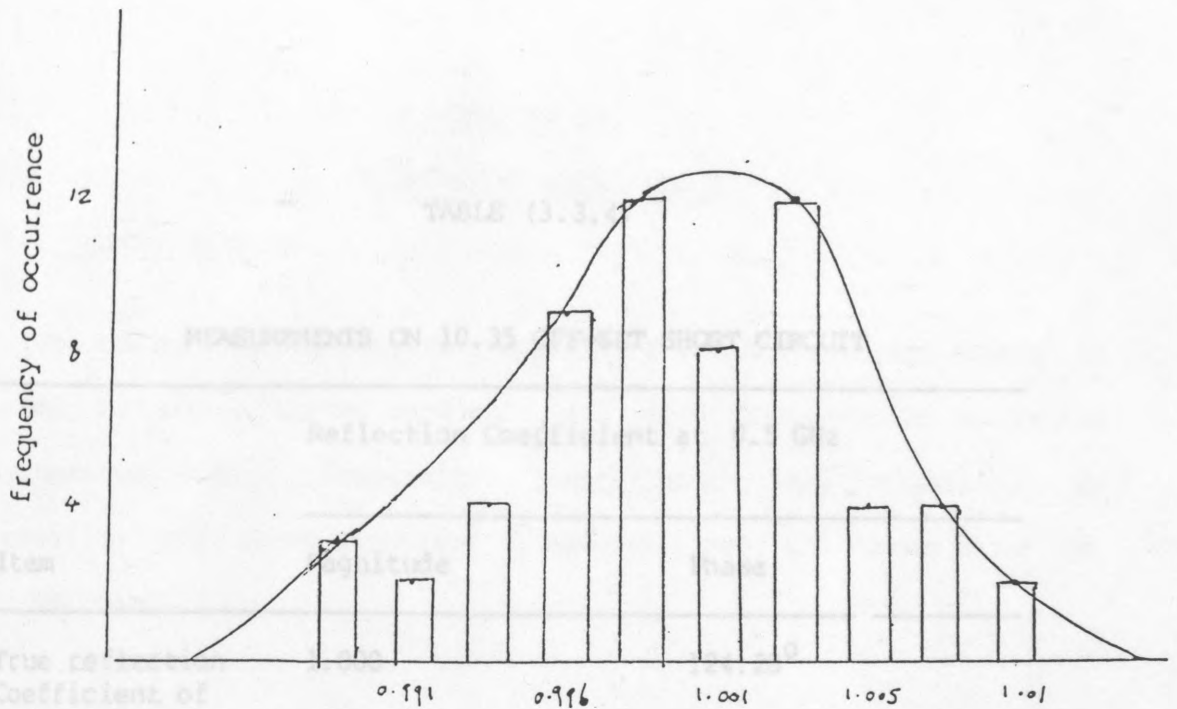


Fig. (3.3.4) Relative frequency of occurrence of magnitude of the reflection coefficient.

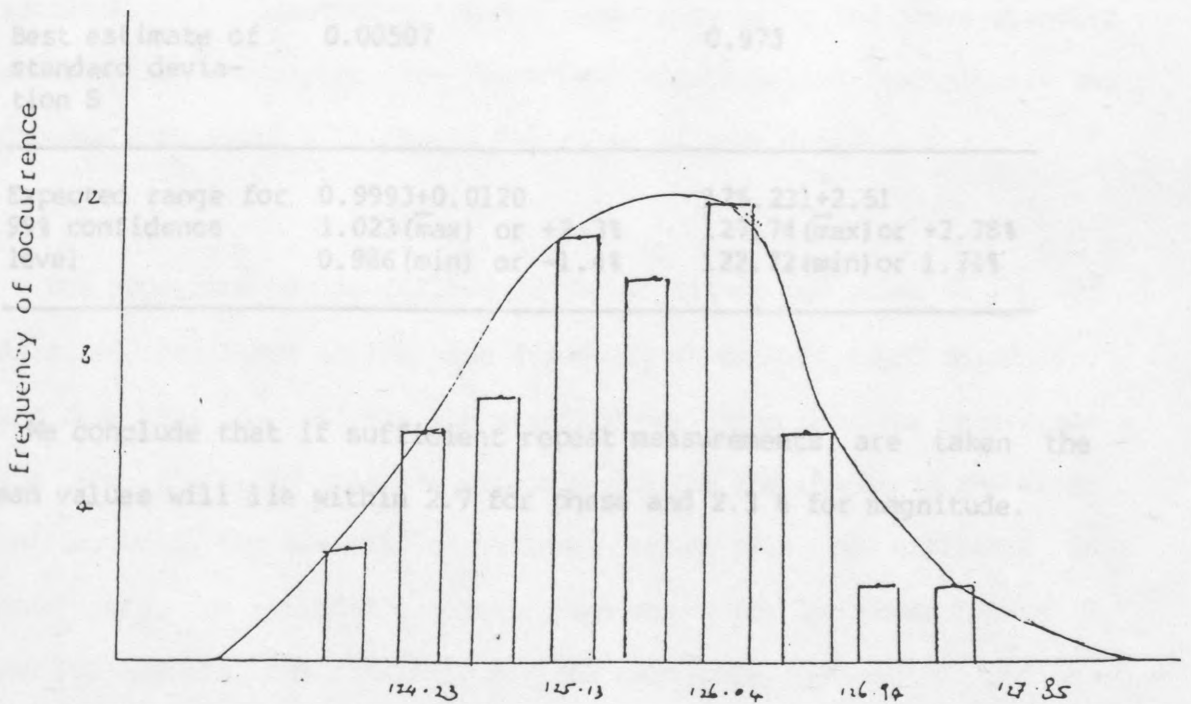


Fig. (3.3.5) Relative frequency of occurrence of the phase of the reflection coefficient.

CHAPTER (4)

MEASUREMENT UNCERTAINTY

TABLE (3.3.4)

4.1 Introduction

MEASUREMENTS ON 10.35 OFF-SET SHORT CIRCUIT

Reflection Coefficient at 0.5 GHz

Item	Magnitude	Phase
True reflection Coefficient of test device	1.000	124.28°
Mean M of 60 measurement	0.99934	125.231°
Best estimate of standard deviation S	0.00507	0.973
Expected range for 99% confidence level	0.9993+0.0120 1.023 (max) or +2.3% 0.986 (min) or -1.4%	125.231+2.51 127.74 (max) or +2.78% 122.72 (min) or 1.24%

We conclude that if sufficient repeat measurements are taken the mean values will lie within 2.7 for phase and 2.3 % for magnitude.

## CHAPTER (4)

### MEASUREMENT UNCERTAINTY

#### 4.1 Introduction :

The calibration of network analyzer for reflection measurements is based on using three standards for each frequency to solve the systematic error (Directivity, Source match, and Tracking). By repeating the above measurements several times, the random error can be estimated.

These errors, have been found by using the following steps : (1) Measuring each of eight standards, ten times. (2) Assigning a standard deviation for the phase and magnitude by means of the analysis of variance. (3) Generating random numbers by using the above standard deviation and applying the bivariate distribution technique. The procedure followed will now be described in more detail.

The procedure was as follows :- The magnitude and phase of  $\rho_{11}$  was measured ten times at the same frequency on each of eight standards, and from this we estimate the standard deviation for the magnitude and the phase. In this way we could predict the change in the error matrix. Using the analysis of variance, which will be explained in next part, we assigned a standard deviation for the phase between 0 and 180 degrees, and similarly for the magnitude between 0 and 1. Then a series of values of the magnitude of  $\rho_{11}$  for the unknown device were taken and with each value a series of random phases. These were used to correct the device under test. The entire calibra-

tion and the measurement correction was carried out about 300 times, and the whole process was repeated with the same magnitude but different phase for the device under test and the procedure was repeated. Applying the technique for bivariate distribution for the two random variables we calculated the uncertainty. This will be studied in detail in the next section.

The reflection coefficient measurements  $S_{11}$  were carried out ten times at each frequency (5-20GHz) for each of the eight standards (which were available at the time), shown in Table (4.2.1) and Fig (4.2.1). The weighted mean and standard deviation were calculated in Appendix (7.5). We have in Tables (4.2.2,4.2.4) and Tables (4.2.3,4.2.5) the weighted mean and the standard deviation for the measured magnitude and phase of the  $S_{11}$  (measured in dB and degrees respectively). From Table (4.2.4) and Table (4.2.5) the standard deviation in phase higher than in dB for the standards.

TABLE (4.2.1)

standard no (1)		short-circuit
standard no (2)	10.35	offset-short
standard no (3)	20.35	offset-short
standard no (4)	30.70	offset-short
standard no (5)		open-circuit
standard no (6)	10.35	offset-open
standard no (7)	20.35	offset-open
standard no (8)	30.70	offset-open

standards used in the calibration procedure

#### 4.2 Analysis of experimental work:

As mentioned before, the errors in the system have been found by using three steps. This section deals with the first part of the procedure

The reflection coefficient measurements  $S_{11}$  were carried out ten times at each frequency (.5-2GHz) for each of the eight standards (which were available at the time), shown in Table (4.2.1) and Fig (4.2.1). The weighted mean and standard deviation were calculated in Appendix (7.5). We have in Tables (4.2.2,4.2.4) and Tables (4.2.3,4.2.5) the weighted mean and the standard deviation for the measured magnitude and phase of the  $\rho_{11}$  (measured in dB and degrees respectively). From Table (4.2.4) and Table (4.2.5) the standard deviation in phase higher than in dB for the standards.

TABLE (4.2.1)

standard no (1)		short-circuit
standard no (2)	10.35	offset-short
standard no (3)	20.35	offset-short
standard no (4)	30.70	offset-short
standard no (5)	.	open-circuit
standard no (6)	10.35	offset-open
standard no (7)	20.35	offset-open
standard no (8)	30.70	offset-open

standards used in the calibration procedure

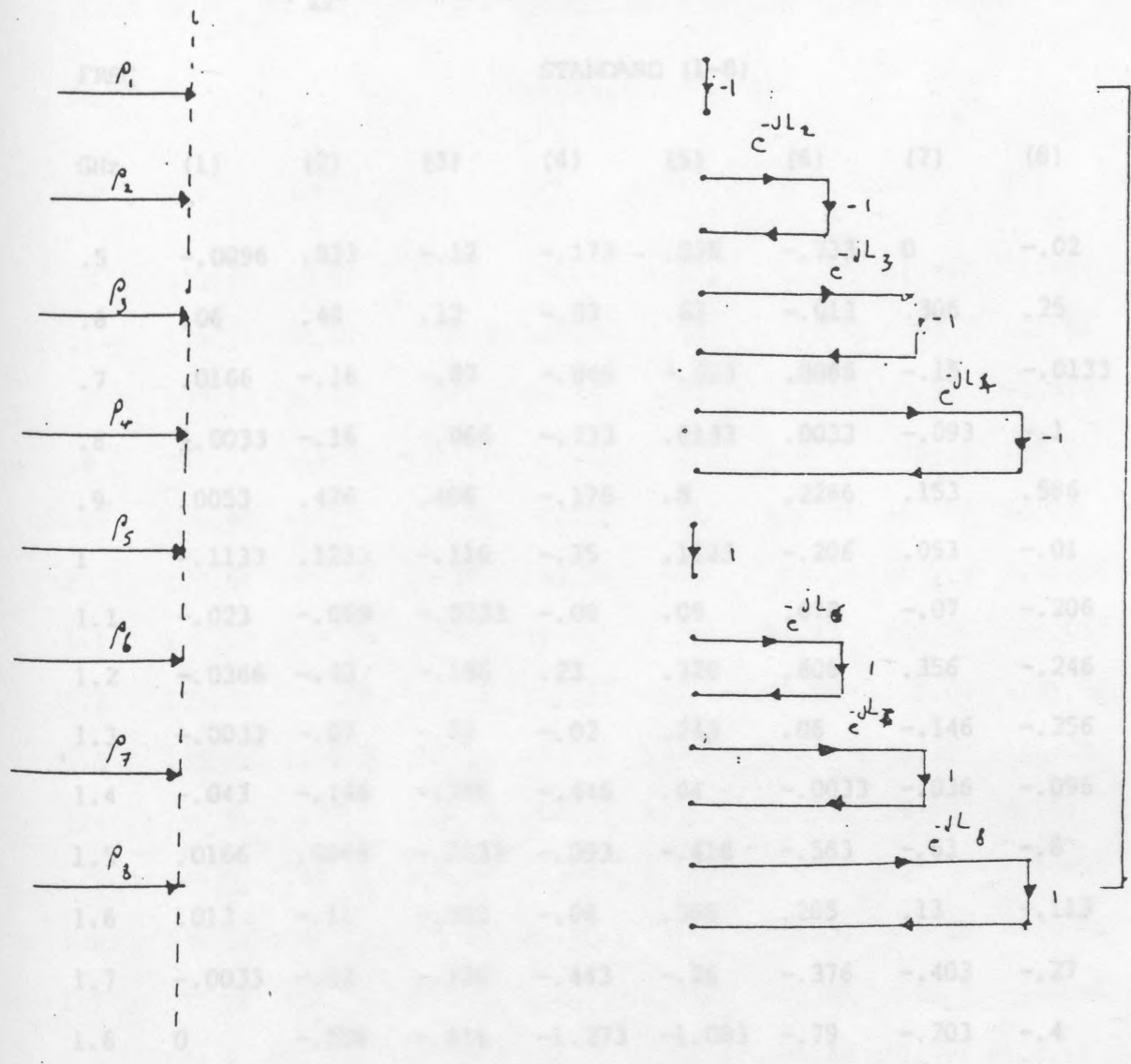
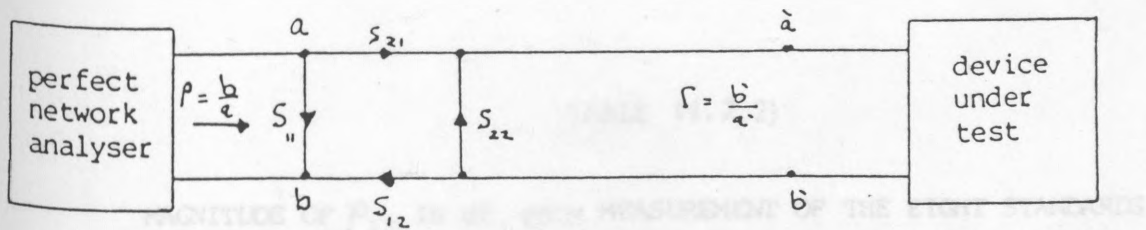


Fig.(4.2.1) Signal-flow graphs of system under calibration..

TABLE (4.2.2)

MAGNITUDE OF  $\rho_{11}$  IN dB FROM MEASUREMENT OF THE EIGHT STANDARDS

FREQ GHz	STANDARD (1-8)							
	(1)	(2)	(3)	(4)	(5)	(6)	(7)	(8)
.5	-.0096	.033	-.12	-.173	.036	-.733	0	-.02
.6	.06	.48	.12	-.03	.63	-.013	.306	.25
.7	.0166	-.16	-.87	-.846	-.033	.0066	-.15	-.0133
.8	-.0033	-.16	-.066	-.233	.0133	.0033	-.093	-.1
.9	.0053	.426	.406	-.176	.8	.2266	.153	.586
1	-.1133	.1233	-.116	-.35	.1133	-.206	.053	-.01
1.1	-.023	-.069	-.0233	-.08	.09	.078	-.07	-.206
1.2	-.0366	-.43	-.196	.23	.326	.606	.356	-.246
1.3	-.0033	-.07	-.02	-.02	.243	.06	-.146	-.256
1.4	-.043	-.146	-.386	-.446	.04	-.0033	-.036	-.096
1.5	.0166	.0066	-.1133	-.093	-.416	-.583	-.63	-.8
1.6	.013	-.11	-.093	-.08	.366	.285	.13	-.113
1.7	-.0033	-.02	-.126	-.443	-.26	-.376	-.403	-.27
1.8	0	-.536	-.816	-1.273	-1.083	-.79	-.203	-.4
1.9	-.033	.17	.13	-.316	.363	-.056	-.11	.16
2	.04	-.646	-.68	-.216	-.686	-.176	-.283	-.875

TABLE (4.2 3)

PHASE OF  $\rho_{11}$  IN DEGREES FROM MEASUREMENTS OF THE EIGHT STANDARDS

FREQ GHz	STANDARD NO (1-8)							
	(1)	(2)	(3)	(4)	(5)	(6)	(7)	(8)
.5	179.67	59.66	-60.7	174.93	.739	-122.7	117.47	-4.04
.6	179.77	34.02	-112.5	100.98	1.12	-149.05	8.2	-81.33
.7	179.63	9.063	-159.7	29.25	.185	-173.4	19.913	-153.73
.8	179.73	-17.54	151.38	-47.46	1.181	159.58	-30.36	131.09
.9	179.86	-44.01	101.85	-123.3	1.311	134.07	-81.97	56.07
1	179.61	-69.29	58.98	162.59	.647	109.72	-130.9	-19.106
1.1	179.83	-94.16	4.95	90.46	1.155	84.45	178.95	-94.03
1.2	179.91	-120.0	-50.41	12.32	1.67	56.85	126.84	-171.96
1.3	179.87	-144.2	-98.43	-62.14	1.48	32.58	79.39	114.89
1.4	179.91	-169.7	-149.7	-140.2	1.151	6.653	29.62	40.84
1.5	179.9	164.35	163.49	148.9	1.167	-19.61	-21.5	-34.42
1.6	179.88	141.31	116.79	77.26	.516	-44.37	-71.28	-109.52
1.7	179.98	114.73	64.76	4.66	1.314	-72.97	-121.3	-184.45
1.8	179.9	89.81	67.89	-72.35	1.827	-94.32	-167.6	102.36
1.9	179.6	64.44	-36.8	-147.57	.615	-121.09	142.1	27.59
2	179.33	37.65	-84.01	142.66	3.57	-143.66	91.91	-50.1

TABLE (4.2.4)

STANDARD DEVIATION OF THE MAGNITUDE  $\rho_{11}$  IN dB FROM MEASUREMENT OF THE EIGHT  
STANDARDS

FREQ GHZ	STANDARD NO (1-8)							
	(1)	(2)	(3)	(4)	(5)	(6)	(7)	(8)
.5	.0005	.1171	.01	.04	.0116	.055	0	.016
.6	.0608	.036	.0173	.07	.05	.051	.0461	.086
.7	.0208	.043	1.412	1.026	.049	.0152	.0458	.0901
.8	.0057	.1216	.081	.057	.015	.0057	.0057	.01
.9	.0092	.047	.032	.049	0	.0057	.0058	.127
1	.140	.149	.189	.055	.0208	.0305	.061	.026
1.1	.049	.0525	.0057	.0173	.0172	.0115	.03	.0115
1.2	.055	.1044	.1305	.111	.141	.11	.089	.119
1.3	.0057	.1126	.1	.072	.045	.0529	.055	.056
1.4	.075	.062	.032	.15	.105	.1124	.126	.116
1.5	.076	.0305	.080	.0115	.104	.0896	.086	.086
1.6	.041	.026	.0115	.01	.135	.104	.134	.126
1.7	.0057	.0173	.055	.075	.04	.068	.058	.06
1.8	.01	.158	.551	.11	.09	.085	.025	.1
1.9	.057	.036	.026	.076	.023	.045	.03	.086
2	.052	.047	.115	.023	.080	.068	.028	.094

TABLE (4.2.5)

STANDARD DEVIATION OF THE PHASE  $\theta_{11}$  IN DEGREES FROM MEASUREMENTS OF THE EIGHT STANDARDS

FREQ GHz	STANDARD NO (1-8)							
	(1)	(2)	(3)	(4)	(5)	(6)	(7)	(8)
.5	.56	.588	1.124	4.465	.734	.609	3.117	2.6
.6	.31	.96	1.697	1.0	1.12	1.0	.586	2.07
.7	.224	1.605	.404	1.29	.185	1.216	1.811	1.418
.8	.378	.506	1.06	.796	1.812	.52	1.57	1.012
.9	.23	1.726	1.231	1.523	1.311	1.007	.04	1.008
1	.871	1.229	2.66	1.027	.647	1.11	.121	1.54
1.1	.208	1.449	2.73	2.34	1.155	2.35	1.002	1.668
1.2	.076	.945	2.411	3.05	1.67	.79	1.77	4.39
1.3	.213	.415	.511	.248	1.485	1.229	2.256	2.007
1.4	.228	.696	1.932	2.59	1.15	1.166	2.13	1.88
1.5	.721	.563	1.5	.863	1.16	1.206	1.322	1.92
1.6	.202	1.19	2.08	1.61	.516	1.471	1.24	1.75
1.7	.023	1.35	1.36	.577	1.314	3.03	1.446	1.37
1.8	.173	.317	1.94	2.51	1.82	1.14	2.32	.623
1.9	.69	.95	2.98	.739	.615	1.63	.1	1.027
2	1.15	2.06	3.44	2.08	3.57	1.52	1.866	6.06

#### 4.3 The logic of the analysis of variance:-

The purpose of the simple analysis of variance is to determine the probability that the means of several groups deviate from one another merely by sampling error. Two estimates of the variance in the population are computed. One of these estimates is based upon the deviation of the group means about the grand mean (mean over all groups in the total analysis). Because this variance estimate is based upon the deviation of group means about the grand mean, it is called the between-groups estimate of the population variance. In contrast, one can also estimate the variance of the groups in the population from the deviation of individuals about their respective group means. It can be shown that such an estimate is not influenced by differences in group means but only by the random variability of individual observations. Since this estimate is determined by the deviation of individuals within each group about their mean, it is known as the within-groups estimate of the population variance.

The two variance estimates differ only by virtue of the fact that the between-groups estimate is sensitive to differences between the group means while within-groups estimate is not, therefore the analysis of variance provides these two estimates of the population variance. Applying the F-test to these variances indicates whether there is a significant difference between them or not. The analysis of variance and the F-test is explained in Appendix(7.6).

The analysis of variance was applied to Table (4.2.4) in order to see whether the standard deviation of S was related to frequency or to the standards used, and similarly to the data of Table (4.2.5).

Referring to table (4.3.1) and Table (4.3.2), it is seen that the variance between standards is greater than the variance within frequency for both the magnitude and phase. This shows that the deviation is related to the standards used. Also applying the F-test for both the magnitude and phase, in confidence levels 95% and 99%, the F-test was found only to be significant in phase.

TABLE (4.3.1)

ANALYSIS OF VARIANCE FOR THE dB IN TABLE (4.2.4)

source of variation.	sum of squares	degrees of freedom	variance estimate
between standards	.2367	7	.033822
within frequency	2.9311	120	.0244
total	3.167	127	

$$F = .0338 / .0244 = 1.38$$

F(7,120) from the table = 2.07 (5%) and 2.76 (1%)

not significant.

$$\text{standard deviation} = \sqrt{.033} = .183$$

TABLE (4.3.2)

ANALYSIS OF VARIANCE FOR THE PHASE IN TABLE (4.2.5)

source of variance	sum of squares	degrees of freedom	variance estimate
between standards	29.01	7	4.144
within frequency	89.68	120	.747
total	118.69	127	

$$F = 4.14/.747 = 4.54$$

significant (ie the variation within the sets is different from the variation between sets)

$$\text{standard deviation} = \sqrt{4.14} = 2.035$$

From table (4.3.1) and (4.3.2) the estimated standard deviation in dB = .183 and the estimated standard deviation in phase = 2.035. These enable the variation of the error matrix for the network to be predicted. Using these two standard values, to generate a random number to the measured reflection coefficient for the eight standards, picking any three depending on the frequency used to calculate a set of s-parameter error, then correct the device under test. i.e from the experimental work by measurement of each of the eight standards ten times at each frequency we are able to predict and estimate the

variation in the error matrix, using the computer program to find the uncertainty in the network analyzer.

The previous work with a normal distribution of random errors deals with only one-dimensional linear error theory. To examine the accuracy of a quantity in a plane with respect to two axes, however a further error analysis must be employed. The distribution which deals with two-number variables is the bivariate distribution (see K. A. Brownell). When the variables are normally distributed, their joint distribution is called a bivariate normal distribution.

A single measurement of  $S_{11}$  was corrected using synthesized standard corrections to which random variations had been applied. This correction was repeated 20 times and the distribution of magnitude and phase were studied.

A hypothetical bivariate distribution for the magnitude and the phase is illustrated in Figure (4.4.1). The density for the magnitude and the phase may be represented by a bell-shaped surface as shown in Fig (4.4.1). If we are merely having an axis, we now have a magnitude phase plane. The height of the bars shows the frequency of each event which is the number of a pair (mag. phase). A point on the plane indicates a value as shown in Fig (4.4.1).

Fig (4.4.1) is a graphical illustration of a joint distribution of two variables. When we have a frequency surface instead of a frequency curve, we are studying population at some phase, say (phase=9.8). As Fig (4.4.1) shows, we have a frequency distribution

#### 4.4 Two-dimensional errors (general theory):-

The previous work with a normal distribution of random errors deals with only one-dimensional linear error theory. To examine the accuracy of a position in a plane with respect to two axes, however a further error analysis must be employed. The distribution which deals with two-random variables is the bivariate distribution (see K A. Brownlee). When two variables are normally distributed, their joint distribution is called a bivariate normal distribution.

A single measurement of  $S_{ii}$  was corrected using synthesized standard corrections to which random variations had been applied. This correction was repeated 73 times and the distribution of magnitude and phase were studied.

A hypothetical bivariate distribution for the magnitude and the phase is illustrated in Table (4.4.1). The density for the magnitude and the phase may be represented by a bell-shaped surface as shown in Fig (4.4.1). Instead of merely having an axis, we now have a magnitude phase plane, and the height of the bars shows the frequency of each event which is made up of a pair (mag. phase). A point on the plane indicates an event as in Fig (4.4.1).

Fig (4.4.1) is a generalised illustration of a joint distribution of two variables, where we now have a frequency surface instead of a frequency curve. Let us slice this population at some phase, say (phase=9.8). As Fig (4.4.1) shows, we have a frequency distribution

of magnitude for the given phase. That is, we have a subpopulation of magnitudes corresponding to a given phase, and this subpopulation is shown by the column corresponding to phase in Table (4.4.1).

But now let us slice the population at a magnitude, say ( $\text{mag} = .997$ ). Then we have a corresponding subpopulation of phase which is given by the row corresponding to the magnitude = .997 i.e in Table (4.4.1) we have a family of subpopulation of magnitudes corresponding to a given phase.

Any plane parallel to the (mag. phase) plane which cuts the surface will intersect it in an elliptical curve.

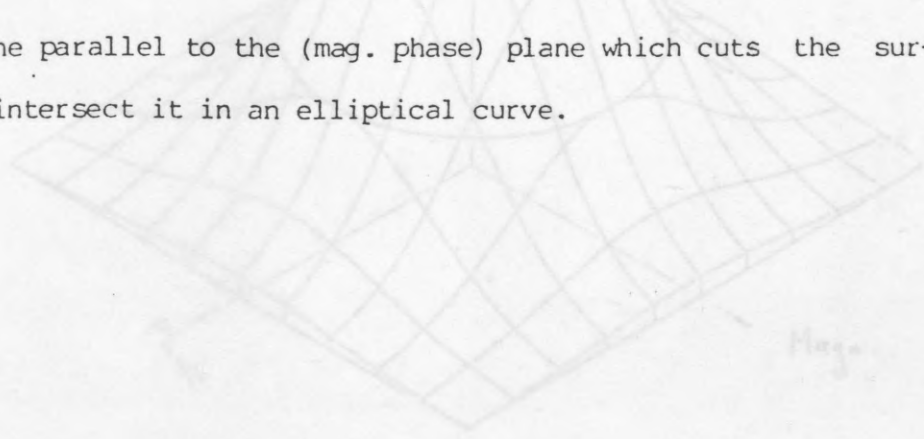


Fig. (4.4.3) The density for the magnitude and phase represented by a bell-shaped surface.



Elliptical error probability

If we consider that  $x$  is the error in the magnitude and  $y$  the error resulting from phase error, assuming that each is random and independent, then the two-dimensional probability density distribution...

TABLE (4.4.1)

A hypothetical bivariate distribution

$$f(x,y) = \frac{1}{2\pi\sigma_x\sigma_y} \exp\left\{-\frac{1}{2}\left[\frac{x^2}{\sigma_x^2} + \frac{y^2}{\sigma_y^2}\right]\right\} \quad (4.4.1)$$

	8.94	9.33	9.76	9.8	9.82	9.82	10	10.03	10.26	10.85	magt.
.989	1										1
.990		1	1	1							3
.991		2	2	2	1						7
.992			3	3	2						8
.994			2	4	2	1					9
.997				3	4	3	2				12
.999				3	4	3	2				12
.998				2	4	2	1	1			10
1.0					2	1	2	1	1		7
1.01							1	1	1	1	4
phase	1	3	9	18	20	9	7	3	3	2	73

where  $\sigma$  is the standard deviation

This shows that as the value of  $\sigma$  varies from zero to infinity, a family of equal probability density ellipses will occur with axes  $\sigma_x$  and  $\sigma_y$  and  $\sigma_x\sigma_y$  respectively, as shown in Fig (3.4.2). The integral of the probability density function is the probability distribution function. The probability of being within an ellipse is given by the distribution function.

Elliptical error evaluation:-

If we consider that  $\pm x$  is the error in the magnitude and  $\pm y$  the error resulting from phase error, assuming that each is random and independent, then the two-dimensional probability density distribution. and that there is a 99% probability that the actual position in x and y will fall simultaneously within that area.

$$P(x) \cdot P(y) = \frac{1}{S(x) \cdot S(y) 2\pi} \exp\left\{-\left(\frac{x^2}{2S(x)^2} + \frac{y^2}{2S(y)^2}\right)\right\} \dots\dots\dots(4.4.1)$$

Solving this equation for a given value of K yields the values of probability distribution shown in the accompanying table.

Since for given value of P(x) and P(y), the left hand side is a constant

$$K^2 = \frac{x^2}{S(x)^2} + \frac{y^2}{S(y)^2}$$

where K is the probability constant

S(x) , S(y) the standard deviation

This shows that for values of K varying from zero to infinity, a family of equal probability density ellipses will occur with axis K S(x) and K S(y) (see B.A.Barry) as shown in Fig (4.4.2). The integral of the probability density function is the probability distribution function. The probability of being within an ellipse is given by the distribution function:

$$P(x,y) = 1 - \exp(-K^2/2)$$

This means for example, that when  $K = 3.5$  the axes of the ellipse are  $3.5 S(x)$  and  $3.5 S(y)$  and that there is a 99% probability that the actual position error in  $x$  and  $y$  will fall simultaneously within that area.

Solving this equation of various value of  $K$  yields the values of probability percentages shown in the accompanying table.

Probability, P

(%)             $K$

---

90            2.146

95            2.44

99            3.5

#### 4.5 Non-Linear Transformation

In a previous section, equation (3.2.3) shows that the measured reflection coefficient  $\rho$  is related to the true reflection coefficient  $\Gamma$  of the device under test by:

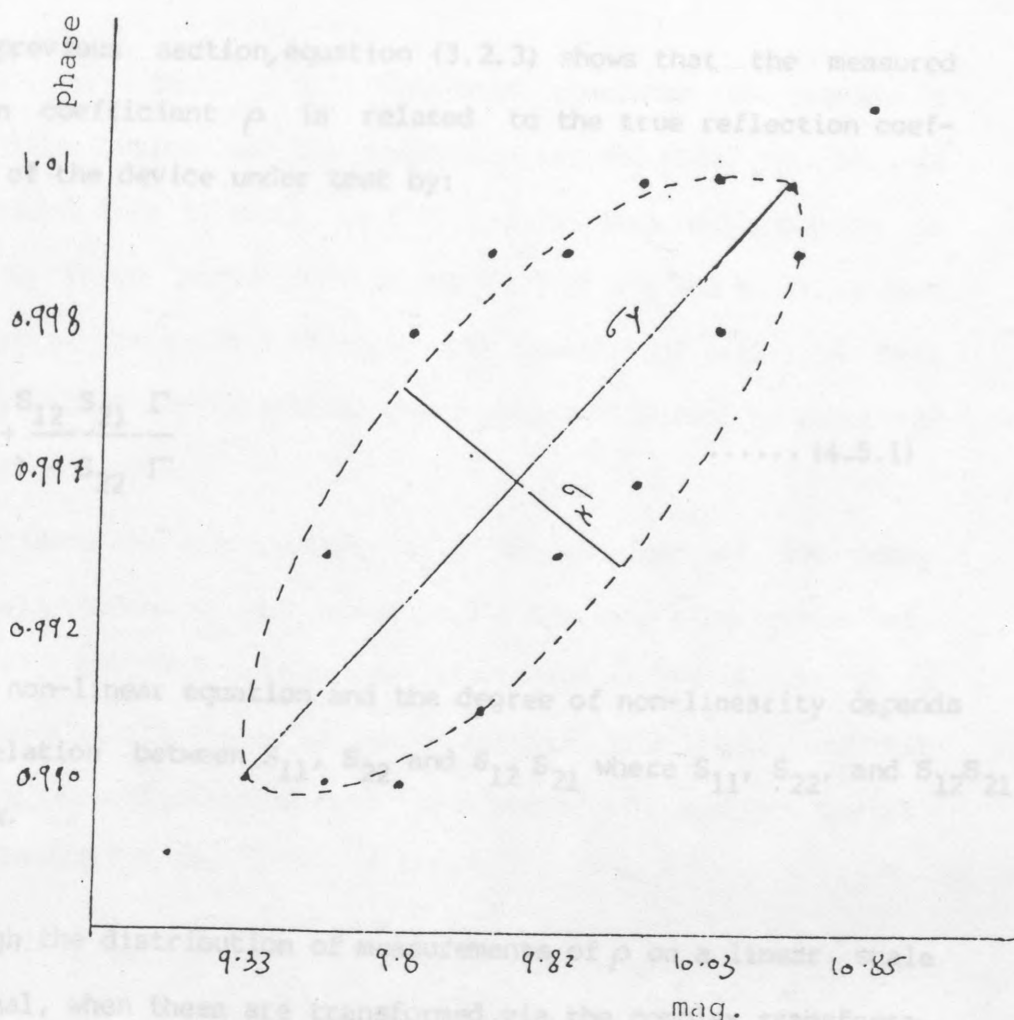


Fig. (4.4.2) Probability density ellipse.

(A hypothetical bivariate distribution in Table (4.4.1))

#### 4.5 Non-Linear Transformation:-

In a previous section, equation (3.2.3) shows that the measured reflection coefficient  $\rho$  is related to the true reflection coefficient  $\Gamma$  of the device under test by:

$$\rho = S_{11} + \frac{S_{12} S_{21} \Gamma}{1 - S_{22} \Gamma} \quad \dots\dots (4.5.1)$$

This is non-linear equation and the degree of non-linearity depends on the relation between  $S_{11}$ ,  $S_{22}$  and  $S_{12} S_{21}$  where  $S_{11}$ ,  $S_{22}$ , and  $S_{12} S_{21}$  are complex.

Thus although the distribution of measurements of  $\rho$  on a linear scale may be normal, when these are transformed via the complex transformation to values of  $\Gamma$  the distribution will be skew. However, if the dispersion is small, it may still be justified to use the normal distribution on the new scale. also the student t-test and Fisher F-test show that this assumption is justified.

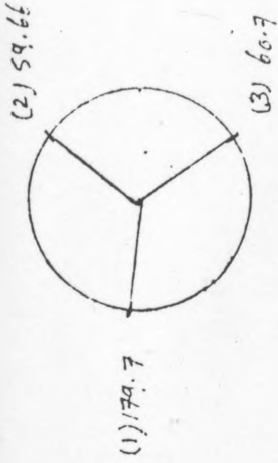
table (4.5.1) shows the distribution (300 random) of the true ( $\Gamma$ ) reflection coefficient for the measured value  $\rho = .5 \angle 10$  at the frequency .5GHz with the 3-standards used in the calibration procedure

[short circuit, 10.35 offset-short circuit and 20.35 offset-short circuit].

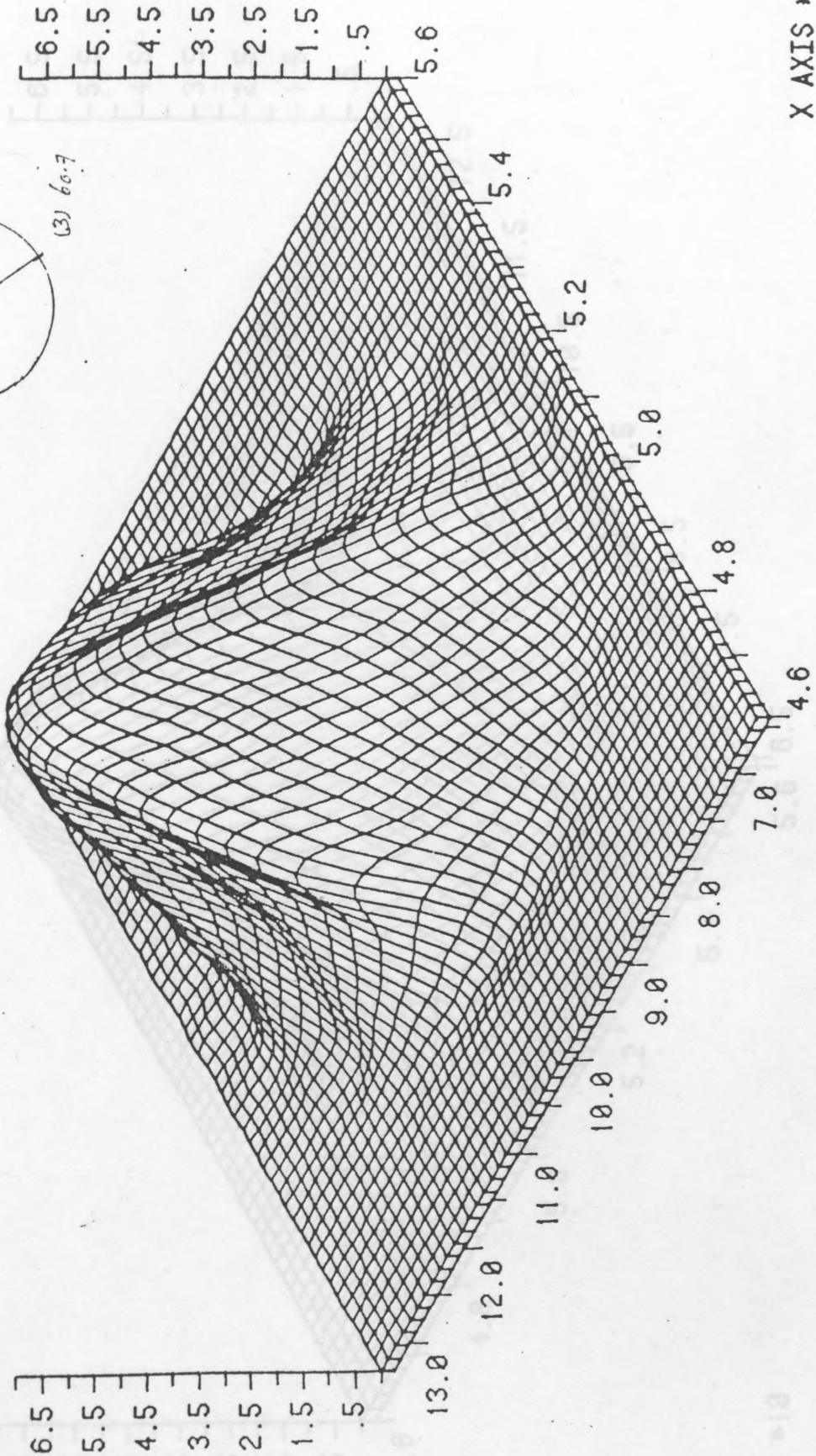
The results from Table (4.5.1) have been cumulated to provide a frequency distribution on the magnitude (x) and phase (y). this is shown in tabulat form in table (4.5.2). This same distribution is displayed in three projections in Fig (4.5.1) a,b and c. It is seen that the form of the surface is reasonably smooth, and bell-like. This it will be recalled used standards whose phases different by about 120 degrees from each other

To investigate the effects which will be obtained if the phase angle between standards is close to 360 the same calculations were repeated for .7 GHz. The results are illustrated in Fig (4.5.2). It is seen that the distribution is no longer anything like normal, and that the nonlinear transformations lead to a number of spurious maxima and minima in the curves.

- (1) short-circuit
- (2) 10.35 offset-short
- (3) 20.35 offset-short



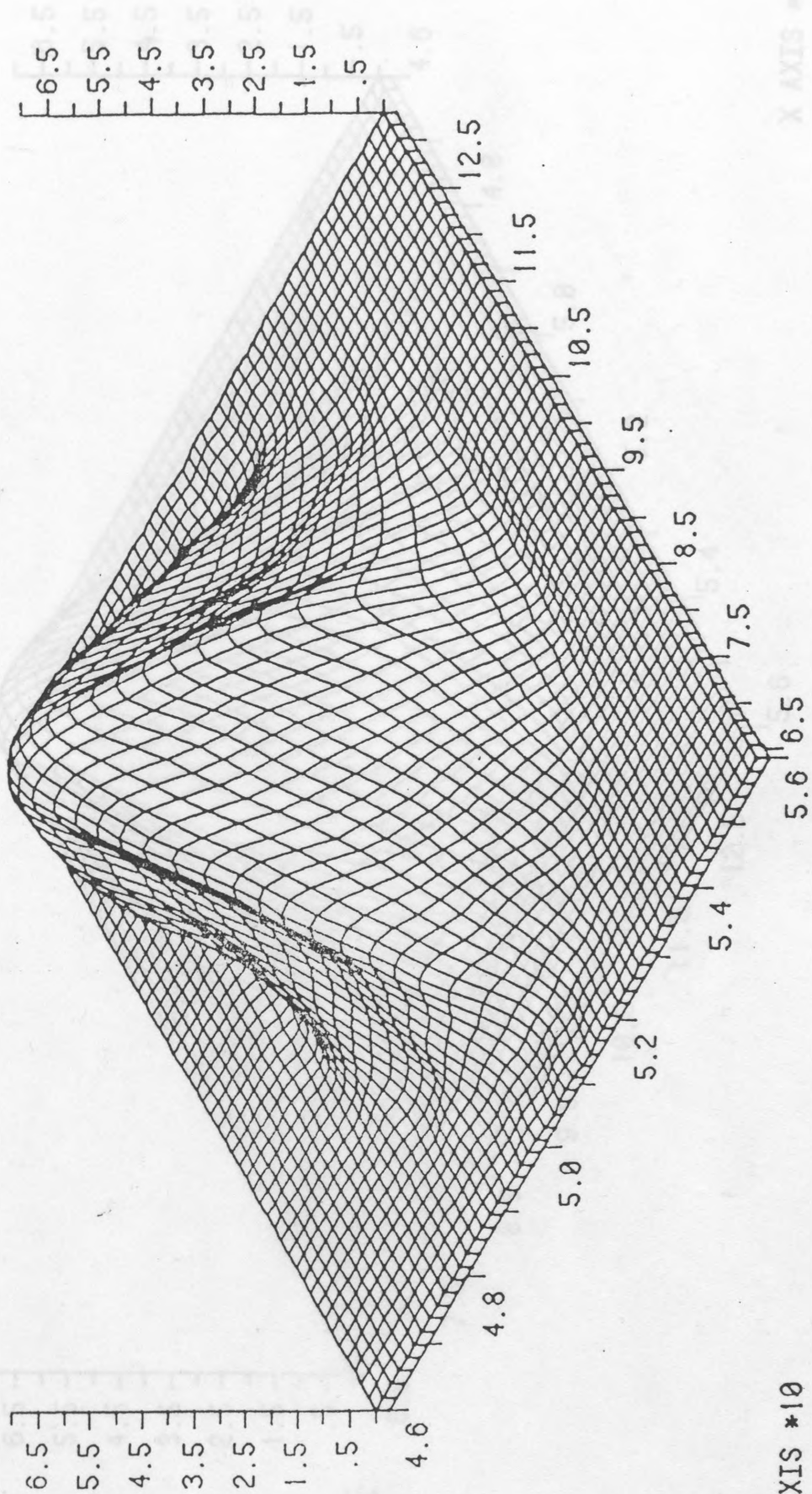
Freq. = .5GHz



X AXIS \*10

Fig (4.5.1)a. The density distribution for the magnitude and phase in Table (4.5.2).

Rotating Fig (4.5.1)a  $90^\circ$



X AXIS \*10

X AXIS \*10

Fig (4.5.1)b

Rotating Fig (4.5.1)  $\alpha 180^\circ$

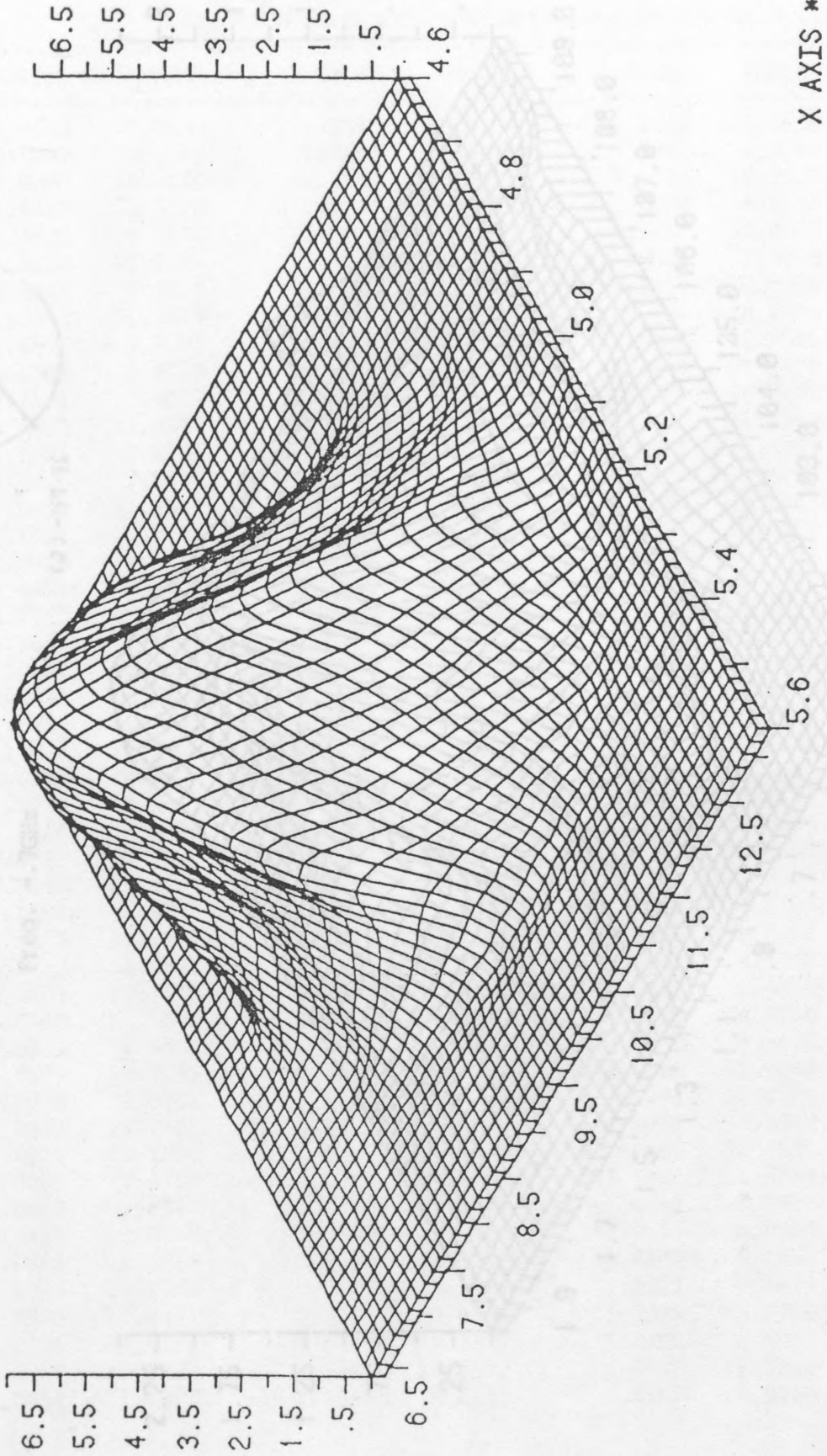
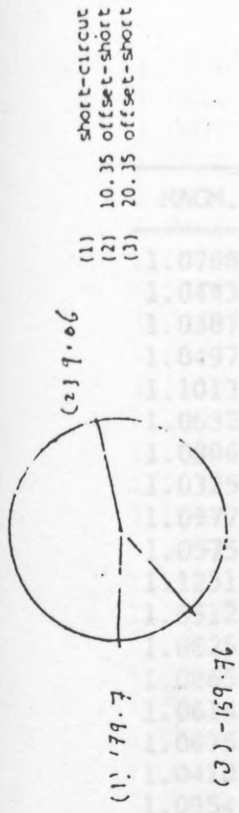


Fig (4.5.1)c



Freq. = .7GHz

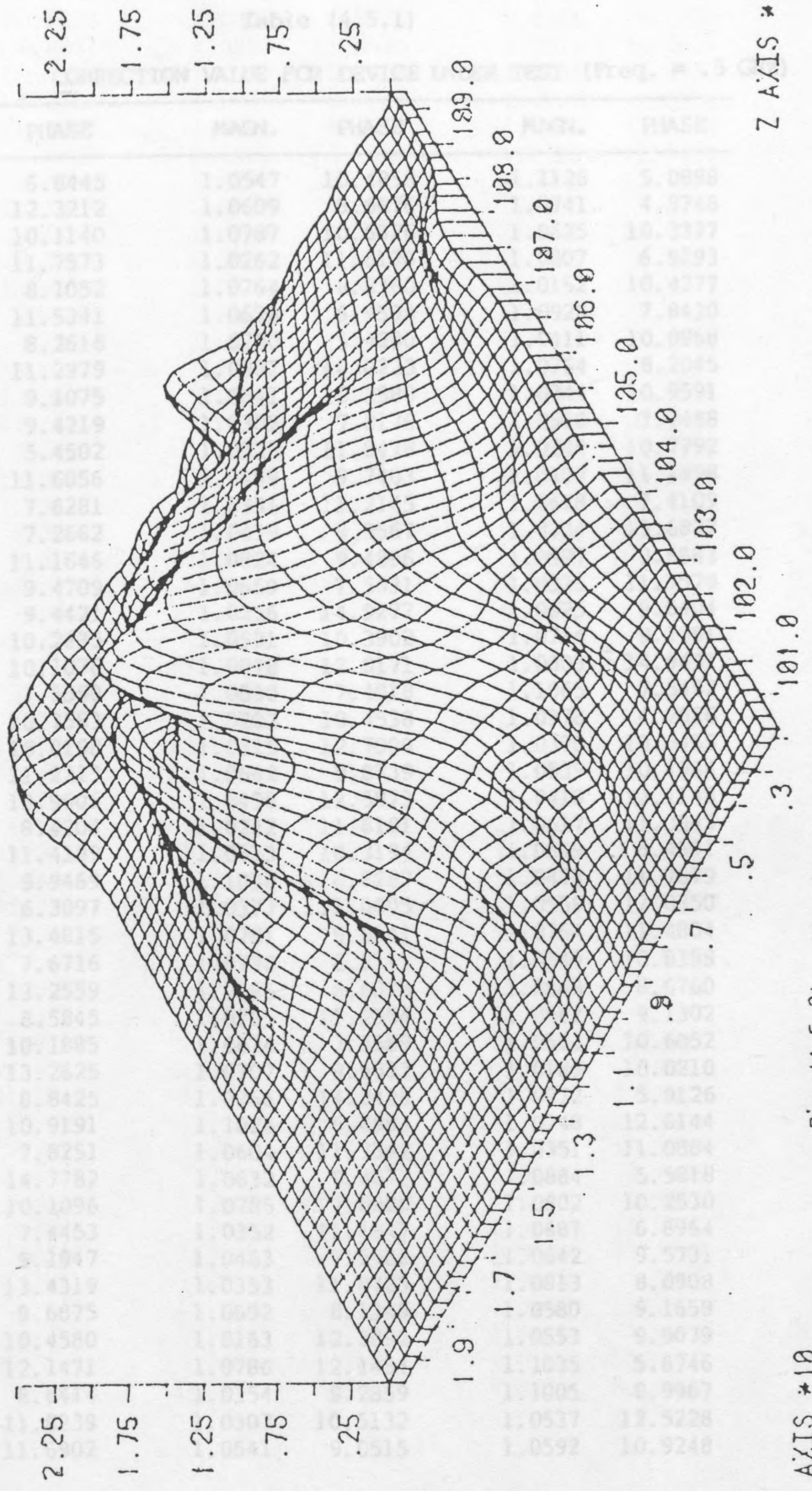


Fig. (4.5.2) The density distribution for the magnitude and phase

Table (4.5.1)

CORRECTION VALUE FOR DEVICE UNDER TEST (Freq. = .5 GHz)

MAGN.	PHASE	MAGN.	PHASE	MAGN.	PHASE
1.0768	6.8445	1.0547	10.4858	1.1128	5.0898
1.0443	12.3212	1.0609	8.6676	1.0741	4.9748
1.0387	10.1140	1.0787	10.6326	1.0625	10.3377
1.0497	11.7573	1.0262	11.6176	1.0807	6.9293
1.1013	8.1052	1.0764	8.8360	1.0152	10.4277
1.0632	11.5341	1.0678	6.9594	1.0928	7.8430
1.0806	8.2616	1.0700	5.4290	1.0411	10.0968
1.0325	11.2979	1.0902	10.0225	1.0764	8.2045
1.0977	9.1075	1.0641	10.2588	1.0344	10.9591
1.0575	9.4219	1.0302	7.8176	1.0968	7.7488
1.1231	5.4502	1.0323	11.8478	1.0240	10.7792
1.0512	11.6056	1.0499	9.7403	1.0407	11.1898
1.0825	7.6281	1.0331	11.2145	1.0678	7.4109
1.0865	7.2662	1.0439	9.9567	1.0334	13.6827
1.0614	11.1646	1.0824	9.4896	1.0927	9.6883
1.0675	9.4709	1.0659	7.5631	1.0335	11.7579
1.0410	9.4421	1.0236	14.9277	1.0625	9.6404
1.0954	10.2235	1.0591	10.3902	1.0714	9.1291
1.0785	10.1076	1.0078	12.8171	1.0003	14.9431
1.0697	7.5550	1.0630	7.4018	1.1065	7.5482
1.0667	10.7583	1.0202	10.4538	1.0978	4.2826
1.0172	15.0198	1.0315	12.7000	1.0370	10.6455
1.0466	11.2213	1.0642	9.8739	1.0539	10.1964
1.0017	13.9606	1.0498	12.5873	1.0410	13.1148
1.0799	8.4204	1.0242	11.6191	1.0617	11.3943
1.0345	11.4189	1.0673	10.3194	1.0549	8.4591
1.0596	9.9469	1.1038	6.8287	1.0473	11.7679
1.0892	6.3897	1.0377	11.0005	1.0559	12.0350
1.0367	13.4815	1.0781	9.5541	1.0764	11.4804
1.0896	7.6716	1.0738	8.9111	1.0549	10.8398
1.0217	13.2559	1.0595	8.6078	1.0563	8.6760
1.0732	8.5845	1.0765	11.2354	1.0962	9.1302
1.0609	10.1885	1.0674	7.5589	1.0533	10.6052
1.0160	13.2625	1.0707	9.5533	1.0189	10.0210
1.0839	8.8425	1.0266	14.3420	1.0972	5.9126
1.0575	10.9191	1.1026	6.4983	1.0248	12.6144
1.0846	7.8251	1.0604	11.7342	1.0351	11.0884
1.0142	14.7782	1.0632	9.4072	1.0884	5.5818
1.0922	10.1096	1.0785	7.0020	1.0802	10.2530
1.0855	7.4453	1.0352	11.1847	1.0687	6.8964
1.0808	9.1947	1.0463	7.5562	1.0642	9.5731
1.0489	13.4319	1.0353	11.0725	1.0813	8.0908
1.0969	9.6875	1.0692	8.1349	1.0580	9.1659
1.0755	10.4580	1.0163	12.3892	1.0553	9.9079
1.0290	12.1471	1.0786	12.1454	1.1035	5.6746
1.0576	8.6414	1.0354	9.2859	1.1005	8.9967
1.0365	11.8239	1.0307	10.5132	1.0537	12.5228
1.0454	11.6902	1.0541	9.0515	1.0592	10.9248

1.0550	10.6628	1.0601	8.8403	1.0584	8.2976
1.0617	9.4881	1.0803	11.2636	1.0302	12.0633
1.0677	10.8509	1.0978	6.0594	1.0569	10.4733
1.0519	9.4093	1.0402	9.7810	1.0852	8.0951
1.0437	10.1195	1.0480	8.1954	1.0342	12.6458
1.0485	7.3383	1.1361	5.4990	1.0090	11.7363
1.0557	8.8254	1.0884	8.1056	1.0466	13.7184
0.9829	15.1506	1.0503	9.9453	1.0800	9.0654
1.0743	7.6411	1.0995	8.8861	1.0395	10.9910
1.0698	9.0982	1.0417	12.9206	1.0713	8.2947
1.0639	10.8839	1.0919	5.8509	1.0866	5.3377
1.0409	9.9622	1.0682	10.1058	1.0938	7.5454
1.0470	9.1931	1.0515	7.6704	1.0863	6.8131
1.0433	13.0313	1.0760	8.2683	1.0386	10.9121
1.0298	13.7554	1.0592	7.8258	1.1076	6.0454
1.0295	12.3155	1.0623	9.0614	1.0666	10.0100
1.0461	8.8007	1.0101	10.5169	1.0421	13.1359
1.0542	10.2566	1.0338	11.3334	1.0414	12.3703
1.0631	11.3454	1.0439	11.3310	1.0488	10.2612
1.0505	8.9011	1.0937	6.3688	1.0351	12.0254
1.0844	9.8135	1.0522	13.4689	1.0571	13.7382
1.0570	10.3178	1.0452	11.8989	1.0853	4.3168
1.0749	7.4366	1.1023	6.5303	1.0403	14.0559
1.0013	13.2534	1.0557	11.7381	1.0765	9.7389
1.1004	5.6524	1.0779	9.8158	1.0400	12.4551
1.0656	7.7125	1.0596	9.1057	1.0657	6.6094
1.0529	9.8477	1.0622	9.1793	1.0645	10.8186
1.0563	11.1326	1.0772	7.8535	1.0417	12.0813
1.0123	13.6620	1.0377	11.9991	1.0431	11.7824
1.1164	4.9882	1.0662	11.8813	1.0540	6.5915
1.0510	8.7187	1.0731	11.1736	1.0987	9.6043
1.0211	13.3610	1.0600	8.9947	1.0456	13.6032
1.0531	9.4445	1.0617	12.3156	1.1005	6.8774
1.0426	11.2197	1.0593	11.2948	1.0454	13.2883
1.0798	9.3544	1.0659	8.8586	1.0434	10.5330
0.9902	13.1102	1.1270	6.5474	1.0779	10.4184
1.0681	7.3625	1.0303	13.7186	1.0609	8.2258
1.0529	11.3764	1.0547	9.3106	1.0486	9.7657
1.0746	8.8765	1.0215	11.6943	1.0869	4.2651
1.0845	10.4813	1.0412	13.1019	1.1000	7.8043
1.0507	11.1218	1.0601	8.1188	1.0441	13.8832
1.0444	10.5196	1.0064	15.0727	1.0624	10.3008
1.0782	5.9397	1.0909	10.3058	1.0295	10.4073
1.1202	5.8341	1.0402	11.8497	1.0688	5.1865
1.0633	9.3431	1.0085	13.5213	1.0562	8.9510
1.0943	9.6998	1.0631	10.4873	1.0611	10.2501
1.0708	8.4454	1.0905	6.4918	1.0308	12.4799
1.0564	12.1951	1.0545	9.0101	1.0902	7.0612
1.1067	5.1445	1.1017	8.6428	1.0302	11.3663
1.0679	6.9774	1.1039	4.7593	1.0912	7.9553
1.0652	10.0560	1.0060	13.3394	1.0351	12.8170
1.0621	10.8001	1.0951	5.6451	1.0296	10.4850

Table (4.5.2)

A HYPOTHETICAL BIVARIATE DISTRIBUTION (Freq. = .5 GHz)

X / Y	4.8094	5.8979	6.9865	8.0750	9.1636	10.2521	11.3407	12.4292	13.5178	14.6063	TOTAL X
0.9906	0	0	0	0	0	0	0	0	1	1	2
1.0059	0	0	0	0	0	1	1	1	5	2	10
1.0212	0	0	0	0	0	4	3	2	3	4	16
1.0366	0	0	0	1	2	11	20	13	10	0	57
1.0519	0	0	2	7	15	15	13	6	6	0	64
1.0672	2	1	7	11	18	13	11	1	0	0	64
1.0825	3	3	7	11	7	9	3	1	0	0	44
1.0978	2	7	6	6	9	4	0	0	0	0	34
1.1131	3	2	0	1	0	0	0	0	0	0	6
1.1285	0	2	1	0	0	0	0	0	0	0	3
TOTAL Y	10	15	23	37	51	57	51	24	25	7	300

Table (4.5.3)

CORRECTION VALUE FOR DEVICE UNDER TEST (Freq. = .7 GHz)

MAGN.	PHASE	MAGN.	PHASE	MAGN.	PHASE
1.0474	9.9722	1.0548	10.9154	1.1082	12.1462
1.0769	9.8947	1.0432	5.7377	1.0635	0.8064
1.0777	15.4605	1.0756	18.8204	1.0636	12.2389
1.0637	10.6718	1.0465	4.3087	1.0597	11.1007
1.0630	10.0522	1.0695	14.7195	1.0696	15.9799
1.0554	12.4816	1.0714	9.2022	1.0586	15.9072
1.0693	14.4006	1.0539	11.0184	1.0803	11.2748
1.0702	12.3100	1.0634	12.6744	1.0635	9.2482
1.0587	8.1688	1.0645	5.6777	1.0783	6.9355
1.0347	7.3543	1.0531	9.9439	1.0622	7.8061
1.0819	8.2351	1.0412	16.0583	1.0718	18.5763
1.0578	6.1305	1.0532	9.6443	1.0529	5.9926
1.0571	8.4143	1.0671	9.3307	1.0698	10.6698
1.0734	8.0053	1.0474	6.6835	1.0462	5.9015
1.0528	15.4192	1.0556	4.8355	1.0440	3.4832
1.0597	10.3945	1.0438	7.0053	1.0460	11.1403
1.0236	10.8309	1.0731	11.8530	1.0767	14.2965
1.0677	14.8996	1.0443	6.7477	1.0887	15.4732
1.0290	13.1134	1.0659	11.0295	1.0644	9.0724
1.0641	11.1320	1.0716	7.7627	1.0359	15.7446
1.0716	3.3480	1.0698	12.1663	1.0701	10.6399
1.0670	10.1956	1.0341	8.1424	1.0556	8.3691
1.0558	18.2624	1.0760	9.9376	1.0565	12.0271
1.0453	9.4810	1.0867	11.7331	1.0840	11.3188
1.0436	6.7611	1.0618	7.2115	1.0463	7.6890
1.0564	7.1371	1.0620	6.6510	1.0547	7.2560
1.0482	9.1398	1.0717	9.3576	1.0986	10.1847
1.0481	10.9014	1.0783	13.8788	1.0346	6.4519
1.0511	6.9024	1.0603	9.8047	1.0509	7.7557
1.0688	7.3704	1.0458	11.0112	1.0671	9.8604
1.0487	7.6245	1.0693	8.5019	1.0730	14.2819
1.0690	10.4742	1.0588	2.0270	1.0461	10.0865
1.0514	13.4092	1.0460	8.5496	1.0571	7.3351
1.0411	13.3496	1.0472	9.4252	1.0773	10.8944
1.0600	9.5809	1.0816	9.2060	1.0682	9.1991
1.0665	6.8221	1.0479	8.2754	1.0643	10.1948
1.0660	8.1023	1.0595	11.9358	1.0531	3.4600
1.0679	10.1321	1.0568	9.9480	1.0550	8.9491
1.0681	7.5168	1.0595	12.0209	1.0572	12.3733
1.0507	5.3345	1.0549	11.9735	1.0610	14.3619
1.0406	11.3282	1.0638	10.6584	1.0779	5.7300
1.0562	7.7579	1.0535	7.9280	1.0587	13.1380
1.0383	15.8227	1.0701	10.4428	1.0482	9.6298
1.0605	11.5814	1.0683	6.9162	1.0580	9.0273
1.0657	10.6043	1.0555	10.5378	1.0582	5.2774
1.0591	6.1394	1.0561	7.0392	1.0673	11.1989
1.0633	10.6832	1.0813	8.1456	1.0461	14.3249
1.0539	6.2808	1.0356	2.4963	1.0457	8.1041
1.0579	7.4941	1.0624	9.7813	1.0814	12.3937

1.0238	14.7064	1.0602	12.0502	1.0471	9.5249
1.0542	12.5151	1.0751	13.7908	1.0581	8.4765
1.0481	10.0874	1.0587	12.0669	1.0528	10.6940
1.0513	7.8988	1.0716	12.6741	1.0807	13.8508
1.0490	10.1619	1.0537	8.1105	1.0582	7.6787
1.0531	16.4168	1.0654	14.4032	1.0832	16.1443
1.0556	8.6245	1.0705	10.3087	1.0651	16.7236
1.0810	11.7405	1.0545	16.8076	1.0541	7.3598
1.0426	4.7540	1.0314	14.7082	1.0517	13.5445
1.0475	11.9589	1.0453	10.6985	1.0685	6.9811
1.0695	11.4050	1.0591	9.6280	1.0655	8.1719
1.0454	7.6833	1.0500	9.9182	1.0539	16.6266
1.0572	8.2786	1.0349	12.2639	1.0578	7.2917
1.0578	7.1569	1.0647	2.9213	1.0531	11.4817
1.0572	8.7762	1.0671	13.2265	1.0677	8.5654
1.0613	10.9465	1.0436	11.7902	1.0577	11.0866
1.0485	11.0742	1.0592	11.1297	1.0288	8.0504
1.0649	13.4733	1.0592	8.8490	1.0512	15.2268
1.0423	9.3368	1.0484	8.7897	1.0534	5.8785
1.0501	9.6681	1.0670	11.3756	1.0651	12.2215
1.0604	6.0815	1.0388	11.6517	1.0497	12.6228
1.0514	7.6204	1.0542	13.1630	1.0527	8.7044
1.0488	11.9463	1.0590	9.7531	1.0575	7.8113
1.0742	10.5086	1.0499	9.6493	1.0807	9.1750
1.0470	11.6013	1.0604	8.9524	1.0619	11.7359
1.0658	9.7615	1.0419	9.2376	1.0458	10.3516
1.0498	11.8562	1.0617	15.0936	1.0579	12.0229
1.0600	8.2967	1.0653	14.6043	1.0739	5.8637
1.0577	15.4507	1.0668	6.5952	1.0584	6.6404
1.0655	10.0951	1.0636	11.9079	1.0769	11.6211
1.0511	11.8823	1.0560	9.0631	1.0534	9.3019
1.0477	13.0049	1.0560	7.3318	1.0394	7.2272
1.0567	8.3219	1.0719	10.8967	1.0637	9.2080
1.0569	2.7590	1.0547	13.9704	1.0569	11.5555
1.0556	8.0561	1.0591	12.0975	1.0667	12.3904
1.0710	9.4862	1.0334	7.5269	1.0661	13.6267
1.0456	11.7289	1.0556	10.2645	1.0671	5.6113
1.0452	9.4584	1.0532	10.7477	1.0474	13.8207
1.0732	9.8507	1.0620	14.5969	1.0917	6.8188
1.0579	12.2851	1.0570	10.6626	1.0677	16.3876
1.0302	13.1195	1.0540	11.2722	1.0861	12.6688
1.0701	5.2041	1.0469	8.8892	1.0518	7.2014
1.0600	11.6146	1.0381	9.5636	1.0830	11.0919
1.0639	10.2300	1.0477	8.8251	1.0670	12.5719
1.0612	10.9750	1.0539	10.9443	1.0794	10.4413
1.0660	14.5139	1.0553	11.3306	1.0394	8.1410
1.0662	8.6303	1.0434	7.9260	1.0486	9.3744
1.0496	10.5682	1.0446	13.6476	1.0530	6.6455
1.0441	12.9544	1.0487	12.5887	1.0618	5.4187
1.0599	11.4486	1.0435	1.7255	1.0484	12.0424
1.0676	10.1359	1.0651	12.1650	1.0559	9.0371

Table (4.5.4)

A HYPOTHETICAL BIVARIATE DISTRIBUTION (Freq. = .7 GHz)

X \ Y	1.7071	3.5085	5.3099	7.1113	8.9127	10.7141	12.5155	14.3169	16.1183	17.9197	TOTAL X
1.0054	0	0	0	0	0	0	0	0	0	0	0
1.0162	0	0	0	0	0	0	0	0	0	0	0
1.0270	0	0	0	0	1	1	2	2	0	0	6
1.0379	1	0	2	4	5	1	3	0	3	0	19
1.0487	1	3	4	16	19	20	12	4	4	0	83
1.0595	2	2	7	16	24	23	18	5	3	1	101
1.0703	0	1	3	8	11	18	9	9	3	2	64
1.0811	0	0	1	1	4	7	4	3	2	0	22
1.0919	0	0	0	1	0	0	1	0	1	0	3
1.1028	0	0	0	0	0	1	1	0	0	0	2
TOTAL Y	4	6	17	46	64	71	50	23	16	3	300

#### 4.6 The application of the calibration procedure:-

To study the application of the calibration procedure to a real load, an "unknown" load was made up Fig (4.6.1). This consisted of a 3dB attenuator having type N connectors to which was attached a short circuit at one end and a type N to APC7 connector at the other. The magnitude of  $S_{11}$  should thus nominally be 6dB but the phase would change as the frequency was changed.

The network analyser was used in three conditions to test the ability of the corrections procedure to correct successively increasing values in the error matrix. These conditions were

- (1) Load connected directly to the 8740A reflection unit
- (2) load connected to the unit via two type N to APC' transitions connected back to back
- (3) load connected as (2) above, but with a polystyrene cylinder of length 2.7 cm fitted inside the type N to APC' connectors to give a substantial mismatch varying with frequency. The VSWR is calculated to be about 1.5 when the cylinder is  $\lambda/8$  long this occurs at approximately  $f = 1.3$  GHz.

In each case the calibration was carried out using the short circuit and the open circuit. For the third standard the short circuit offset by 20.35 cm was used over the frequency range 0.65-0.9 GHz, whilst the short circuit offset by 10.35 cm was used for the frequency range 0.9 to 1.1 GHz.

The uncorrected measurements for the three conditions are plotted in fig (4.6.2). This shows the measured reflection coefficient plotted on the cartesian complex plane. It is seen that the unmodified pair of transducers introduce some displacement of the curve, but it has generally the same form. When the polystyrene cylinder is introduced however the curve, noted by solid triangles is no longer recognisable.

In Fig (4.6.3) it will be seen that when the calibration procedure was applied, the curves all lie quite close together even for the measurements through the modified transducer. It is only near to 0.7 GHz that there is substantial divergence.

Fig (4.6.4) shows that when calibration elements include the 7 cm length, that this discrepancy at 0.7 GHz is eliminated and agreement is obtained over the whole frequency range.



Fig.(4.6.3) Full attenuator having type N connector to which was attached a short circuit at one end and a type N to ARC7 connector at the other.

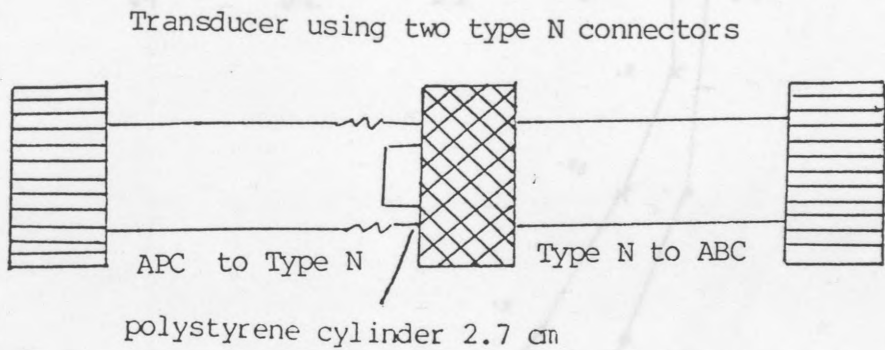
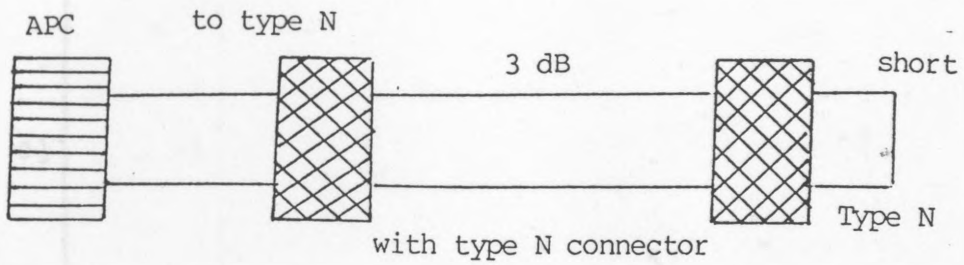


Fig.(4.6.1) 3dB attenuator having type N connector to which was attached a short circuit at one end and a type N to APC7 connector at the other.

Fig.(4.6.2) The measured values of 3-dB with short-circuit measured direct, through 2 type N transducer and "plastic" 2 type N transducer. with no correction

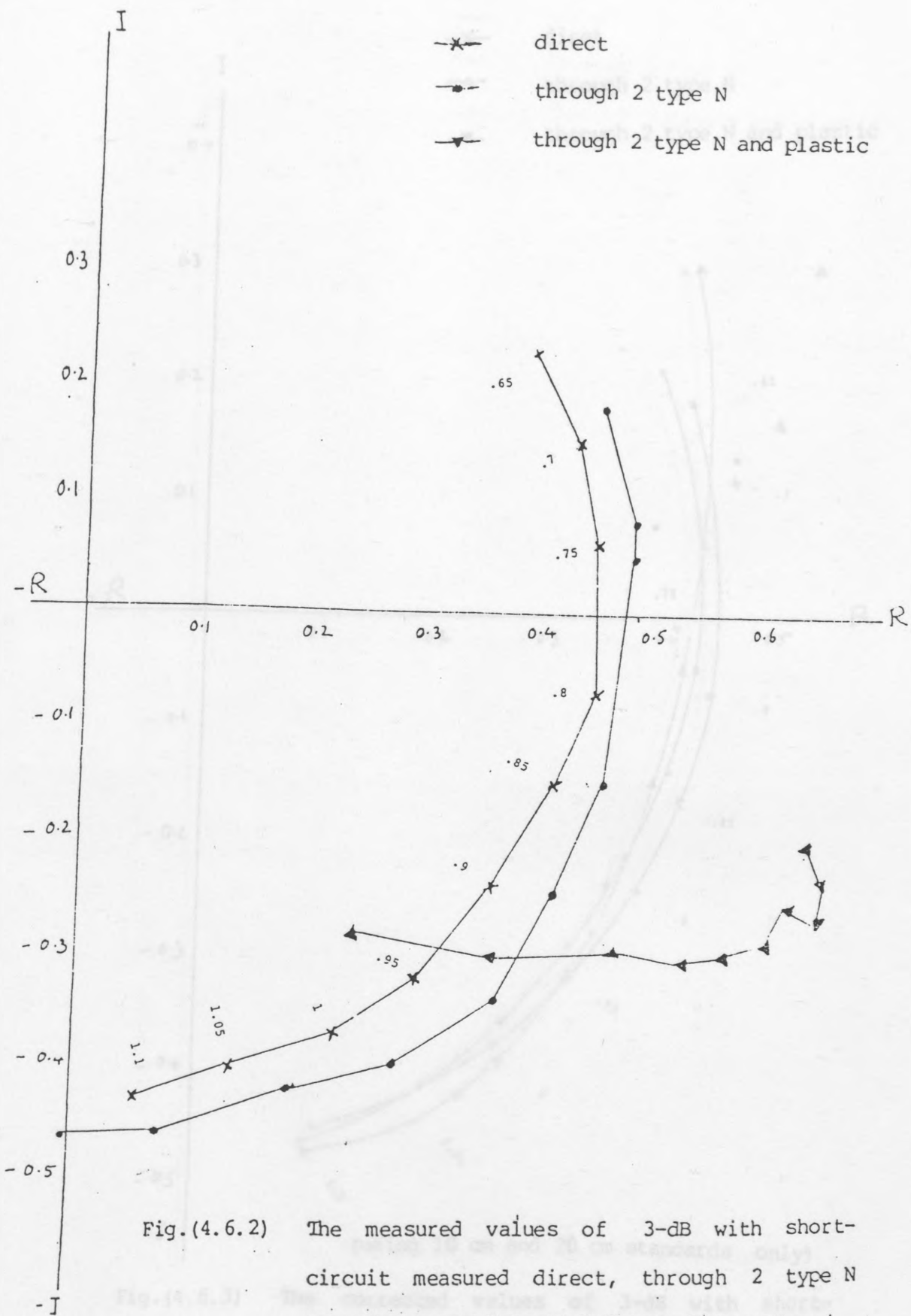


Fig.(4.6.2) The measured values of 3-dB with short-circuit measured direct, through 2 type N transducer and "plastic" 2 type N transducer. with no correction

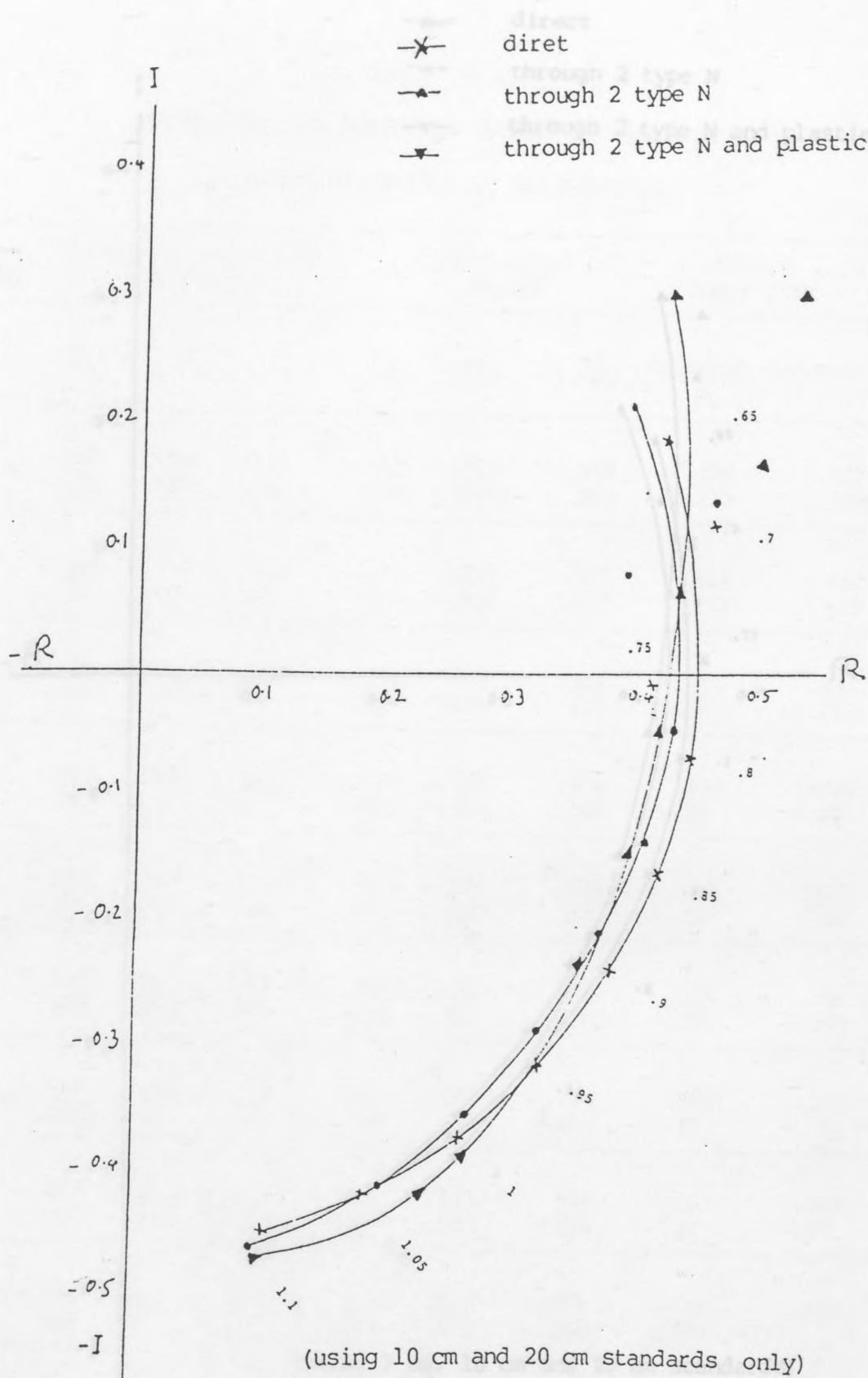


Fig.(4.6.3) The corrected values of 3-dB with short-circuit measured direct, through 2 type N transducer and "plastic" 2 type N transducer.

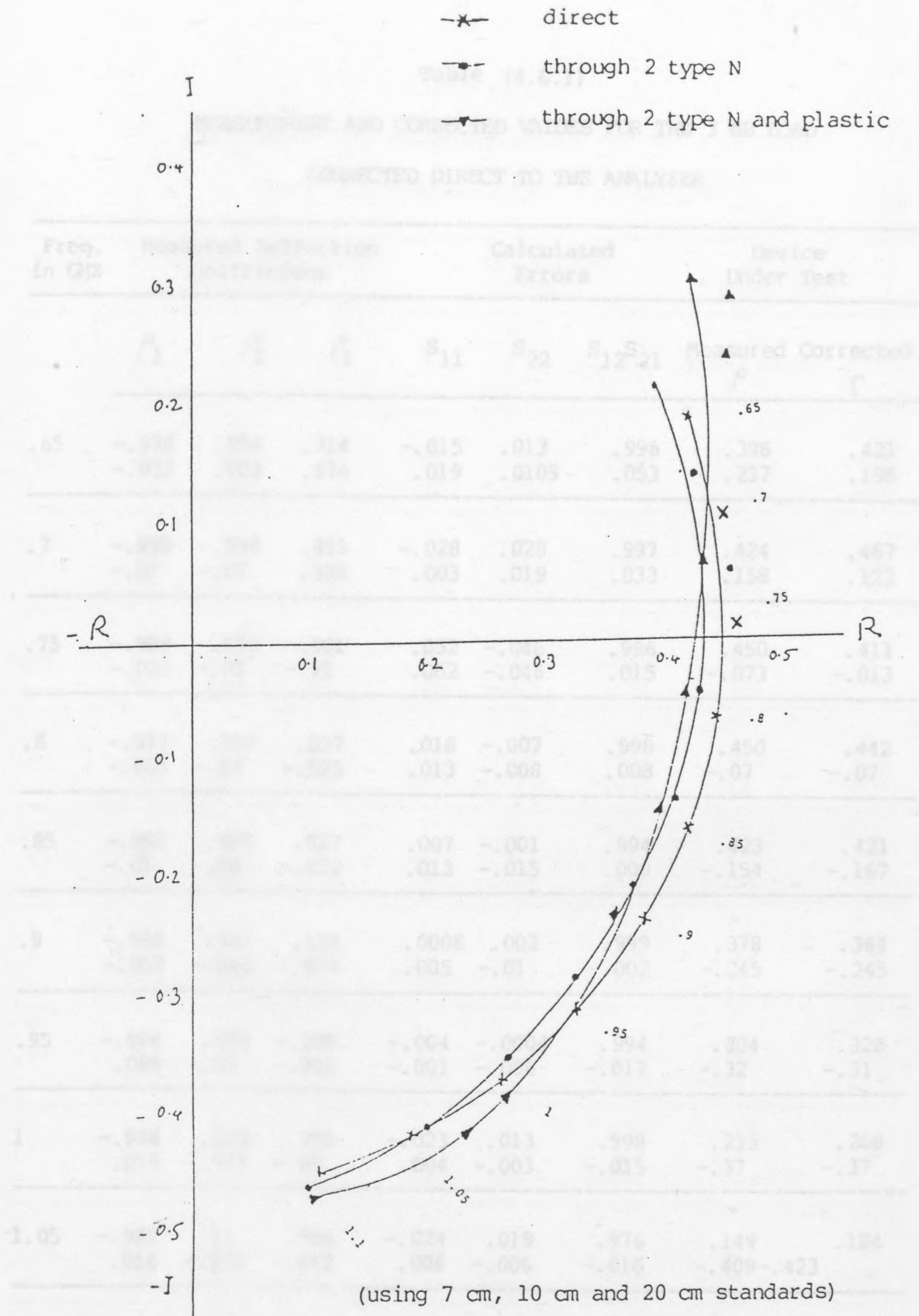


Fig.(4.6.4) The corrected values of 3-dB with short-circuit measured direct, through 2 type N transducer and "plastic" 2 type N transducer.

Table (4.6.1)

## MEASUREMENT AND CORRECTED VALUES FOR THE 3 dB LOAD

CONNECTED DIRECT TO THE ANALYZER

Freq. in GHz	Measured Reflection Coefficient			Calculated Errors			Device Under Test	
	$\rho_1$	$\rho_2$	$\rho_3$	$S_{11}$	$S_{22}$	$S_{12}S_{21}$	Measured $\rho$	Corrected $\rho$
.65	-.998	.994	.714	-.015	.013	.996	.396	.421
	-.022	.003	.674	.019	.0109	.053	.237	.196
.7	-.998	-.998	.939	-.028	.028	.997	.424	.467
	-.01	-.01	.308	.003	.019	.033	.158	.122
.75	-.998	.998	.981	.052	-.046	.996	.450	.411
	-.005	-.01	-.11	.062	-.046	.015	-.073	-.013
.8	-.977	.998	.837	.018	-.007	.998	.450	.442
	-.003	-.03	-.525	.013	-.008	.008	-.07	-.07
.85	-.998	.998	.527	.007	-.001	.994	.423	.421
	-.01	-.04	-.822	.013	-.015	.009	-.154	-.167
.9	-.998	.997	.128	.0008	.002	.999	.378	.384
	-.002	-.046	-.974	.005	-.01	-.002	-.245	-.245
.95	-.998	.988	-.298	-.004	-.0004	.994	.304	.328
	.008	-.05	-.936	-.001	-.006	-.017	-.32	-.31
1	-.998	.329	.998	-.023	.013	.998	.233	.268
	.016	-.931	-.05	.004	-.003	-.015	-.37	-.37
1.05	-.982	.11	.996	-.024	.019	.976	.149	.184
	.016	-.970	-.062	.006	-.006	-.016	-.409	-.423
1.1	-.998	-.109	.995	-.035	.018	.981	.06	.1
	.01	-.959	-.078	.014	-.021	-.015	-.431	-.458

Table (4.6.2)

MEASUREMENT AND CORRECTED VALUES FOR THE 3 dB LOAD

CONNECTED THROUGH 2 TYPE N TRANSDUCER

Freq. in GHz	Measured Reflection Coefficient			Calculated Errors			Device Under Test	
	$\rho_1$	$\rho_2$	$\rho_3$	$S_{11}$	$S_{22}$	$S_{12}S_{21}$	Measured $\rho$	Corrected $\rho$
.65	-.994	.982	.747	-.019	.013	.988	.453	.405
	-.010	.037	.655	.008	-.0069	-.017	.183	.218
.7	-.988	-.986	.954	-.048	.042	.985	.481	.464
	-.01	-.06	.274	-.014	-.009	-.037	.084	.146
.75	-.977	.987	.981	.057	-.055	.979	.486	.392
	-.02	-.05	-.15	.052	-.026	.041	-.051	-.088
.8	-.971	.994	.811	.005	-.007	.983	.465	.432
	-.016	-.05	-.552	.007	-.011	-.035	-.15	-.056
.85	-.988	.997	.5	.006	-.011	.992	.426	.410
	-.01	-.05	-.852	.011	-.004	.033	-.246	-.147
.9	-.988	.984	.089	.01	.009	.986	.362	.375
	-.017	-.069	-.984	.024	-.002	-.044	-.33	-.219
.95	-.995	.986	-.338	-.018	-.014	.994	.286	.328
	.015	-.07	-.928	-.026	-.007	-.057	-.40	-.28
1	-.978	.308	.985	-.043	.016	.943	.191	.278
	.038	-.951	-.08	.021	.009	-.051	-.424	-.37
1.05	-.948	.08	.985	-.046	.022	.923	.08	.193
	.049	-.983	-.088	.011	.012	-.051	-.46	-.428
1.1	-.981	-.135	.979	-.055	.021	.949	.009	.09
	.04	-.967	-.077	.01	-.001	-.032	-.46	-.466

Table (4.6.3)

MEASUREMENT AND CORRECTED VALUES FOR THE 3 dB LOAD  
CONNECTED THROUGH "PLASTIC" 2 TYPE N TRANSDUCER

Freq. in GHz	Measured Reflection Coefficient			Calculated Errors			Device Under Test	
	$\rho_1$	$\rho_2$	$\rho_3$	$S_{11}$	$S_{22}$	$S_{12}S_{21}$	Measured $\rho$	Corrected $\rho$
.65	-.982	.962	.94	-.203	-.217	.92	.641	.438
	-.005	-.222	.255	-.214	-.034	-.213	.207	.301
.7	-.977	-.984	.974	.151	-.159	.961	.656	.537
	-.09	-.01	.052	-.206	.038	-.212	-.239	.311
.75	-.966	.977	.956	.228	-.224	.916	.655	.508
	.205	.09	-.16	-.053	-.043	-.252	-.26	-.117
.8	-.956	.987	.918	.349	-.347	.855	.633	.443
	.238	-.04	-.298	.043	-.01	-.17	-.25	-.077
.85	-.907	.993	.860	.363	-.354	.851	.618	.407
	.394	-.04	-.488	.004	-.079	-.15	-.284	-.044
.9	-.956	.988	.699	.3548	-.33	.848	.575	.391
	.459	.109	-.658	.05	.121	-.121	-.306	-.155
.95	-.814	.984	-.241	.320	-.2964	.864	.533	.365
	.519	.17	-.901	-.096	-.155	-.121	-.30	-.215
1	-.80	.831	.93	-.242	-.224	.868	.470	.278
	.52	-.48	.33	.238	.213	.004	-.29	-.41
1.05	-.783	.69	.902	.223	-.257	.824	.366	.238
	.528	-.660	.272	.181	.226	-.023	-.304	-.421
1.1	-.758	.428	.923	.212	-.212	.841	.24	.1 03
	.56	-.841	.336	.244	.236	-.019	-.281	-.461

#### 4.7 Final work:-

The technique evolved here takes advantage of the random number generator available in a time-sharing computer.

A phase angle between 0 and  $2\pi$  and magnitude between 0 and 1 was assigned to each of the three standards. Then a series of values of the magnitude of S and random phase for the unknown device were taken. These were used to correct the device under test. The entire calibration and the measured correction was carried out about 300 times, and the whole process was repeated with the same magnitude but different phase for the device under test. The procedure was repeated and the technique for a bivariate distribution was applied for the two random variables in order to calculate the uncertainty.

The curves of Fig (4.7.1) show the complete results in the range from .1 to 2 GHz in two different confidence levels (95 % and 99 %). These curves were obtained using the standard software which took the average of 300 measurements. The final result is shown in Table (4.7.2) for the magnitude and Table (4.7.2) for the phase.

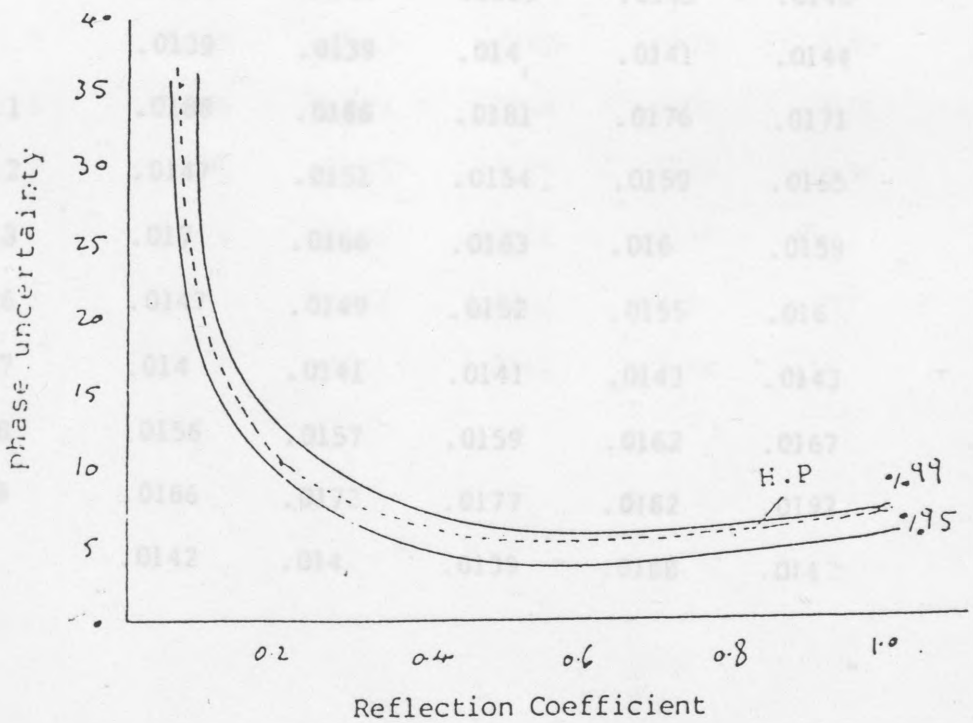
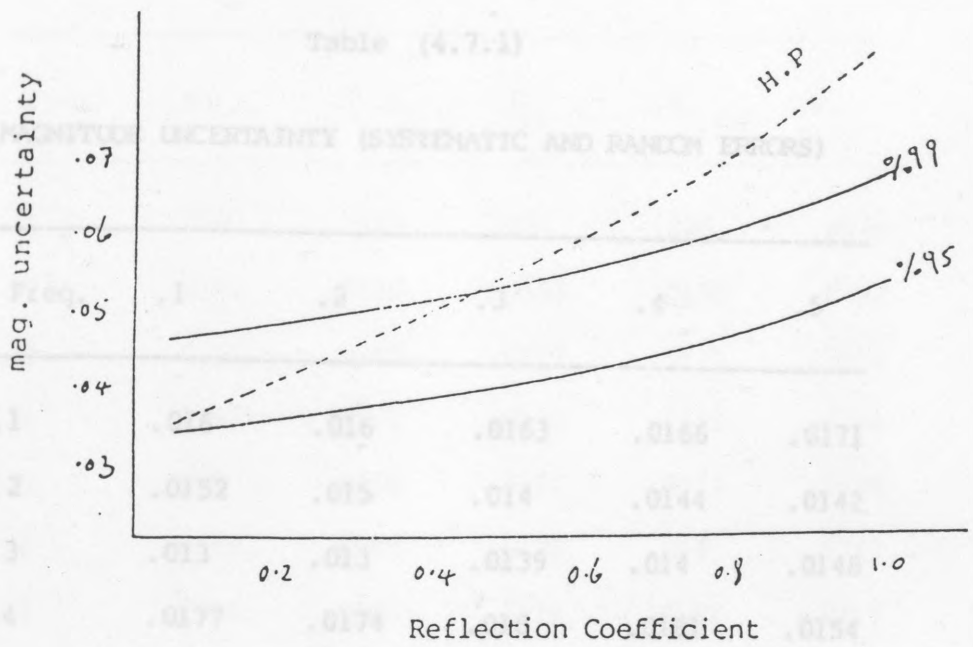


Fig. (4.7.1) The uncertainty curve for the magnitude and phase for systematic and random errors

Table (4.7.1)

MAGNITUDE UNCERTAINTY (SYSTEMATIC AND RANDOM ERRORS)

Freq.	.1	.2	.3	.4	.5
.1	.016	.016	.0163	.0166	.0171
.2	.0152	.015	.014	.0144	.0142
.3	.013	.013	.0139	.014	.0148
.4	.0177	.0174	.018	.0161	.0154
.5	.0152	.015	.0149	.0148	.0148
.6	.014	.0139	.0139	.014	.0143
.9	.0136	.0137	.0139	.0143	.0148
1	.0139	.0139	.014	.0141	.0144
1.1	.0188	.0186	.0181	.0176	.0171
1.2	.0147	.0151	.0154	.0159	.0165
1.3	.017	.0166	.0163	.016	.0159
1.6	.0147	.0149	.0152	.0155	.016
1.7	.014	.0141	.0141	.0143	.0143
1.8	.0156	.0157	.0159	.0162	.0167
1.9	.0166	.0172	.0177	.0182	.0192
2	.0142	.014	.0139	.0168	.014

cont .

Freq.	.6	.7	.8	.9	1
.1	.018	.0192	.02	.025	.0248
.2	.0142	.0146	.0153	.0165	.0182
.3	.0153	.0163	.0177	.0194	.0215
.4	.0147	.0143	.0144	.0151	.0166
.5	.015	.0155	.0164	.0177	.0194
.6	.0149	.0158	.0173	.019	.0213
.9	.0156	.0166	.0179	.0197	.0215
1	.0148	.0156	.0166	.018	.0198
1.1	.0167	.0165	.0166	.0172	.0184
1.2	.0173	.0183	.0195	.021	.0228
1.3	.0159	.0162	.0169	.0179	.0195
1.6	.0166	.0175	.0184	.0199	.0216
1.7	.0149	.0155	.0165	.0177	.0194
1.8	.0173	.0183	.0194	.0209	.022
1.9	.02	.0216	.0233	.025	.027
2	.0144	.0151	.0163	.0179	.02
2.1	.0171	.0181	.0191	.0204	.0216
2.2	.0171	.0181	.0191	.0204	.0216
2.3	.0171	.0181	.0191	.0204	.0216

Table (4.7.2)

## PHASE UNCERTAINTY (SYSTEMATIC) AND RANDOM ERRORS)

Freq.	.1	.2	.3	.4	.5
.1	9.96	5.0	3.48	2.73	2.34
.2	7.54	3.81	2.73	2.21	1.94
.3	10.33	5.15	3.59	2.76	2.34
.4	8.56	4.16	2.8	2.11	1.76
.5	8.06	4.1	2.86	2.24	1.92
.6	9.78	5.18	3.72	2.94	2.58
.9	9.28	4.76	3.37	2.67	2.31
1	8.23	4.31	3.1	2.49	2.16
1.1	9.25	4.43	3.0	2.29	1.91
1.2	9.14	4.7	3.35	2.68	2.33
1.3	7.43	4.03	2.93	2.38	2.1
1.6	7.64	3.84	2.68	2.11	1.82
1.7	9.27	4.71	3.29	2.59	2.22
1.8	9.74	4.97	3.48	2.74	2.36
1.9	9.71	4.85	3.4	2.69	2.33
2	8.33	4.19	2.94	2.34	2.03

cont.

Freq.	.6	.7	.8	.9	1
.1	2.124	1.99	1.91	1.88	1.87
.2	1.79	1.71	1.67	1.66	1.67
.3	2.08	1.92	1.81	1.75	1.71
.4	1.55	1.43	1.36	1.34	1.34
.5	1.74	1.63	1.58	1.56	1.56
.6	2.35	2.2	2.11	2.06	2.03
.9	2.1	1.97	1.87	1.86	1.84
1	1.97	1.85	1.78	1.74	1.73
1.1	1.69	1.55	1.46	1.42	1.4
1.2	2.12	2.0	1.93	1.89	1.87
1.3	1.94	1.84	1.79	1.76	1.78
1.6	1.66	1.57	1.53	1.51	1.522
1.7	2.0	1.87	1.8	1.76	1.76
1.8	2.15	2.02	1.94	1.911	1.9
1.9	2.12	2.0	1.93	1.9	1.9
2	1.85	1.75	1.7	1.68	1.68

Conclusion

It is concluded that large systematic errors may be removed from uncalibrated measurements of reflection coefficients by means of a parameter transformation. This involved taking measurements of three known standards. This use of standardizing one-ports comprising a short circuit, an open circuit and one of the above offset by a calibrated length of rigid coaxial line having at each end APC-7 connectors has been studied and it has been shown that such reference elements are satisfactory in the frequency range 100-1300 MHz. Furthermore by studying the change of measured phase with frequency, a measurement of the electrical length could be obtained for the length of rigid line.

The effect of an incorrect value for the electric length in one of the standards was analysed assuming that two of the calibrating elements, the short and the open circuit were perfectly defined. Equations giving the uncertainty in the magnitude and phase in the final corrected measurement of the unknown have been obtained and the uncertainty evaluated for a particular case.

The desirable choice of standards depends on the frequency. The best results are obtained when the three measured reflection coefficients plotted in the complex plane lie on the unit circle and have their phase angles well spaced. It was confirmed that it is essential

to change the set of standards as the frequency is changed, rather than use the same set for all frequencies.

When the measurements are repeated many times on a single standard which is disconnected and reconnected the spread in the measurement obtained when the frequency is held as constant to within  $\pm 0.005$  MHz. enables the standard error of a single measurement to be calculated.

To solve for the overall system error (both systematic and random) a statistical approach has been used. Ten measurements were taken at one frequency on each of eight standards, then, using the analysis of variance, a standard deviation was assigned to the phase and the magnitude. Taking advantage of the random number generator available in the computer and using these estimated values the distribution of measurements on the complex plane was calculated. To do this the entire calibration procedure was repeated about three hundred times. The distribution was near normal when the standards were well chosen, but if two standards differed in phase close to 360, the distribution become irregular.

The validity of the calibration procedure was tested when a stable load was measured through different mismatching transducers. One of the transducers would introduce a V.S.W.R of 1.5 at certain frequencies when measuring a matched load. It was demonstrated that, even when measuring through such a poor transducer, the corrected results would agree with those measured directly, to within 0.01 in the magnitude.

APPENDIX (7.1)

The necessary computer program is included which will enable results to be repeated for any given value of spread of phase in a single measurement. Furthermore, the computer program may be used for any other system.

The uncertainties in magnitude and phase derived above have been compared with those quoted by Hewlett-Packard in the frequency range 0.1-2 Ghz. The measurements of phase were in good agreement, but the measurements of magnitude slightly different.

$$V_1 = a_1 S_{11} + a_2 S_{12} \quad \dots\dots (7.1.1)$$

$$V_2 = a_1 S_{21} + a_2 S_{22} \quad \dots\dots (7.1.2)$$

By definition, the reflection coefficient ( $\Gamma$ ) is defined by:

$$\Gamma = \frac{\text{Reflected wave}}{\text{Incident wave}}$$

Hence, the reflection coefficient ( $\rho$ ) looking into the two port network is:

$$\rho = \frac{b_1}{a_1} \quad \dots\dots (7.1.3)$$

and the reflection coefficient ( $\Gamma_L$ ) of the load terminating port 2 is:

$$\Gamma_L = \frac{a_2}{b_2} \quad \dots\dots (7.1.4)$$

Substituting equation (7.1.4) into equation (7.1.2)

APPENDIX (7.1)

BILINEAR TRANSFORMATIONS OF SCATTERING PARAMETERS

The purpose of this part is to show the relationship between scattering parameters and bilinear transformations.

Scattering Coefficients of a 2-port network:-

In Figure (6.1.1)  $a_1$ ,  $a_2$  and  $b_1$ ,  $b_2$  are defined as the incident and reflected waves into the two port network.

$$b_1 = a_1 S_{11} + a_2 S_{12} \quad \dots\dots (7.1.1)$$

$$b_2 = a_1 S_{21} + a_2 S_{22} \quad \dots\dots (7.1.2)$$

By definition the reflection coefficient ( $\Gamma$ ) is defined by:

$$\Gamma = \frac{\text{Reflected wave}}{\text{Incident wave}}$$

Hence, the reflection coefficient ( $\rho$ ) looking into the two port network is:

$$\rho = \frac{b_1}{a_1} \quad \dots\dots (7.1.3)$$

and the reflection coefficient ( $\Gamma_L$ ) of the load terminating port 2 is:

$$\Gamma_L = \frac{a_2}{b_2} \quad \dots\dots (7.1.4)$$

Substituting Equation (7.1.4) into Equation (7.1.2)

$$b_2 = \frac{a_2}{\Gamma_L} = S_{21} a_1 + S_{22} a_2 \quad \text{APPENDIX (7.2)}$$

GENERAL DESCRIPTION OF THE STANDARDS

$$a_2 (1/\Gamma - S_{22}) = S_{21} a_1$$

This section describes the points common to the coaxial standards

$$\frac{a_2}{a_1} = \frac{S_{21}}{(1/\Gamma - S_{22})} = \frac{S_{21}\Gamma_L}{1 - S_{22}\Gamma_L} \quad \dots\dots (7.1.5)$$

Substituting Equation (7.1.3) and (7.1.5) into Equation (7.1.1) gives:

$$b_1 = S_{11}a_1 + S_{12}a_2$$

The connector line is constructed from special silver lined and

$$\frac{b_1}{a_1} = \rho = S_{11} + \frac{S_{12}S_{21}\Gamma_L}{1 - S_{22}\Gamma_L} \quad \dots\dots (7.1.6)$$

Or

$$\rho = \frac{-(S_{11}S_{22} - S_{12}S_{21})\Gamma_L + S_{11}}{-S_{22}\Gamma_L + 1}$$

Or

$$\rho = \frac{A\Gamma_L + B}{C\Gamma_L + D}$$

Where

$$A = -(S_{11}S_{22} - S_{12}S_{21}) = -\Delta S$$

$$B = S_{11}$$

$$C = -S_{22}$$

$$D = 1$$

Hence reflection coefficients between two measuring planes have also been shown to be related by a bilinear transformation.

## APPENDIX (7.2)

### GENERAL DESCRIPTION OF THE STANDARDS

This section describes the points common to the coaxial standards particular details of the individual standards will be described in later sections.

#### (I) The connector line:-

The connector line is constructed from special silver lined and silver-overlay precision drawn tubes. It is fitted with a type  $A_1$  Connector ( $A_1$  means suitable for all types of measuring instruments) at each end, and the inner conductor is supported by the mating connectors. The special design feature of complete freedom from discontinuities is a necessary - condition to allow precise admittance transformation through the line. It must be uniform and its connectors must have a common plane of cleavage for the ends of both inner and outer conductors. The following requirements must also be met.

- 1) The series impedance introduced by the contacts between pairs of inner and outer conductors must not exceed a few millic hms.
- 2) The diameters of the conductors must be sufficient, within the limitation imposed by the upper frequency limit, to enable the line to be made and measured to adequately close tolerances so that, apart from residuals, the characteristic impedance can be determined accurately from dimensional measurements.

- 3) The mating lines should provide uniform extensions at each end of the standards for a distance of about three times the air gap between inner and outer conductor, at which distance the supports may be placed. with the measurement reflectometers whose parts are also connected with APC-7 Connectors.
- 4) The connectors must be sexless so that the line can be reversed, and connection and disconnection can be achieved with ease. their physical dimensions.
- 5) Choice of diameter of the standard coaxial line is governed by both mechanical and electrical considerations the diameters ratio of the outer - to inner conducting surface is of course fixed by the nominal characteristic resistance, usually 50 ohms.

Two types of precision connectors should be specified.

- 1) A General Precision Connector (GPC) having a self contained dielectric support.
- 2) A Laboratory Precision Connector (LPC) using only air dielectric. The laboratory precision connector should be used where the electrical length and characteristic impedance of the connector must be known to the highest accuracy.

3) The mechanical dimensions of these connectors are held within tolerances of  $\pm 0.0025$  mm.

4) Easy interface with the measurement reflectometers whose parts are also connected with APC-7 Connectors.

5) Easy machining of the inner and outer conductors due to their physical dimensions.

A variety of coaxial connector sizes was discussed. It was finally agreed that two basic sizes should satisfy the bulk of the applications for precision coaxial connectors, the 14 mm and 7 mm (same dimensions essentially as the type N connector).

TABLE (7.2.1)

Dimensions of 7 mm and 14 mm 50ohm line

	14mm line		7mm line	
	mm	inches	mm	inches
OD of outer conductor	13.2875	0.5231	7.000	0.2756
OD of inner conductor	6.2041	0.2442	3.048	0.1199

(2) Line size:-

In 1964 (D.E.Fossum) a great deal of discussion took place about what line size would find best application in instrumentation. Obviously, larger coaxial line would provide more precise connectors because of relative ease in holding comparatively close tolerance. On the other hand, smaller size coaxial line would work better at higher frequencies and can handle a larger total spectrum

A variety of coaxial connector sizes were discussed. It was finally agreed that two basic sizes should satisfy the bulk of the applications for precision coaxial connectors, the 14 mm and 7 mm (same dimensions essentially as the type N connector).

TABLE (7.2.1)

Dimensions of 7 mm and 14 mm 50ohm line

---

	14mm line		7mm line	
	mm	inches	mm	inches
ID of outer conductor	13.2875	0.5625	7.000	0.2756
OD of inner conductor	6.2041	0.24425	3.040	0.1197

---

2) General precision for the 7-mm (0.275 inch) laboratory connector parameters:

The range of environmental conditions over which the performance of the 7-mm laboratory precision connector (APC-7) described in the following specifications is a connection arrangement which includes mechanical means for joining the electrical paths of the inner and outer conductors or precision air-dielectric coaxial lines whose characteristic impedance is 50.0 ohms at 23°C, 760 mm Hg, 50 percent relative humidity, and infinite conductivity for the conductors.

A) Mechanical properties

1) Connect - disconnect life:-

1) Line diameter and tolerances:-

ID of outer conductor: 7.000 mm (0.275 inch)

OD of inner conductor: 3.040 mm (0.1197 inch)

tolerance on the inner and outer diameters shall produce a characteristic impedance accuracy of better than  $\pm 0.2$  percent, with a maximum tolerance on the ID of the outer conductor of  $\pm 0.005$  mm ( $\pm 0.0002$  inch)

2) VSWR limits

The maximum VSWR shall be less than

2) Environmental condition, operating:-

The range of environmental conditions over which the performance of the connections shall remain within electrical specifications covers the following:-

Temperature 13 to 33C

Humidity 20 to 80 per cent

Pressure 590 to 780 mm Hg.

3) Connect - disconnect life:-

The electrical performance shall remain within specifications when the function is subjected to 1000 complete connection cycles. Non-abrasive cleaning is permitted at any time.

B) Electrical parameters:-

1) Maximum frequency limits

The maximum frequency at which the specifications shall apply is 18 HGz.

2) VSWR limits

The maximum VSWR shall be less than

SIMPLE LINEAR REGRESSION (line length 7 cm)

VSWR = 1.002 + 0.0015 x freq (GHz)

HOW MANY OBSERVATIONS ON EACH VARIABLE? 12

3) Insertion loss:

VARIABLE	MEAN	VARIANCE	STD DEVIATION
X	113.1917	3613.943	5.625531
Y	1.002	0.000225	0.015

The insertion loss in dB shall be less than

INDEX	MEAN	STDEV	STD ERROR
1	113.1917	5.625531	0.453114

dB =  $5 \times 10^{-3}$  x / freq. (GHz)

4) DC contact resistance: The DC contact resistance of the mated inner and outer conductor joints shall be less than the following:

PARAMETER	MEAN	95 PCT CONFIDENCE LIMITS
A	5.018407	2.707154
B	17.13142	17.28440

Inner outer

5 milliohms 0.5 milliohms

ESTIMATED VALUES OF Y (FROM THE REGRESSION) AND CONFIDENCE LIMITS FOR INDIVIDUAL VALUES OF X, FOR EACH VALUE OF X:				
X-ACTUAL	Y-ACTUAL	Y-CALC	95 PCT CONFIDENCE LIMIT	
2.5	37.3	38.96666	37.1617	40.7715
3.3	56	56.09444	54.14294	57.8540
6.3	72.9	73.2101	71.51531	74.9452
9.3	90	90.32572	88.67819	92.0468
12.3	107.8	107.4413	105.431	109.156
15.3	126	124.5569	122.9735	126.77
18.3	143	141.6725	140.1853	143.407
21.3	159.5	158.7881	157.2765	160.252
24.3	176	175.9037	174.3373	177.707
27.3	192.2	193.0193	191.433	194.86
30.3	210	210.1349	208.5293	212.043
33.3	228	227.2505	225.6117	229.221

APPENDIX (7.3)

SIMPLE LINEAR REGRESSION (line length 7 cm)

EQUATION:  $Y = A + B \cdot X$

HOW MANY OBSERVATIONS ON EACH VARIABLE? 12

VARIABLE	MEAN	VARIANCE	STD DEVIATION
X	3	13	3.605551
Y	133.1917	3615.943	61.77336

INDEX (R <sup>2</sup> )	EXPL VAR	STDEXPL VAR	STD ERROR
.9993773	3497.532	.4204407	.643614

PARAMETER	VALUE	95 PCT CONFIDENCE LIMITS	
A	-3.362881	-5.018607	-2.707154
B	17.13182	16.99917	17.26446

ESTIMATED VALUES OF Y (FROM THE REGRESSION) AND CONFIDENCE LIMITS FOR INDIVIDUAL VALUES OF Y, FOR EACH VALUE OF X:

X-ACTUAL	Y-ACTUAL	Y-CALC	95 PCT CONFIDENCE LIMIT	
2.5	37.3	38.96666	37.1617	40.7716
3.5	56	56.09348	54.34294	57.8540
4.5	72.5	73.2303	71.51531	74.9452
5.5	90	90.36212	88.67819	92.0460
6.5	107.8	107.4939	105.831	109.156
7.5	126	124.6258	122.9735	126.27
8.5	141	141.7576	140.1053	143.409
9.5	159.5	158.8894	157.2265	160.552
10.5	176	176.0212	174.3373	177.705
11.5	192.2	193.153	191.438	194.86
12.5	210	210.2848	208.5293	212.040
13.5	228	227.4167	225.6117	229.221

S I M P L E L I N E A R R E G R E S S I O N (line length 10 cm)

EQUATION:  $Y = A + B \cdot X$

HOW MANY OBSERVATIONS ON EACH VARIABLE? 12

VARIABLE	MEAN	VARIANCE	STD DEVIATION
X	8	13	3.605551
Y	-201.9958	8296.036	91.08258

INDEX ( $R^2$ )	EXPL VAR	UNEXPL VAR	STD ERROR
.9999574	7604.375	.3242188	.5694021

PARAMETER	VALUE	95 PCT CONFIDENCE LIMITS	
A	.093956	-.9209408	1.108853
B	-25.26122	-25.3777	-25.14474

ESTIMATED VALUES OF Y (FROM THE REGRESSION) AND CONFIDENCE LIMITS FOR INDIVIDUAL VALUES OF Y, FOR EACH VALUE OF X:

X-ACTUAL	Y-ACTUAL	Y-CALC	95 PCT CONFIDENCE LIMITS	
2.5	-63.2	-63.0591	-64.64412	-61.47409
3.5	-88.74	-88.32033	-89.86196	-86.7787
4.5	-113.83	-113.5816	-115.0876	-112.0755
5.5	-138.25	-138.8428	-140.3215	-137.364
6.5	-163.26	-164.104	-165.5643	-162.6437
7.5	-188.81	-189.3652	-190.8162	-187.9143
8.5	-214.79	-214.6265	-216.0774	-213.1755
9.5	-240.21	-239.8877	-241.3479	-238.4274
10.5	-266.5	-265.1489	-266.6276	-263.6702
11.5	-290.33	-290.4101	-291.9161	-288.9041
12.5	-315.67	-315.6713	-317.213	-314.1297
13.5	-340.36	-340.9326	-342.5176	-339.3476

SIMPLE LINEAR REGRESSION (line length 20 cm)

EQUATION:  $Y = A + B \cdot X$  (line length 30 cm)

HOW MANY OBSERVATIONS ON EACH VARIABLE? 12

VARIABLE	MEAN	VARIANCE	STD DEVIATION
X	8	13	3.605551
Y	-396.8325	31977.12	178.8215

INDEX (R <sup>2</sup> )	EXPL VAR	UNEXPL VAR	STD ERROR
.9999875	29311.59	.3671875	.60596

PARAMETER	VALUE	95. PCT CONFIDENCE LIMITS	
A	-.065773	-1.14583	1.014284
B	-49.59584	-49.7198	-49.47188

ESTIMATED VALUES OF Y (FROM THE REGRESSION) AND CONFIDENCE LIMITS FOR INDIVIDUAL VALUES OF X, FOR EACH VALUE OF X:

X-ACTUAL	Y-ACTUAL	Y-CALC	95 PCT CONFIDENCE LIMITS	
2.5	-124.24	-124.0554	-125.7422	-122.3686
3.5	-174.22	-173.6512	-175.2918	-172.0106
4.5	-223.7	-223.2471	-224.8498	-221.6444
5.5	-271.98	-272.8429	-274.4166	-271.2692
6.5	-321.63	-322.4388	-323.9928	-320.8847
7.5	-371.35	-372.0346	-373.5787	-370.4905
8.5	-421.5	-421.6304	-423.1745	-420.0663
9.5	-471.79	-471.2263	-472.7803	-469.6723
10.5	-521.86	-520.8221	-522.3958	-519.2484
11.5	-570.86	-570.418	-572.0207	-568.8153
12.5	-619.29	-620.0138	-621.6544	-618.3732
13.5	-669.57	-669.6096	-671.2964	-667.9229

APPENDIX (7.4)

THE EFFECT OF ELECTRIC-LENGTH OF REFERENCE SHORT-CIRCUIT IN NETWORK

ANALYSIS OF REGRESSION

SIMPLE LINEAR REGRESSION (line length 30 cm)

EQUATION:  $Y = A + B \cdot X$

HOW MANY OBSERVATIONS OF EACH VARIABLE? 12

VARIABLE	MEAN	VARIANCE	STD DEVIATION
X	3	13	3.605551
Y	559.375	69521.5	263.6643

INDEX (R <sup>2</sup> )	EXPL VAR	UNEXPL VAR	STD ERROR
.9999874	63727.37	.6772461	.3229476

PARAMETER	VALUE	95 PCT CONFIDENCE LIMITS	
A	-25.65159	-27.11341	-24.18477
B	73.12532	72.95997	73.29667

ESTIMATED VALUES OF Y (FROM THE REGRESSION) AND CONFIDENCE LIMITS FOR INDIVIDUAL VALUES OF Y, FOR EACH VALUE OF X:

X-ACTUAL	Y-ACTUAL	Y-CALC	95 PCT CONFIDENCE LIMITS	
2.5	153.5	157.1672	154.3734	159.46
3.5	230	230.2975	228.0694	232.5256
4.5	301.8	303.4259	301.2492	305.6025
5.5	376	376.5542	374.417	378.6914
6.5	450.9	449.6825	447.572	451.773
7.5	522.6	522.8108	520.7133	524.9079
8.5	595.7	595.9391	593.8421	598.0362
9.5	668.5	669.0675	666.957	671.178
10.5	742.7	742.1958	740.0586	744.333
11.5	816	815.3241	813.1475	817.5007
12.5	883.6	883.4524	886.2243	890.6835
13.5	961	961.5803	959.29	963.8716

APPENDIX (7.4)

THE EFFECT OF ELECTRIC-LENGTH OF REFERENCE SHORT-CIRCUIT IN NETWORK ANALYSER CALIBRATION

By assuming  $|\Gamma_c| = |\hat{\Gamma}_c| = 1$

and let  $|\Gamma| = r$

From Equation (3.4.8) in Chapter (3)

$$\begin{aligned} \hat{\Gamma} &= r (\cos a + j \sin a) - (\cos b + j \sin b) + (\cos b + j \sin b) \\ &\quad - r (\cos a + j \sin a) (\cos b + j \sin b) (\cos b + j \sin b) / \\ &\quad - 1 - r (\cos a + j \sin a) (\cos b + j \sin b) + r (\cos a + j \sin a) \\ &\quad (\cos b + j \sin b) - (\cos b + j \sin b) (\cos b + j \sin b) \\ &\dots\dots (7.4.1) \end{aligned}$$

Since,

$$\sin (A+B) = \sin A \cos B + \cos A \sin B$$

$$\cos (A+B) = \cos A \cos B - \sin A \sin B$$

Equation (7.4.1)

$$\begin{aligned} \hat{\Gamma} &= [r \cos a - \cos b + \cos b - r \cos (a+b)] \\ &\quad + j [r \sin a - \sin b + \sin b - r \sin (a+b)] \\ &\quad [1 - r \cos (a+b) + r \cos (a+b) - \cos (b+b)] \\ &\quad j [-r \sin (a+b) + r \sin (a+b) - \sin (b+b)] \dots\dots (7.4.2) \end{aligned}$$

Therefore,

$$\begin{aligned}
 |\Gamma|^2 &= [r \cos a - \cos b + \cos \hat{b} - r \cos (a+b\hat{b})]^2 \\
 &+ [r \sin a - \sin b + \sin \hat{b} - r \sin (a+b\hat{b})]^2 / \\
 &[1-r \cos (a+b) + r \cos (a\hat{b}) - \cos (b\hat{b})]^2 \\
 &+ [-r \sin (a+b) + r \sin (a\hat{b}) - \sin (b\hat{b})]^2] \dots\dots (7.4.3)
 \end{aligned}$$

Differentiation  $|\Gamma|^2$  with respect to  $\theta$  and equal to zero:

$$\begin{aligned}
 B [2\{r \cos \theta - \cos b + \cos \hat{b} - r \cos (a+b\hat{b})\} \\
 [-r \sin a + r \sin (a+b\hat{b})] \\
 + 2\{r \sin a - \sin b + \sin \hat{b} - r \sin (a+b\hat{b})\} \\
 \{r \cos a - r \cos (a+b\hat{b})\} \\
 + A [2\{1-r \cos (a+b) + r \cos (a\hat{b}) - \cos (b\hat{b})\} \\
 \{r \sin (a+b) - r \sin (a\hat{b})\} \\
 + 2\{-r \sin (a\hat{b}) + r \sin (a\hat{b}) - \sin (b\hat{b})\} \\
 \{-r \cos (a+b) + r \cos (a\hat{b})\}] = 0 \dots\dots (7.4.4)
 \end{aligned}$$

Therefore,

$$\begin{aligned}
 B [\sin (a+b) - \sin (a\hat{b}) + \sin (a\hat{b}) - \sin (a\hat{b})] \\
 + A [\sin (a\hat{b}) - \sin (a\hat{b}) + \sin (a\hat{b}) - \sin (a\hat{b})] = c
 \end{aligned}$$

Therefore,

$$[\sin(a+b) - \sin(a-b) + \sin(a+b) - \sin(a-b)] [A+B] = 0$$

Therefore,

$$\sin(a-b) - \sin(a-b) + \sin(a+b) - \sin(a-b) = 0$$

Therefore,

$$\sin a (\cos b - \cos b) = 0 \quad \dots\dots (7.4.5)$$

$$0 = 0$$

The definitions and notations are listed below:-

1.  $x_i$  is a measurement value assigned to the  $i$ th measurement.
2.  $n$  is the total number of measurements.
3. The mean  $\bar{x}$  is defined as the average of the 'n' measurements

of  $x_i$ .

$$\bar{x} = \frac{1}{n} \sum_{i=1}^n x_i$$

4. The variance  $s^2$  is defined as:

where  $n_i$  = number of measurements for that particular  $x_i$ .

- 5: The deviation  $d_i$  of a measurement  $x_i$  in a set of (n) measurements is defined as:

APPENDIX (7.5)

SOME STATISTICAL DEFINITIONS

The purpose of this appendix is to define and clarify the procedure used in deriving the results of Chapter (4). Most of the information comes from Yamanee 1967.

Derivation of the equations used here will not be given as they have already been derived in their references.

The definitions and equations are listed below:-

1.  $x_i$  is a measurement value assigned to the "i"th measurement.
2. n is the total number of measurements.
3. The mean ( $X_n$ ) is defined as the average of the 'n' measurements

of  $x_i$ .

$$X_n = 1/n \sum_{i=1}^{i=n} x_i$$

4. The weighted mean ( $\bar{x}$ ) is defined as:

$$\bar{x} = \frac{\sum_{i=1}^{i=n} W_i x_i}{\sum_{i=1}^{i=n} W_i}$$

Where  $W_i$  = number of measurements for that particular  $x_i$ .

5. The deviation ( $S_i$ ) of a measurement  $x_i$  in a set of (n) measurements is defined:

$$S_i = x_i - X_n$$

6: The precision of Standard deviation ( $\sigma$ ) of a set of 'n' measurements is given by:

$$\sigma = \sqrt{\frac{1}{n} \sum_{i=1}^{l=n} S_i^2} = \sqrt{\frac{1}{n} \sum_{i=1}^{i=n} (x_i - x_n)^2}$$

7: The best estimate of the standard deviation ( $S_n$ ) is defined as:

$$\bar{S}_n = \sigma \sqrt{\frac{(n)}{(n-1)}} = \sqrt{\frac{1}{(n-1)} \sum_{i=1}^{i=n} S_i^2}$$

8: The variance ( $\sigma^2$ ) is defined as the square of the standard deviation.

$$(\sigma^2) = \frac{1}{n} \sum_{i=1}^{i=n} S_i^2$$

It follows from (6) and (7) that:

$$(S_n^2) = \frac{1}{(n-1)} \sum_{i=1}^{i=n} S_i^2$$

9: The standard deviation of the mean [ $\sigma(x_n)$ ] is given by:

$$\sigma(x_n) = \sigma \sqrt{n}$$

10: The best estimate of the standard deviation of the mean [ $S_n(x_n)$ ] is defined as:

$$S_n(x_n) = \bar{S}_n \sqrt{n} \text{ The above is also called the Standard error.}$$

11: If the overall result of 'n' measurements (X) is written as:

$$X = \bar{X}_n \pm S_n$$

and if a Gaussian distribution is assumed.

$S_n = 1.65 \bar{S}_n$ , is determined with a confidence level of 90%.

$S_n = 2 \bar{S}_n$ , is determined with a confidence level of 95%.

$S_n = 3 \bar{S}_n$ , is determined with a confidence level of 99%.

1) The samples are normally and independently distributed.

2) The samples have the same variance.

3) Each sample has been "treated" differently and the treatments have had additive effects on the samples.

Suppose that a number of observations fall naturally into separate sets, and that the  $i$ th set contains  $n_i$  observations has a mean  $\bar{y}_i$  where

$$\bar{y}_i = \frac{1}{n_i} \sum_{j=1}^{n_i} y_{ij}$$

and  $S_i$  is the within group variance of each reading. By calculating the within group variance of the variables between sets and  $S_2$  of the standard error of the overall mean level of the variation within the sets.

TABLE (7.6.1)  
APPENDIX (7.6)

ANALYSIS OF VARIANCE

Analysis of variance is a technique used to trace the different sources that bring about the variation between the observed and true mean of a sample. The splitting of the variation helps to eliminate the effect of interfering variables and, thereby increases the sensitivity of the experiment. All common analysis of variance tests to the following assumptions:-

- 1) The samples are normally and independently distributed.
- 2) The samples have the same variance.
- 3) Each sample has been "treated" differently and the treatments have had additive effect on the samples.

Suppose that a series of  $n$  observations fall naturally into  $r$  separate sets, and that the  $j^{\text{th}}$  set containing  $n_j$  observations has a mean  $y_j$  where

$$y_j = \frac{\sum W_{ij} Y_{ij}}{\sum W_{ij}}$$

and  $W_{ij}$  is the weight appropriate to each reading. By calculating an estimate  $S_1$  based on the variation between sets and  $S_2$  of the standard error of the overall mean based on the variation within the sets.

i.e. The F-test can be used to check whether the variation within the sets is different from the variation between sets.

TABLE (7.6.1)

Analysis of variance

source of variation	sum of square	degree of freedom	variance estimate
between sample	$S_1^2 = W_{ij} (Y_j - \bar{y})^2$ $(r-1)W_{ij}$	$(r-1)$	$S_1^2$ $(r-1)$
within sample	$S_2^2 = W_{ij} (Y_{ij} - \bar{y}_j)^2$ $(n-r) W_{ij}$	$(n-r)$	$S_2^2$ $(n-r)$

F-test (Fisher test):

If  $S_1^2$  is smaller or only slightly larger than  $S_2^2$  there is no justification for assuming that a real difference exists among the expected values of the group. If however  $S_1^2$  is considerably larger than  $S_2^2$  then there arises the suspicion that the expected values in the groups are in fact different.

To test this suspicion one take the ratio of the two variance and enters these in the statistical table for the F test (eg. Yamanee 1967 table 5a) for the appropriate degrees of freedom of each variance. The Table given the variance ratio for different levels of significance.

i.e The F-test can be used to check whether the variation within the sets is different from the variation between sets.

APPENDIX (7.7)

CORRECTION USING ANY THREE STANDARDS

To calculate the parameters in the usual three parameter error model. Use any three standards terminated in short circuit, open circuit

$$\rho_1 = S_{11} + \frac{qS_{12}S_{21}\Gamma_1}{1 - qS_{22}\Gamma_1} \quad \dots\dots(7.7.1)$$

$$\rho_2 = S_{11} + \frac{qS_{12}S_{21}\Gamma_2}{1 - qS_{22}\Gamma_2} \quad \dots\dots(7.7.2)$$

$$\rho_3 = S_{11} + \frac{qS_{12}S_{21}\Gamma_3}{1 - qS_{22}\Gamma_3} \quad \dots\dots(7.7.3)$$

where  $q = -1$  for short circuit and  $q = 1$  for open circuit (7.7.4)

Here  $\rho_1, \rho_2$  and  $\rho_3$  are the measured results and  $\Gamma_1, \Gamma_2$  and  $\Gamma_3$  are the known calibration standards. It should be noted that both  $\rho$  and  $\Gamma$  are complex quantities.

For the computer  $S(11) = S_{11}$  similiary for  $S(22)$  and  $S(12)S(21)$

$$S(11) + S(22)\rho(1)\Gamma(1) = \rho(1) + v\Gamma(1) \quad \dots\dots(7.7.4)$$

$$S(11) + S(22)\rho(2)\Gamma(2) = \rho(2) + v\Gamma(2) \quad \dots\dots(7.7.5)$$

$$S(11) + S(22)\rho(3)\Gamma(3) = \rho(3) + \nabla\Gamma(3) \quad \dots\dots\dots(7.7.6)$$

where  $\nabla = S(11)S(22) - S(12)S(21)$

from equation (6.6.4) and (6.6.5)

$$S(22)[\rho(1)\Gamma(1) - \rho(2)\Gamma(2)] = [\rho(1) - \rho(2)] + \nabla[\Gamma(1) - \Gamma(2)] \quad \dots\dots\dots(7.7.7)$$

from equation (6.6.5) and (6.6.6)

$$S(22)[\rho(2)\Gamma(2) - \rho(3)\Gamma(3)] = [\rho(2) - \rho(3)] + \nabla[\Gamma(2) - \Gamma(3)] \quad \dots\dots\dots(7.7.8)$$

equation (6.6.7) and (6.6.8) can be put in the form:

$$S(22)A(1) + \nabla B(1) = C(1) \quad \dots\dots\dots(7.7.9)$$

$$S(22)A(2) + \nabla B(2) = C(2) \quad \dots\dots\dots(7.7.10)$$

where

$$A(\Gamma) = \rho(1)\Gamma(1) - \rho(2)\Gamma(2)$$

$$A(2) = \rho(2)\Gamma(2) - \rho(3)\Gamma(3)$$

$$B(1) = \rho(1) - \rho(2)$$

$$B(2) = \rho(2) - \rho(3)$$

$$C(1) = \Gamma(1) - \Gamma(2)$$

$$C(2) = \Gamma(2) - \Gamma(3)$$

From equation (6.6.9) and (6.6.10)

$$S(22) = C(1)B(2) - C(2)B(1) / A(1)B(2) - A(2)B(1) \dots\dots (7.7.11)$$

$$\Delta = C(1)B(2) - C(2)B(1) / \Delta$$

where

$$\Delta = A(1)B(2) - A(2)B(1)$$

Also from equation (7.7.9) and (7.7.10)

$$v = A(1)C(2) - A(2)C(1) / A(1)B(2) - A(2)B(1)$$

$$= A(1)C(2) - A(2)C(1) / \Delta$$

$$= S(3) \dots\dots (7.7.12)$$

From equation (7.7.2)

$$S(11) = \Gamma(2) + S(3)\rho(2) - S(22)\rho(2)\Gamma(2) \dots\dots (7.7.13)$$

From equation (7.7.1)

$$S(12)S(21) = [\Gamma(1) - S(11)][1.0 - S(22)\rho(1)] / \rho(1) \dots\dots (7.7.14)$$

## APPENDIX (7.8)

### MANUAL SOFTWARE

#### Introduction:-

Practical applications of the equations in Appendix(7.5) require long and tedious computations of complex numbers. A short computer program is developed to solve explicitly a very useful reflectometer error model currently receiving high utilization in microwave measurement systems. The program architecture is designed to enhance its utilization as a stand-alone subroutine operating in conjunction with a measurement program, or to replace iterative solution software in existing automated measurements systems.

The history of automated network analyzers is well documented and their contribution to accurate and high speed microwave measurements is nothing short of phenomenal. However, because of heavy capital equipment investments required to purchase a fully automated system, many manual systems are still being utilized. Software manual routines programs may be utilized to process the data thus required. The accuracy enhancement software removes directivity, source match and frequency response errors from reflection magnitude and phase measurements. Finally, as mentioned before it was decided to solve the problem statistically taking advantage of a computer driven random number generator. This is the technique that has resulted in the current accuracy specification.

Program description

A very important attribute of these systems are that if the measurement system is properly modelled, measurements can be made upon sets of precision standards and the users model can be solved. Unknowns can then be measured and corrected for errors. High degrees of accuracy are thus possible for measurements of unknown two-port. A basic language program has been written to implement the model in flowcharts (1) and (2).



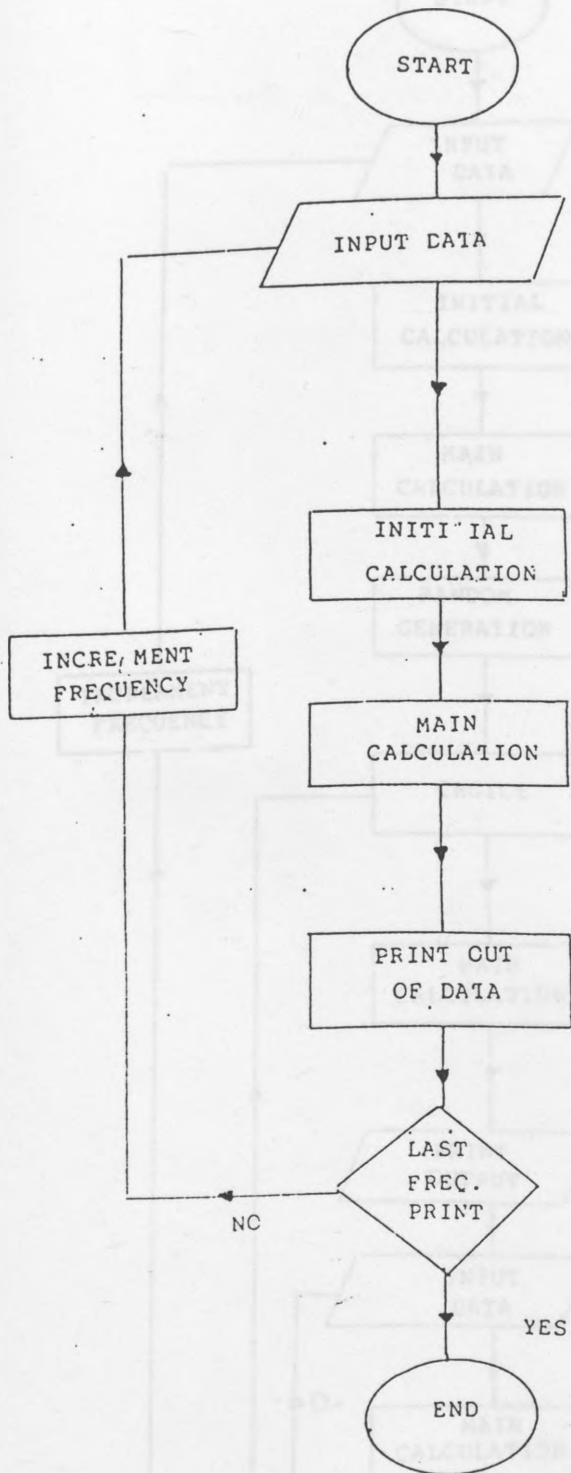
Calculate of effective electrical lengths between standards.

Calculate error network parameter equations (8), (9) and (10) (Appendix 7.7), and corrected reflection coefficient of the device under test.

Write out input data, error network parameters and corrected reflection coefficient of unknown device.

FLOW CHART (1) FCR GENERAL 3-STANDARD

(MANUAL PROGRAM)



Initial Fortran program.

Read input data which consists of frequency, and physical length for 3-standards.

Read input data which consists of frequency, (magnitude and phase of Reflection Coefficient of 1<sup>st</sup>, 2<sup>nd</sup>, 3<sup>rd</sup> and unknown.

Calculate of effective electrical lengths between standards.

Calculate error network parameter equations (8), (9) and (10) (Appendix 7.7), and corrected reflection coefficient of the device under test.

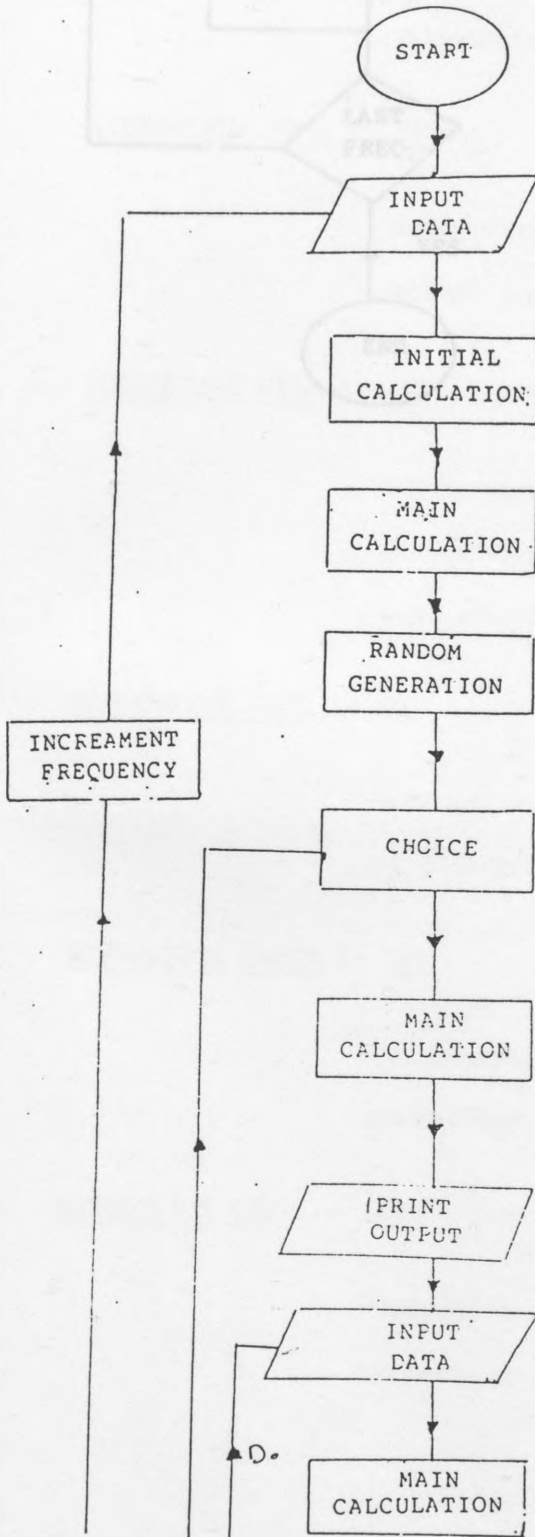
Write out input data, error network parameters and corrected reflection coefficient of unknown device.

Print out error network parameters.

Input measured reflection coefficient for the device under test.

Calculate the corrected reflection coefficient.

FLOW CHART (2) FOR GENERAL RANDOM NUMBER FOR 8-STANDARD.  
(MANUAL PROGRAM)



Initiate Fortran program.

Read input data which consists of frequency, and physical length for 8-standards.

Calculate the ideal reflection coefficient for the standard (represents the actual reflection coefficient).

Generate random numbers normally distributed by using certain standard deviation for the dB and phase for the ideal field. (represent the measured  $\rho$  reflection coefficient).

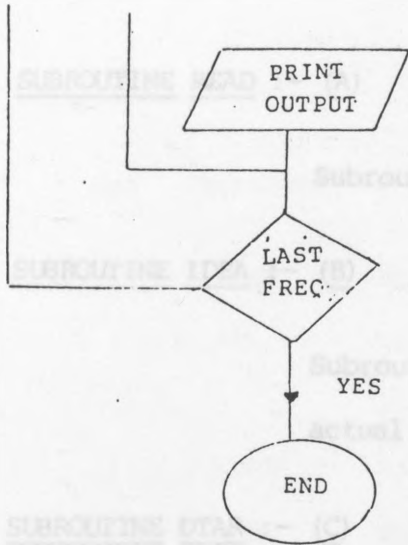
Pick up any 3-standard give reasonable correction accordingly to this frequency.

Calculate error network parameters equation (8), (9) and (10) (Appendix 7.7).

Print out error network parameters.

Input measured reflection coefficient for the device under test.

Calculate the corrected reflection coefficient.



Print out the correction reflection coefficient.

Subroutine for input data.

Subroutine for creating an ideal subfile (represent actual reflection coefficient) for any frequency.

Subroutine for producing normally distributed random numbers for the ideal subfile according to given standard deviation for the dB and phase.

SUBROUTINE PLOT :- (D)

Subroutine for picking up any combination consists of 3-standard reasonable to this frequency.

SUBROUTINE ERROR :- (E)

Subroutine for calculating one set of error parameters.

SUBROUTINE BEST :- (F)

Subroutine for correcting measurements using error parameters.

SUBROUTINE READ :- (A)

TABLE (7.8.2)

Set Required Subroutine for input data.

SUBROUTINE IDEA :- (B) No. of the frequencies

2 NF No. of the combinations each one consists of  
Subroutine for creating an ideal subfile (represent  
actual reflection coefficient) for any frequency.

SUBROUTINE DTAR :- (C) No. of the data to be corrected.

5 NR Generating random numbers.  
6 SDDB Standard deviation of the dB  
7 DTAR Standard deviation of the phase.  
8 DTAR dB of the data to be corrected.

SUBROUTINE PROT :- (D) Phase of the data to be corrected.

Subroutine for picking up any combination consists  
of 3-standard reasonable to this frequency.

SUBROUTINE ERROR :- (E)

Subroutine for calculating one set of error  
parameters.

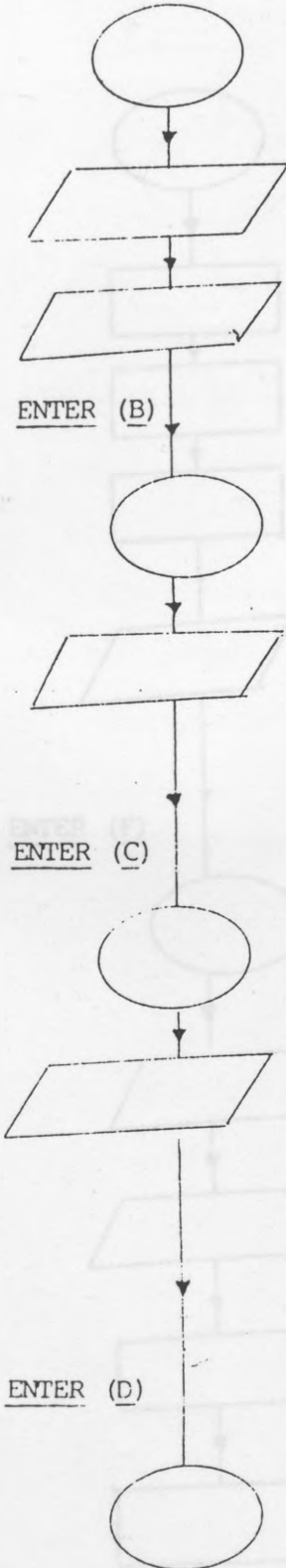
SUBROUTINE BETT :- (F)

Subroutine for correcting measurements using error  
parameters.

TABLE (7.8.1)

Set	Register	Register
1	NFRE	No. of the frequencies
2	NP	No. of the combinations each one consists of 3-standards
3	NDAT	No. of the standard (S-standards)
4	MCOR	No. of the data to be corrected.
5	MR	Generating random numbers.
6	SDDB	Standard deviation of the dB
7	SDPH	Standard deviation of the phase.
8	XMAG	dB of the data to be corrected.
9	XANG	Phase of the data to be corrected.

ENTER (A)



Sub. READ

Read input data in Table (1)

Print out data in Table (1)

ENTER (B)

Sub. IDEAL

Print out DB(I), PHA(I), I=1,8

ideal(true) reflection coefficient  
for the S-standards.

ENTER (C)

Sub. DTAR

Print out ZMAG(I), ZANG(I), I=1,8

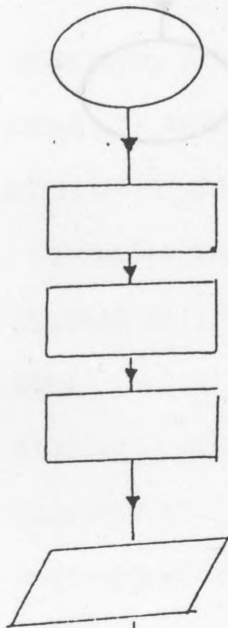
[first random group for DB(I),  
PHA(I), represent mag. reflection  
coefficient.

ENTER (D)

Sub. PROT

Pick up first combination

ENTER (E)



Print out reflection coefficient in  
polar form.

Sub. ERROR

USE /ANGDE, and rectangular form SE

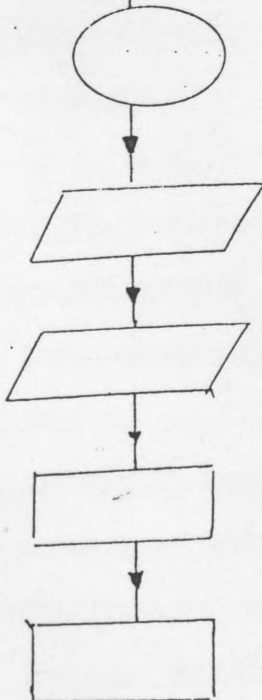
Calculate the total value for  $S_{11}$   
( $A_{11}$ )

Calculate the total value for  $S_{22}$   
( $A_{22}$ )

Calculate the total value for  $S_{12}S_{21}$   
( $A_{12}$ )

print out  $A_{11}$ ,  $A_{22}$  and  $A_{12}$  in rec-  
tangular form.

ENTER (F)



Sub. BEIT

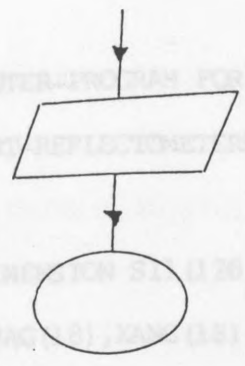
Input measured reflection coef-  
ficient for the device under test

Print out measured reflection coef-  
ficient XMAG(I), XANG(I), I=1,NCOR

Commences calculation to yield cor-  
rected reflection coefficient.

Continues calculations to yield  
reflection coefficient.

A COMPUTER PROGRAM FOR THE DIRECT CALIBRATION OF TWO-PORT REFLECTOMETERS FOR MICROWAVE MEASUREMENT.



Print out reflection coefficient in polar form.

EEM /ANGEE, and rectangular form EE

```

10 DIMENSION S11(120,8),S22(120,8),S12(120,8),G(24),AL(8),
20 COMA(8),XDM(8),FREQ(30) END (8),DANG(8),
30 WC(3),CB(3),PWA(3),SDB(30),P11(8),P22(8),P12(8),SDB(8),SDB(8)
40 DIMENSION RR(6,120,30),PT(6,120,30)
50 COMPLEX S11,S22,S12,P11,P22,P12,C,EE
60 NTA=1
70 AL(1)=0
80 AL(2)=10.35
90 AL(3)=20.75
100 AL(4)=30.70
110 AL(5)=0.11
120 AL(6)=10.46
130 AL(7)=30.46
140 AL(8)=30.81
150 DO 5 I=1,8
160 5 AL(I)=16.*XDM(I)*AL(I)/2.99792458
170C LAYER NBI DICES AL*PI*10
180 CALL HEADS(FR,FA,FB,FOAT,FOCR,IR,IRAG,IRAG,FRBO,STEB,STEB,NL,MR)
190 IG=1
200 IF(IRAG(1).EQ.1)GOTO 6
210 6 DO 60 IG=1,NFVE
220 CALL IDRA(AL,CB,PWA,FREQ(IG))
230 IF(PWA(2).EQ.0)GOTO 14

```

2 A COMPUTER PROGRAM FOR THE DIRECT CALIBRATION OF TWO-

250 PORT REFLECTOMETERS FOR MICROWAVE MEASUREMENT

260 WRITE (6, 200) ((I, DB(I), PHA(I)), I=1, NFRE)

10 DIMENSION S11 (120, 8), S22 (120, 8), S12 (120, 8), LN (24), AL (8),

20 &XMAG (18), XANG (18), FREQ (30), ZMAG (8), ZANG (8),

30 &C (3), DB (8), PHA (8), ARR (30), P11 (8), P22 (8), P12 (8), SDDB (8), SDPH (8)

40 DIMENSION RR (6, 120, 20), FF (6, 120, 20) (C, ENG, MR, AL, NEAT)

50 COMPLEX S11, S22, S12, P11, P22, P12, C, EE

60 MT=1 WRITE (6, 200)

70 AL (1)=0 (6, 210) ((I, ENG(I), ENG(I)), I=1, NEAT)

80 AL (2)=10.35

90 AL (3)=20.35 (AL, P11, P22, P12, LN, NEAT, MR, ZMAG, ZANG, FREQ)

100 AL (4)=30.70

110 AL (5)=0.11 (MR)

120 AL (6)=10.46 (P11 (C))

130 AL (7)=20.46 (P22 (C))

140 AL (8)=30.81 (P12 (C))

150 DO 5, I=1, 8 (GOTO 25)

160 5 AL (I)=16.\*ATAN (1.) \*AL (I) / 2.99792E10 (C, S12 (ID, EN))

170C LATER PSI BECCMES AL \* FREQ

180 CALL READ (NFRE, MA, NP, NDAT, MCOR, LN, XMAG, XANG, FREQ, SDDB, SDPH, NL, MR)

190 IG=1 (6, 211)

200 IF (NFRE.EQ.1) GOTO 6

210 6 DO 60 IG=1, NFRE

220 CALL IDEA (AL, DB, PHA, FREQ (IG))

230 IF (MA.GE.2) GOTO 14

```

240     WRITE (6, 205) FREQ (IG)
250     WRITE (6, 199)
260     WRITE (6, 200) ((I, DB (I), PHA (I)), I=1, NDAT)
270 14 CONTINUE
280     DO 30 ID=1, MR
290     PRINT, 'MR AND ID ARE', MR, ID
300     CALL DTAR (DB, PHA, FREQ, SDDB, SDPH, ZMAG, ZANG, MR, AX, NDAT)
310     IF (MA.GE.3)GOTO 15
320     WRITE (6, 209)
330     WRITE (6, 210) ((I, ZMAG (I), ZANG (I)), I=1, NDAT)
340 15 CONTINUE
350     CALL PROT (AL, P11, P22, P12, LN, NDAT, NP, ZMAG, ZANG, FREQ)
360     WRITE (6, 214)
370     DO 25 IC=1, NP
380     S11 (ID, IC) = P11 (IC)
390     S22 (ID, IC) = P22 (IC)
400     S12 (ID, IC) = P12 (IC)
410     IF (MA.GE.4)GOTO 25
420     WRITE (6, 215) (IC, S11 (ID, IC), S22 (ID, IC), S12 (ID, IC))
430 25 CONTINUE
440     IF (MCOR.EQ.0)GOTO 30
450     WRITE (6, 224)
460     DO 35 IB=1, MCOR
470     PMAG=XMAG (IB)
480     PANG=XANG (IB)
490     DO 40 IC=1, NP

```

```

500     C(1)=S11 (ID, IC)
510     C(2)=S22 (ID, IC)
520     C(3)=S12 (ID, IC)
530     CALL BETT (C(1) ,C(2) ,C(3) ,PMAG, PANG, EEM, ANGEE, EE, AAM, AAP, XX, YY)
540     RR (IC, ID, IB) =REAL (EE)
550     FF (IC, ID, IB) =AIMAG (EE)
560     40 CONTINUE
570     35 CONTINUE
580     30 CONTINUE
590     DO 12 II=1, MCOR
600     DO 50 I=1, MR
610     WRITE (6, 105) (RR (J, I, II) ,FF (J, I, II) ,J=1, NP)
620     105 FORMAT (2X, 12F10.4)
630     50 CONTINUE
640     12 CONTINUE
650     DO 8 II=1, MCOR
660     DO 2 J=1, NP
670     HR=0
680     HRR=0
690     DO 75 I=1, MR
700     HR=RR (J, I, II) +HR
710     75 HRR=FF (J, I, II) +HRR
720     HA=HR/120
730     HAA=HRR/120
740     WRITE (6, 300) HA, HAA
750     300 FORMAT (2X, 2F12.4)

```

```

760      XX=0
770      XXX=0
780      DO 125 I=1,MR
790          XX=(RR(J,I,II)-HA)**2+XX
800      125 XXX=(FF(J,I,II)-HAA)**2+XXX
810      WRITE(6,500)XX,XXX
820      500 FORMAT(2X,2F12.4)
830      ZZ=SQRT(XX/119)
840      ZZZ=SQRT(XXX/119)
850      WRITE(6,700)ZZ,ZZZ
860      700 FORMAT(2X,2F12.4)
870      2 CONTINUE
880      8 CONTINUE
890      60 CONTINUE
900      STOP
910      199 FORMAT(2X,15HIDEAL DATA FILE)
920      200 FORMAT(2X,1I2,2F12.4)
930      205 FORMAT(2X,11HFREQUENCY =,1E14.4)
940      209 FORMAT(2X,15HRANDOMIZED DATA)
950      210 FORMAT(2X,1I2,2F12.4)
960      214 FORMAT(2X,16HERROR PARAMETERS)
970      215 FORMAT(2X,1I2,3(2X,2F8.4))
980      224 FORMAT(2X,14HCORRECTED DATA)
990      END

```

```

1000     SUBROUTINE IDEA (AL, ZMAG, ZANG, FREQ)
1010C  SUBROUTINE FOR CREATING AN IDEAL SUBFILE FOR ANY FREQUENCY.
1020     DIMENSION AL (8) , ZMAG (8) , ZANG (8)
1030     DO 70 I=1,8
1040     IF (I.GE.5)GOTO 80
1050     PHS=-AL(I)*FREQ*45./ATAN(1.)
1060     GO TO 90
1070 80 PHS=-AL(I)*FREQ*45./ATAN(1.)-180.
1080 90 ZANG(I)=AMOD(PHS,360.)+180.
1090     ZMAG(I)=0.
1100 70 CONTINUE
1110     RETURN
1120 240 FORMAT(2X,1I2,2F12.4)
1130     END

1140     SUBROUTINE PROT (AL,S11,S22,S12, LN,NDAT,NP,ZMAG,ZANG,FREQ)
1150     DIMENSION AL(8),J(3),S11(8),S22(8),S12(8),FI(3),
1160     &RHO(3),ZMAG(8),ZANG(8),LN(24)
1170     COMPLEX RHO,S11,S22,S12,CS1,CS2,CS3
1180     TMAG(A)=EXP(0.05*ALOG(10.)*A)
1190     DO 20 I=1,NP
1200     J(1)=LN(3*I-2)
1210     J(2)=LN(3*I-1)
1220     J(3)=LN(3*I)
1230     DO 25 K=1,3

```

```

1240     YMAG=IMAG(ZMAG(J(K)))
1250     YANG=ZANG(J(K))*ATAN(1.)/45
1260     FI(K)=AL(J(K))*FREQ
1270     RHO(K)=YMAG*CEXP(CMPLX(0.0,YANG))
1280 25 CONTINUE
1290     CALL ERRO(RHO,J,FI,CS1,CS2,CS3,MA)
1300     S11(I)=CS1
1310     S22(I)=CS2
1320     S12(I)=CS3
1330 20 CONTINUE
1340     RETURN
1350     END

1600 100 FORMAT(V)
1610 110 FORMAT(V)

1360     SUBROUTINE READ(NFRE,MA,NP,NDAT,MCOR,LN,XMAG,XANG,
1370     &FREQ,SDDB,SDPH,NL,MR)
1380     DIMENSION LN(24),XMAG(18),XANG(18),FREQ(30),SDDB(8),SDPH(8)
1390     READ(3,100)NFRE,MA,NP,NDAT,MCOR,MR
1400     WRITE(6,200)NFRE,MA,NP,NDAT,MCOR,MR
1410     WRITE(6,205)
1420     NL=3*NP
1430     READ(3,110)(LN(I),I=1,NL)
1440     WRITE(6,210)(LN(I),I=1,NL)
1450     DO 41 I=1,8
1460     READ(3,120)(SDDB(I),SDPH(I))
1470 41 WRITE(6,220)(SDDB(I),SDPH(I))

```

```

1480 240 IF(NFRE.EQ.1)GOTO 3
1490 READ(3,130)(FREQ(I),I=1,NFRE)
1500 WRITE(6,230)(FREQ(I),I=1,NFRE)
1510 GOTO 5
1520 3 READ(3,129) FREQ(1)
1530 WRITE(6,229)FREQ(1)
1540 5 IF(MCOR.EQ.0)GOTO 11
1550 READ(3,140)((XMAG(I),XANG(I)),I=1,MCOR)
1560 WRITE(6,239)
1570 WRITE(6,240)((XMAG(I),XANG(I)),I=1,MCOR)
1580 11 CONTINUE
1590 RETURN
1600 100 FORMAT(V)
1610 110 FORMAT(V)
1620 120 FORMAT(V)
1630 129 FORMAT(V)
1640 130 FORMAT(V)
1650 140 FORMAT(V)
1660 200 FORMAT(2X,4HNFRE,2X,4H MA,6H NP,6H NDAT,6H MCOR,6H MR
1670 &/2X,1I2,5I6)
1680 205 FORMAT(2X,31HTHE TRIOS OF CORRECTION NUMBERS)
1690 210 FORMAT(2X,8(2X,3I2))
1700 220 FORMAT(2X,5HSDOB=,1F6.4,2X,5HSDPH=,1F6.4)
1710 229 FORMAT(2X,1E12.4)
1720 230 FORMAT(2X,11HFREQUENCIES/1E12.4)
1730 239 FORMAT(2X,20HDATA TO BE CORRECTED)

```

```

1740 240 FORMAT(2X,2F12.4) I, S11, S12, RHO, RHO, EDI, ANGE, BEI, AM, AP, XX, YI)
1750      END
1760      SUBROUTINE ERRO(RHO,J,FI,A11,A22,A12,MA)
1770C    CALCULATES ONE SET OF ERROR PARAMETERS
1780      DIMENSION RHO(3),J(3),A(3),B(3),C(3),FI(3),ALF(3)
1790      COMPLEX RHO,ALF,A,B,C,DEL,A11,A22,A12
1800      DO 10 I=1,3
1810      MP=1
1820      IF(J(I).LE.4) MP=-1
1830      ALF(I)=MP*CEXP(CMPLX(0.,FI(I)))
1840 10 CONTINUE
1850      DO 20 K=1,2
1860      A(K)=ALF(3)-ALF(K)
1870      B(K)=RHO(3)-RHO(K)
1880      C(K)=RHO(3)*ALF(3)-RHO(K)*ALF(K)
1890 20 CONTINUE
1900      DEL=A(1)*B(2)-A(2)*B(1)
1910      A11=(C(1)*B(2)-C(2)*B(1))/DEL
1920      A22=(A(1)*C(2)-A(2)*C(1))/DEL
1930      A12=(RHO(1)-A11)*(ALF(1)-A22)
1940      RETURN
1950      END

```

```

1960   SUBROUTINE BETT (S11,S22,S12,PMAG,PANG,EEM,ANGEE,BEE,AAM,AAP,XX,YY)
1970C  CORRECTS MEASUREMENTS USING ERROR PARAMETERS
1980   DIMENSION RR (4,20),FF (4,20)
1990   COMPLEX S11,S22,S12,RO,EE,BEE
2000   XMAG=EXP (0.05*ALOG (10.0) *PMAG)
2010   XANG=PANG*ATAN (1.)/45
2020   RO=XMAG*CEXP (CMPLX (0.0,XANG))
2030   EE=(RO-S11)/(S22*RO+S12-S11*S22)
2040   BEE=EE
2050   30 EEM=CABS (EE)
2060   ANGEE=(ATAN2 (AIMAG (EE),REAL (EE)) *57.2958)
2070   AAM=XMAG-EEM
2080   AAP=XANG*57.2958-ANGEE
2090   XX=AAM*COS (AAP*.01745)
2100   YY=AAM*SIN (AAP*.01745)
2110   WRITE (6,225) (EE,EEM,ANGEE,AAM,AAP,XX,YY)
2120 225 FORMAT (2X,2F8.4,2X,6(2X,F8.4))
2130   RETURN
2140   END
2150   SUBROUTINE DTAR (DB,PHA,FREQ,SDDB,SDPH,DC,PHC,MT,AX,NK)
2160C  RETURNS A RANDOMIZED DATA FILE
2170   DIMENSION DB (8),PHA (8),NB (8),DC (8),PHC (8),NC (8),SDDB (8),SDPH (8)
2180   IF (MT.NE.1)GOTO 5
2190   AX=RANDT (1.0)

```

```

2200      5 CONTINUE
2210      DO 10 K=1,NK
2220      CALL NUMA(GAU,AX)
2230      DC(K)=DB(K)+SDDB(K)*GAU
2240      CALL NUMA(GAU,AX)
2250      PHC(K)=PHA(K)+SDPH(K)*GAU
2260      10 CONTINUE
2270      RETURN
2280      END

2290      SUBROUTINE STAR(X)
2300C     STARTS PRODUCING RANDOM NUMBERS
2310      K=RANDI(1.0)*100+100
2320      X=.5716931
2330      DO 20 I=1,K
2340      X=RAND(X)
2350      20 CONTINUE
2360      WRITE(6,201)
2370      201 FORMAT(6X,9HSTAR USED)
2380      RETURN
2390      END

2400      SUBROUTINE NUMA(GAU,X)
2410C     PRODUCES NORMALLY DISTRIBUTED RANDOM NUMBERS.  SD=1

```

```

2420     SUM=0
2430     DO 30 J=1,12
2440     X=RANDT(1.0)
2450     SUM=SUM+X
2460     30 CONTINUE
2470     GAU=SUM-6
2480     RETURN
2490     END

```

REFERENCES

- (1) S.F. De Silva: "Precision Automatic Microwave Measurement System", *IEEE Trans. AP-16*, p.p:308-311.
- (2) R.W. Beatty: "Invariance Of The Cross Ratio Applied To Microwave Network Analysis", National Bureau Of Standards, Issued September 1972.
- (3) K.A. Brownlee: "Statistical Theory And Methodology In Science And Engineering".
- (4) N.A. Barry: "Error In Practical Measurement In Science, Engineering, And Technology".
- (5) B. Bianco, A. Corana, S. Ridella: "Evaluation Of Errors In Calibration Procedures For Measurements Of Reflection Coefficient", *IEEE Trans-AP 27*, December 1978.
- (6) S.F. De Silva and N.K. McPhun: "Calibration Of Microwave Network Analyzer For Computer Corrected S-Parameter Measurements", *Electronics Letters* 12th March 1973, p.p:126-128.
- (7) S.F. De Silva and N.K. McPhun: "Calibration Of An Automatic Network Analyzer Using Transmission Lines Of Unknown Characteristic Impedance, Loss And Dispersion", *The Radio And Electronic Engineer*, May 1978.
- (8) S.F. De Silva and N.K. McPhun: "Calibration Techniques For One Port Measurement", *Microwave Journal*, June 1978, p.p:97-100.

REFERENCES

- (1) S.F. Adam: "A New Precision Automatic Microwave Measurement System". IEEE Trans. 1968 IM-17, p.p:308-313.
- (2) R.W. Beatty: "Invariance Of The Cross Ratio Applied To Microwave Network Analysis". National Bureau Of Standards, Issued September 1972.
- (3) K.A. Brownlee: "Statistical Theory And Methodology In Science And Engineering". of the 5th European Microwave Conference, p.p:69-73, 1975.
- (4) B.A. Barry: "Error In Practical Measurement In Science, Engineering, And Technology". Microwave Journal, Vol. 21, May 1978, p.p:63-66.
- (5) B. Bianco, A. Corana, S. Ridela: "Evaluation Of Errors In Calibration Procedures For Measurements Of Reflection Coefficient". IEEE Trans IM 27, December 1978.
- (6) E.F. Da Silva And M.K. McPhun: "Calibration Of Microwave Network Analyzer For Computer, Corrected S-Parameter Measurements". Electronics-Letters 22nd March 1973, p.p:126-128.
- (7) E.F. Da Silva and M.K. McPhun: "Calibration Of An Automatic Network Analyzer Using Transmission Lines Of Unknown Characteristic Impedance, Loss And Dispersion". The Radio And Electronic Engineer, May 1978.
- (8) E.F. Da Silva and M.K. PcPhun: "Calibration Techniques For One Port Measurement". Microwave Journal, June 1978, p.p:97-100.

- (9) O.J.Davies, R.B.Doshi, B.Nagenthiram "Correction of microwave network analyser measurements of a two-port devices" Electronics-letters 1973, p.p:543-544
- (10) G.F. Engen: "Calibration Technique For Automated Network Analyzer With Application To Adapter Evaluation". IEEE Trans. MTT-22, December 1974, p.p:1255-1260.
- (11) N.R. Franzen and R.A. Special: "A New Procedure For System Calibration And Error Removal In Automated S-Parameters Measurements". Proceeding of The 5th European Microwave Conference, p.p:69-73, 1975.
- (12) J. Fitzpatrick "Error Model For Systems Measurements". Microwave Journal, No.21, May 1978, p.p:63-66.
- (13) D.E. Fossum: "Progress Report Of The 'IEEE Instrumentation And Measurement ist 500-chnical Subcommittee On Precision Coaxial Connector". IEEE Trans IM 1964, p.p:285-291.
- (14) V.G.Gelnovatch "A computer program for the direct calibration of two port reflectometers for automated microwave measurements" IEEE Trans. 1976, MIT 24, p.p:45-47.
- (15) J.W. Gould And G.M. Rhodes: "Computer Correction Of A Microwave Network Analyzer Without Accurate Frequency Measurement". Electronics-Lett. 18th Oct. 1973, Vol.9, No.21, p.p:494-495.
- (16) J.K. Hunton "Analysis Of Microwave Measurement Techniques By Means Of Signal Flow Graphs". I.R.E. Trans. MTT-8, p.p:206-212, March 1960.

- (17) B.P. hand: "Developing Accuracy Specification For Automatic Network Analyzer System". Hewlett Packard S. 1970, p.p:16-19.
- (18) I. Kasa: "Closed-Form Mathematical Solution To Some Network Analyzer Calibration Equations". IEEE Trans. Vol.IM-23, No.4, December 1974.
- (19) I. Kasa: "Exact Solution Of Network Analyzer calibration And Two Port Measurements By Sliding Termination". CPEM Digest 1974, p.p:90-72. *lett. 1973, No.9, p.p:323-324.*
- (20) W. Kruppa and K.F.Sodomsy "An explicit solution for the scattering parameters of a linear two-port measured with an imperfect test port" IEEE Trans. MTT 19, December 1971, p.p:122-123.
- (21) N. Kuhn: "Simplified Signal Flow Graph Analysis" Microwave Journal, November 1963, p.p:59-66. *7, p.p:7-9.*
- (22) P. Lacy And W. Oldfield: "A Precision Swept Reflectometer". The Microwave Journal, April 1973, p.p:31-34. *Conference Proceeding No.6 European Microwave Conference 1976.*
- (23) N. Marcuvitz "Waveguide Handbook". M.I.T. Rad. Lab. Ser. Vol.10, new York, McGraw-Hill, 1950 Sec.4.3. *(32) measurements". IEEE Monograph 19, Peter Peregrinus 1977.*
- (24) S.Rehnmark "On the calibration process of automatic network analyser system" IEEE Trans. 1974, MTT 22, p.p:457-458. *(31) Impedance Standards. The Microwave Journal, June 1964, p.p:47-50.*
- (25) S. Ridella "Computerized Microwave Measurements Accuracy Analysis". Proceedings Of The European Microwave Conference. Paper 13, 34. 1973. *(34) on Equations". Electron. Lett. 1975, 11, p.p:403-405.*

- (26) S. Ridella "Computerized reflection Measurements". C.P.E.M. Digest 1978, p.p:51-53.
- (27) E.W. Risley: "Discontinuity Capacitance Of A Coaxial Line Terminated In A Circular Waveguide". IEEE Trans. Vol.MTT 17, February 1969.
- (28) H.V. Shurmer: "Calibration Procedure For Computer-Corrected S-Parameter Characterization Of Devices Mounted In Microstrip". Electron, Lett. 1973, No.9, p.p:323-324.
- (29) P.I. Somla: "The Computation Of Coaxial Line Step Capacitances". IEEE Trans. MTT 15 January 1976.
- (30) P.I. Somla: "The Discontinuity Capacitance And The Effective Position Of A Shielded Open Circuit In A Coaxial Line". Proc. I.R.E.E. Australia January 1967, p.p:7-9.
- (31) H. Vifian: "A New Principle For Measuring Electrical Length And Deviation From Linear Phase". Conference Proceeding No.6 European Microwave Conference 1976.
- (32) F. Warner: "Microwave Attenuation Measurements". IEEE Monograph 19, Peter Peregrinus 1977.
- (33) B.O. Wetschel: "Air-Filled Coaxial Lines As Absolute Impedance Standards". The Microwave Journal, June 1964, p.p:47-50.
- (34) D. Wood: "Rigorous Derivation Of Computer-Corrected Network - Analyzer Calibration Equations". Electron, Lett. 1975, 11, p.p:403-405.

- (35) D. Wood: "A Coaxial Connector System For Precision R.F. Measuring Instruments And Standards". Proc. IEE Part B, Vol.108, 1961.
- (36) D. Wood: "Immittance Transformation Using Precision Air-Dielectric Coaxial Lines And Connectors". Proc. IEE. Vol.118, No.11, November 1971.
- (37) D. Wood: "Shielded-Open Circuit Discontinuity Capacitance Of Coaxial Line". Proc. IEE, No.12, December 1972.
- (38) T. Yamane "Statistics, an introductory analysis" 1967.
- (39) J. Zorzy: "Skin Effect Corrections In Immittance And Scattering Coefficient Standards Employing Precision Air Dielectric Coaxial Line". IEEE Trans. Vol.IM. 15, No.4, December 1960.